

Technische Universität München  
Lehrstuhl für Biofunktionalität der Lebensmittel

# Phenotypic and functional characterization of macrophages during type 2 immune responses

Silke Huber

Vollständiger Abdruck der von der Fakultät Wissenschaftszentrum Weihenstephan für Ernährung, Landnutzung und Umwelt der Technischen Universität München zur Erlangung des akademischen Grades eines

Doktors der Naturwissenschaften

genehmigten Dissertation.

Vorsitzender: Univ.-Prof. Dr. M. Schemann  
Prüfer der Dissertation: 1. Univ.-Prof. Dr. D. Haller  
2. Univ.-Prof. Dr. D. Vöhringer  
(Friedrich-Alexander-Universität Erlangen-Nürnberg)

Die Dissertation wurde am 01.03.2011 bei der Technischen Universität München eingereicht und durch die Fakultät Wissenschaftszentrum Weihenstephan für Ernährung, Landnutzung und Umwelt am 26.07.2011 angenommen.

*Für meine Familie*

---

## PUBLICATIONS

Huber S., Hoffmann R., Muskens F., Voehringer D. (2010). Alternatively activated macrophages inhibit T-cell proliferation by Stat6-dependent expression of PD-L2. *Blood*. 116 (17): 3311-20.

Wagner C.J., Huber S., Wirth S, Voehringer D. Chitin induces up-regulation of B7-H1 on macrophages and inhibits T cell proliferation. *Eur J Immunol*. 40 (10): 2882-90.

Messlik A., Schmechel S., Kisling S., Bereswill S., Heimesaat MM., Fischer A., Göbel U., Haller D. (2009). Loss of Toll-like receptor 2 and 4 leads to differential induction of endoplasmic reticulum stress and proapoptotic responses in the intestinal epithelium under conditions of chronic inflammation. *J Proteome Res*. 8 (10): 4406-17.

Glas J., Seiderer J., Pasciuto G., Tillack C., Diegelmann J., Pfennig S., Konrad A., Schmechel S., Wetzke M., Török HP., Stallhofer J., Jürgens M., Griga T., Klein W., Epplen JT., Schiemann U., Mussack T., Lohse P., Göke B., Ochsenkühn T., Folwaczny M., Müller-Myhsok B, Brand S. (2009). rs224136 on chromosome 10q21.1 and variants in PHOX2B, NCF4, and FAM92B are not major genetic risk factors for susceptibility to Crohn's disease in the German population. *Am J Gastroenterol*. 104 (3): 665-72.

Glas J., Konrad A., Schmechel S., Dambacher J., Seiderer J., Schroff F., Wetzke M., Roeske D., Török HP., Tonenchi L., Pfennig S., Haller D., Griga T., Klein W., Epplen JT., Folwaczny C., Lohse P., Göke B., Ochsenkühn T., Mussack T., Folwaczny M., Müller-Myhsok B., Brand S. (2008). The ATG16L1 gene variants rs2241879 and rs2241880 (T300A) are strongly associated with susceptibility to Crohn's disease in the German population. *Am J Gastroenterol*. 103 (3): 682-91.

Seiderer J, Elben I, Diegelmann J, Glas J, Stallhofer J, Tillack C, Pfennig S, Jürgens M, Schmechel S., Konrad A, Göke B, Ochsenkühn T, Müller-Myhsok B, Lohse P, Brand S. (2008). Role of the novel Th17 cytokine IL-17F in inflammatory bowel disease (IBD): upregulated colonic IL-17F expression in active Crohn's disease and analysis of the IL17F p.His161Arg polymorphism in IBD. *Inflamm Bowel Dis*. 14 (4): 437-45.

Schmechel S., Konrad A., Diegelmann J., Glas J., Wetzke M., Paschos E., Lohse P., Göke B., Brand S. (2008). Linking genetic susceptibility to Crohn's disease with Th17 cell function: IL-22 serum levels are increased in Crohn's disease and correlate with disease activity and IL23R genotype status. *Inflamm Bowel Dis*. 14 (2): 204-12.

Glas J, Seiderer J, Wetzke M, Konrad A, Török HP, Schmechel S., Tonenchi L, Grassl C, Dambacher J, Pfennig S, Maier K, Griga T, Klein W, Epplen JT, Schiemann U, Folwaczny C, Lohse P, Göke B, Ochsenkühn T, Müller-Myhsok B, Folwaczny M, Mussack T, Brand S. (2007). rs1004819 is the main disease-associated IL23R variant in German Crohn's disease patients: combined analysis of IL23R, CARD15, and OCTN1/2 variants. *PLoS One*. 5;2(9) : e819.

---

# TABLE OF CONTENTS

<b>PUBLICATIONS</b> .....	<b>iii</b>
<b>ZUSAMMENFASSUNG</b> .....	<b>vii</b>
<b>ABSTRACT</b> .....	<b>ix</b>
<b>1 INTRODUCTION</b> .....	<b>1</b>
1.1 Basic concepts in immunology .....	1
1.1.1 Differentiation of T helper cells .....	2
1.1.2 Type 2 immune responses .....	3
1.1.3 Interleukin-4 receptor signaling .....	4
1.2 Macrophages .....	6
1.2.1 Origin and differentiation of macrophages .....	6
1.2.2 Classically activated macrophages (CAM) .....	8
1.2.3 Alternatively activated macrophages (AAM) .....	9
1.3 B7:CD28 family members: PD-1 and its ligands.....	11
1.4 Nematode infection: <i>Nippostrongylus brasiliensis</i> model .....	13
1.5 Aims of the work.....	14
<b>2 MATERIAL</b> .....	<b>15</b>
2.1 Equipment and consumable material .....	15
2.2 Reagents and chemicals .....	17
2.3 Buffer and cell culture media .....	20
2.4 Antibodies .....	21
2.5 Primer sequences.....	22
2.6 Biological material .....	23
<b>3 METHODS</b> .....	<b>25</b>
3.1 Cellular and immunological methods .....	25
3.1.1 Removal of mouse organs and preparation of single cell suspensions .....	25
3.1.2 <i>Nippostrongylus brasiliensis</i> infection.....	27
3.1.3 Flow cytometry and cell sorting.....	28
3.1.4 Generation of macrophages and dendritic cells .....	29
3.1.5 Cell culture .....	30

---

3.1.6	<i>In vivo</i> blockade of PD-L2 .....	31
3.1.7	Mixed bone marrow chimeras.....	31
3.1.8	5-Bromo-2'-deoxyuridine (BrdU)-staining.....	32
3.1.9	Immunohistochemistry.....	32
3.2	Molecular biology methods.....	33
3.2.1	RNA isolation and polymerase chain reaction (PCR).....	33
3.2.2	Microarrays .....	35
3.2.3	Retroviral transduction of macrophages .....	35
3.3	Statistics .....	39
<b>4</b>	<b>RESULTS</b> .....	<b>40</b>
4.1	The inhibitory effect of AAM on T cell proliferation.....	40
4.1.1	IL-4-exposed macrophages suppress T cell proliferation in a Stat6-dependent manner.....	40
4.1.2	T cell suppression is dependent on cell-cell contact .....	43
4.2	PD-L2 expression on AAM.....	44
4.2.1	PD-L2 is expressed on AAM in a Stat6-dependent manner .....	44
4.2.2	PD-L2 is the only B7 family member which is induced by IL-4 on macrophages in a Stat6-dependent manner .....	49
4.2.3	PD-L2 expression correlates with other established AAM markers .....	52
4.3	Stat6 dependence and plasticity of PD-L2 expression .....	54
4.4	Inhibitory activity of PD-L2 on AAM .....	56
4.4.1	PD-L2 is required to mediate the inhibitory activity of AAM.....	56
4.4.2	PD-L2 is sufficient to mediate the inhibitory activity of AAM.....	58
4.5	PD-L2 expression on macrophages <i>in vivo</i> .....	60
4.5.1	PD-L2 is induced on alveolar macrophages during <i>N. brasiliensis</i> infection.....	60
4.5.2	T cell derived IL-4/IL-13 is required for PD-L2 expression on AAM <i>in vivo</i> .....	63
4.6	Macrophage recruitment during <i>N. brasiliensis</i> infection.....	64
4.6.1	Accumulation of macrophages in the lung after <i>N. brasiliensis</i> infection is independent of Stat6.....	64
4.6.2	Recruitment of macrophages in the lung after <i>N. brasiliensis</i> infection is independent of CCR2, CCR5 and F4/80.....	67
4.7	PD-1 expression on Th2 cells during <i>N. brasiliensis</i> infection.....	70
4.7.1	PD-L2 expression on macrophages correlates inversely with PD-1 expression on T cells .....	70
4.7.2	PD-1 expression is partly directly regulated by Stat6 in a cell-intrinsic manner.....	73
4.8	Anti-PD-L2 treatment during <i>N. brasiliensis</i> infection.....	75

---

<b>5</b>	<b>DISCUSSION.....</b>	<b>78</b>
	<b>LIST OF FIGURES.....</b>	<b>87</b>
	<b>LIST OF TABLES.....</b>	<b>89</b>
	<b>ABBREVIATIONS.....</b>	<b>90</b>
	<b>ACKNOWLEDGEMENTS.....</b>	<b>94</b>
	<b>REFERENCES.....</b>	<b>95</b>
	<b>CURRICULUM VITAE.....</b>	<b>103</b>
	<b>ERKLÄRUNG.....</b>	<b>105</b>

---

## ZUSAMMENFASSUNG

Makrophagen weisen in Abhängigkeit von ihrer Mikroumgebung eine breite phänotypische Heterogenität auf. Die klassische Aktivierung von Makrophagen wird durch die Interferon- $\gamma$ -abhängige Th1-Typ Immunantwort induziert, während Makrophagen einen alternativen Phänotyp durch die Interleukin-4 (IL-4) oder IL-13-vermittelte Aktivierung des Transkriptionsfaktors Stat6 entwickeln. Während einer Th2-assoziierten Immunantwort, die durch Helmintheninfektionen oder Allergien ausgelöst wird, akkumulieren alternativ aktivierte Makrophagen (AAM) in Geweben. Diese Zellen besitzen die Fähigkeit, T-Zellen in ihrer Aktivität zu hemmen, wobei nicht bekannt ist, wie die Hemmung vermittelt wird.

In dieser Arbeit wurden AAM phänotypisch und funktionell *in vitro* und *in vivo* charakterisiert. Co-Kultur Experimente zeigten, dass AAM Zell-Zell-Kontakt abhängig die T-Zell Aktivierung hemmen und Stat6-vermittelte Signalwege in Makrophagen für die suppressive Aktivität benötigt werden. Durch Microarray-Analysen wurde eine durch IL-4 induzierte Expression des hemmenden Liganden *programmed death-ligand 2* (PD-L2) in Makrophagen von Wildtyp aber nicht von Stat6-defizienten Mäusen festgestellt. Die PD-L2 Expression korrelierte dabei mit etablierten Markern für AAM wie *resistin-like molecule-alpha* (Relm- $\alpha$ ), Arginase1 und *chitinase-like protein* Ym1. PD-L2 wurde daher als bisher einziger bewährter Oberflächenmarker für die Analyse von AAM identifiziert. Eine Antikörper-vermittelte Blockierung von PD-L2 auf AAM konnte die gehemmte T-Zell Proliferation aufheben und eine retrovirale Transduktion von PD-L2 in Stat6-defiziente Makrophagen war ausreichend, um die T-Zell Proliferation zu unterdrücken. Diese Ergebnisse zeigen, dass PD-L2 auf AAM unabhängig von anderen Stat6-regulierten Genen, eine wirksame Inhibierung von T-Zellen vermittelt. Durch Infektion von Mäusen mit dem Helminthen *Nippostrongylus brasiliensis* konnte auch *in vivo* eine Stat6-abhängige Expression von PD-L2 auf Makrophagen nachgewiesen werden. Infektionen von konditional IL-4/IL-13-defizienten Mäusen mit *N. brasiliensis* ergaben, dass die PD-L2 Expression auf Makrophagen abhängig von der IL-4/IL-13 Sekretion der T-Zellen ist. Infektionsversuche mit gemischten Chimären, hergestellt aus Knochenmark von Wildtyp und Stat6-defizienten Mäusen, zeigten eine Stat6-unabhängige Akkumulation von Makrophagen in den Geweben. Jedoch war in den Chimären die Expression von PD-1,

dem Rezeptor für PD-L2, auf Th2-Zellen in der Stat6-defizienten Population höher als in der Wildtyp Population. Durch eine gezielte Blockierung von PD-L2 in Wildtyp Mäusen während einer Infektion mit *N. brasiliensis* konnte nachgewiesen werden, dass ein Fehlen von PD-L2 zu einer erhöhten Expression von PD-1 auf T-Zellen und zu einer Zunahme der Th2-Antwort führt. Diese Ergebnisse verdeutlichen, dass AAM die Th2-Zellen durch die PD-L2 Expression hemmen und dadurch eine übermäßige Entzündungsreaktion vermieden wird.



---

## ABSTRACT

Macrophages display a broad phenotypic heterogeneity depending on their microenvironment. The classical activation of macrophages is mediated by interferon- $\gamma$ -dependent Th1-type immune responses, whereas macrophages undergo alternative activation in response to interleukin-4 (IL-4) or IL-13-induced activation of the transcription factor Stat6. Alternatively activated macrophages (AAM) accumulate in tissues during Th2-associated immune responses such as helminth infections and allergic disorders. These cells possess inhibitory activity against T cells, although it remains unclear how inhibition is exerted.

The aim of this work was to characterize the phenotype and function of AAM *in vitro* and *in vivo*. This study showed that AAM-mediated suppression of T cell proliferation depends on cell-cell contact and requires Stat6-mediated signaling in macrophages. Microarray analysis revealed that the inhibitory ligand programmed death-ligand 2 (PD-L2) is strongly induced by IL-4 in macrophages from wild type but not from Stat6-deficient mice. PD-L2 expression correlates with other well-established markers for AAM, including resistin-like molecule- $\alpha$  (Relm- $\alpha$ ), arginase1 and chitinase like protein Ym1. PD-L2 can thereby be considered as a reliable surface marker for the analysis of AAM. Antibody-mediated blockade of PD-L2 restored T cell proliferation and retroviral transduction of PD-L2 into Stat6-deficient macrophages was sufficient to inhibit T cell proliferation. These results demonstrate that PD-L2 on AAM is critically involved in T cell inhibition, independently of other Stat6-regulated genes. The Stat6-dependent PD-L2 expression on macrophages could also be demonstrated *in vivo* during infection with the helminth *Nippostrongylus brasiliensis*. Infection of conditional IL-4/IL-13-deficient mice with *N. brasiliensis* showed that PD-L2 expression on macrophages is dependent on IL-4/IL-13 secretion from T cells. Further infection analysis with mixed bone marrow chimeras generated with bone marrow from wild type and Stat6-deficient mice, revealed that macrophages accumulate in selected tissues independently of Stat6. However, expression of PD-1, the receptor for PD-L2 on Th2 cells analyzed in chimeric mice was higher in the Stat6-deficient population than in the wild type population. Specific blockade of PD-L2 in wild type mice during *N. brasiliensis* infection revealed that lack of PD-L2 caused an up-regulation of PD-1 on T

cells and an enhanced Th2 response. These results indicate that AAM inhibit Th2 cells by expression of PD-L2 and thereby prevent excessive inflammation.

---

# 1 INTRODUCTION

## 1.1 Basic concepts in immunology

The immune system defends the host against infection by identifying and killing pathogens. It is able to detect a wide variety of infectious agents, from viruses and bacteria to parasitic worms and needs to distinguish them from the organisms own healthy cells and tissues in order to function properly. In vertebrates, two types of immune responses are used to protect the host: innate and adaptive. The innate immune system contains cells that have genetically encoded receptors to detect defined features of invading microbes and provides a rapid initial line of defense. The innate immune cells comprise natural killer cells (NK cells), mast cells, granulocytes and phagocytic cells including dendritic cells (DCs) and macrophages. These cells recognize regular patterns of molecular structures that are present on many microorganisms. The structures are referred to as pathogen-associated molecular patterns (PAMP) and include peptidoglycans and lipopolysaccharides (LPS) in the bacterial cell wall. Recognition of these structures through specific receptors triggers innate immune cells to engulf and degrade pathogens and to secrete cytokines and chemokines, which initiate the process of inflammation. Local inflammation and the phagocytosis of invading bacteria may also be triggered by activation of the complement system. Innate immunity acts as the first line of defense but lacks the ability to recognize certain pathogens as well as cells that provide “memory” to reinfection. Adaptive immunity is based on clonal selection from a repertoire of lymphocytes bearing highly diverse antigen-specific receptors that enable the immune system to recognize any foreign antigen. There are two major types of lymphocytes: B lymphocytes (B cells) and T lymphocytes (T cells). B cells and T cells develop from stem cells in the bone marrow and differentiate in primary lymphoid organs. B cells differentiate in the bone marrow and T cells in the thymus. Once they complete maturation, B cells and T cells enter the bloodstream as mature naïve lymphocytes and circulate through secondary lymphoid organs. These include lymph nodes, spleen, Peyer’s patches and the mucosa associated lymphoid tissues, in which an adaptive immune response is initiated if a lymphocyte meets the antigen. T cells and B cells have distinct recognition systems for the detection of extracellular and intracellular pathogens. B cells have cell-surface immunoglobulin

molecules as receptors for antigens, and upon activation, secrete immunoglobulins (Ig) as soluble antibodies that provide a humoral immunity against extracellular pathogens. T cells have receptors that recognize peptides of intracellular and extracellular pathogens presented by major histocompatibility complex (MHC) molecules on antigen presenting cells (APC). Two classes of MHC molecules transport peptides to the cell surface to present them to distinct types of effector T cells. MHCI presents peptides to cytotoxic CD8<sup>+</sup> T cells that kill infected target cells, whereas MHCII-peptide complexes are recognized by CD4<sup>+</sup> T cells which are mainly involved in activating and directing other immune cells including macrophages and B cells. A key feature of the adaptive immune system in the process of responding to a specific pathogen is the capability to generate increased numbers of differentiated memory lymphocytes, which allows a more rapid and effective immune response to reinfection with the same pathogen [1].

### **1.1.1 Differentiation of T helper cells**

Naïve CD4<sup>+</sup> T cells differentiate at least into four different types of T helper (Th) cells: Th1, Th2, Th17 cells and regulatory T cells (Tregs). Differentiation of CD4<sup>+</sup> T cells into Th1 or Th2 subsets is based on the cytokine milieu [2]. Th1 cells develop in response to interleukin-12 (IL-12) and are characterized by the expression of the T-box transcription factor (T-bet) [3]. These cells are associated with the production of interferon- $\gamma$  (IFN- $\gamma$ ) and tumor necrosis factor- $\alpha$  (TNF- $\alpha$ ) required for efficient immune responses against intracellular pathogens [4]. In addition, these cells also promote help to the production of opsonizing and complement-binding antibodies by plasma cells and increase the phagocytic activity of macrophages [5]. IL-4 has an important role in the differentiation of Th2 cells. Through its action on transcription factor signal transducer and activator of transcription 6 (Stat6), IL-4 up-regulates the expression of GATA-binding protein 3 (GATA-3), the master regulator for Th2 cell differentiation [6, 7]. Th2 cells are characterized by the secretion of IL-4, IL-5 and IL-13, which are critical for immunity against helminths and other extracellular pathogens [8]. IL-4 and IL-13 are particularly important as they generate an autocrine feedback loop that leads to further Th2 cell development [9]. Besides immunity against pathogens, another important feature of these

two CD4<sup>+</sup> T cell subsets is the ability to cross-regulate the generation of the other subset through their signature cytokines IFN- $\gamma$  or IL-4 [4, 5]. The discovery of the IL-17 family of cytokines and the analysis of IL-23-mediated effector functions on T cells have suggested the existence of an additional subset of CD4<sup>+</sup> T cells that produce IL-17 and were designated Th17 cells [10]. The differentiation of Th17 cells requires the combination of the pro-inflammatory cytokine IL-6 and the immunosuppressive cytokine transforming growth factor- $\beta$  (TGF- $\beta$ ) and depends on the activation of the transcription factor retinoid acid-related orphan nuclear hormone receptor- $\gamma$ t (ROR- $\gamma$ t) [11, 12]. IL-23 is involved in the maintenance of these cells [11]. Th17 cells enhance host protection against extracellular bacteria and fungi, which are not efficiently cleared by Th1 and Th2 responses [13]. Tregs are phenotypically characterized by the expression of IL-2R $\alpha$  (CD25) and the transcription factor forkhead box P3 (Foxp3) [14, 15]. Tregs are thought to be important for keeping autoreactive T cells in check that have escaped from negative selection in the thymus. Tregs also participate in peripheral tolerance through suppression of other immune cells [16].

### **1.1.2 Type 2 immune responses**

The immune response against many helminth parasites or allergens is referred to as the type 2 immune response (Th2-type), which includes both innate and adaptive components. Th2-type responses are typically characterized by an increase in the level of IL-4 and other Th2-type cytokines, including IL-5 and IL-13. IL-4 is considered to be a keystone of the Th2-type response and is secreted by Th2 cells, basophils and mast cells [17-19]. Eosinophils have also been reported to be capable of producing IL-4 [20]. IL-4 is important for the differentiation of naïve T cells into Th2 cells and at the same time, suppresses the expression of IFN- $\gamma$ -production of Th1 cells [21]. Although IL-4 signaling is required in driving the Th2 cell development, the initial source of IL-4 remains obscure. IL-4 is also essential for the induction of IgE synthesis by activated B cells and influences class switching to IgG1 as well [22, 23]. IgE binds then to the high-affinity Fc receptor (Fc $\epsilon$ RI) on the surface of basophils and mast cells, thereby linking the innate and the adaptive immune system during a Th2-type immune response [24]. Activated basophils

and mast cells secrete various products, in particular cytokines, chemokines, histamine, heparin and proteases, which result in increased smooth muscle constriction and vascular permeability [24]. By directly acting on epithelial cells and smooth muscle cells IL-4 further promotes mucus production and goblet cell metaplasia [25]. IL-4 stimulates B cells to increase their cell surface expression of MHCII molecules, IL-4 receptor  $\alpha$  and the low affinity IgE receptor (CD23) [26-28]. In addition, macrophages undergo alternative activation in response to IL-4 and/or IL-13. These alternatively activated macrophages (AAM) are implicated in performing immunoregulatory roles [29].

### **1.1.3 Interleukin-4 receptor signaling**

IL-4-induced responses result from the interaction with the IL-4 receptor (IL-4R). The IL-4R $\alpha$  chain associates with either the common  $\gamma$ -chain ( $\gamma_c$ ) to form the type I IL-4R or with the IL-13R $\alpha$  chain to form the type II IL-4R (Figure 1) [30, 31]. The type I receptor has a higher affinity for IL-4 and is expressed predominantly on hematopoietic cells, whereas the type II receptor is expressed mainly on stromal cells. IL-4R engagement results in recruitment of Janus tyrosine kinases (Jaks). Activation of Jaks leads to tyrosine phosphorylation of the IL-4R $\alpha$  chain. Subsequently, adaptor proteins with Src homology 2 domains (SH2) bind to the receptor. Two major pathways for the IL-4R signaling transduction have been described: the Stat6 pathway and the insulin receptor substrate (IRS) pathway (Figure 1) [32, 33].

Signaling through the Stat6 pathway requires the recruitment of Stat6 molecules to the IL-4R $\alpha$  chain. Stat6 binds via the SH2 domain to the specific tyrosine residue in the IL-4R $\alpha$  cytoplasmic region [17]. Bound Stat6 gets phosphorylated by Jaks and Stat6 then disengages from the IL-4R $\alpha$  cytoplasmic tail, forms homodimers with a second phosphorylated Stat6 molecule and translocates to the nucleus, where it activates transcription of IL-4 inducible genes (Figure 1) [34]. Stat6 regulates expression of chemokines like eotaxin-1 (CCL11), thymus and activation-regulated chemokine (CCL17) and macrophage-derived chemokine (CCL22), which mediate recruitment of eosinophils

and other effector cells to target tissues [35, 36]. Stat6 also induces goblet cell hyperplasia and is required for the expulsion of gastrointestinal helminths [37, 38].

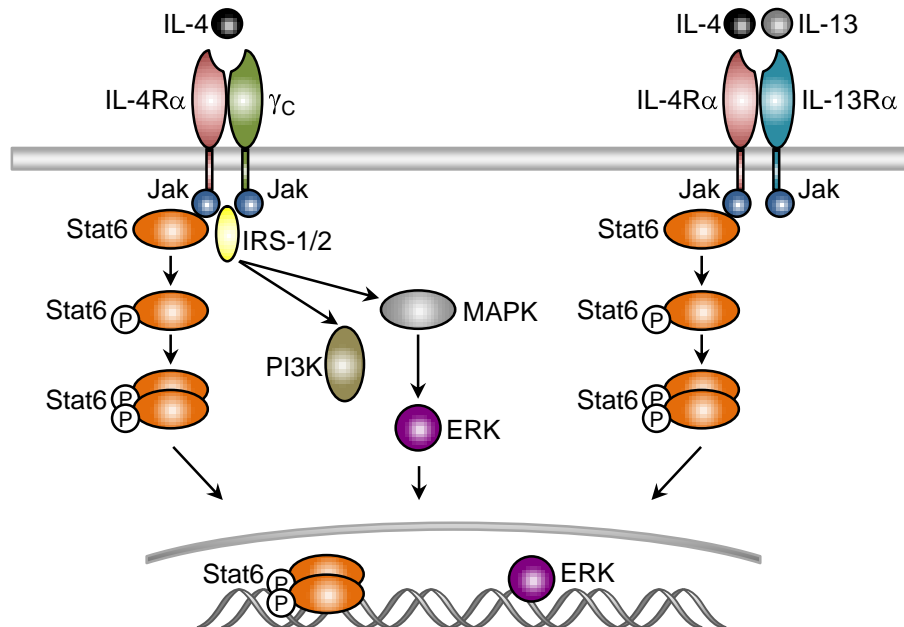


**Figure 1: IL-4R signaling pathway.**

IL-4 binds to the IL-4R $\alpha$  chain. The IL-4R $\alpha$  chain associates with either the common  $\gamma$ -chain ( $\gamma_c$ ) or with the IL-13R $\alpha$  chain. IL-4R engagement results in activation of two distinct signaling pathways: the activation of Stat6 and the IRS-1/2 signaling pathway.

Signaling via the IRS-pathway is initiated by the recruitment of the IRS-1/2 molecules to the IL-4R $\alpha$  chain. Recruited IRS-1/2 molecules are phosphorylated by Jaks and act as adaptor proteins linking further signal transduction molecules to the receptor (Figure 1) [33]. Phosphorylated IRS-1/2 molecules have been described to bind to the regulatory subunit of the phosphoinositide 3-kinase (PI3K). Activated PI3K phosphorylates membrane lipids that act as second messenger and are crucial for cell growth and survival [39]. Another binding partner of phosphorylated IRS-1/2 is the adapter molecule growth factor receptor-bound protein 2 (Grb-2), that establishes a link to the mitogen-activated protein kinase/extracellular-signal-regulated kinases (MAPK/ERK) pathway (Figure 1) [17].

## 1.2 Macrophages

### 1.2.1 Origin and differentiation of macrophages

Macrophages were initially recognized by Elie Metchnikoff in 1883 as phagocytic cells responsible for pathogen elimination [40]. The term macrophage came from the Greek for “large eaters” and was used to distinguish these cells from microphages (from the Greek for “small eaters”; neutrophils). Based on ontogeny and phagocytosis, macrophages belong to the mononuclear phagocyte system, which includes bone marrow-derived precursor cells, monocytes in the peripheral blood and mature macrophages in the tissues [41]. Macrophages are generally considered to be derived from circulating monocytes, which migrate into tissues in the steady state or in response to inflammation [42]. Monocytes develop in the bone marrow from hematopoietic stem cells (HSCs). HSCs first differentiate in response to granulocyte-macrophage colony-stimulating factor (GM-CSF) and macrophage colony-stimulating factor (M-CSF) and under control of the transcription factor PU.1 to monoblasts and to pro-monocytes before becoming monocytes (Figure 2) [42]. Monocytes then exit the bone marrow and enter the bloodstream. Adhesion molecules such as integrins and selectins control the migration of monocytes from the blood into different tissues where they differentiate into tissue-specific macrophages including macrophages of the bone (osteoclasts), alveoli (alveolar macrophages), central nervous system (microglial cells), gastrointestinal tract, liver (Kupffer cells), spleen and peritoneum [29, 42]. Tissue macrophages are about 15-25  $\mu\text{m}$  in diameter and their half-life under homeostatic conditions varies between weeks and months [43, 44].

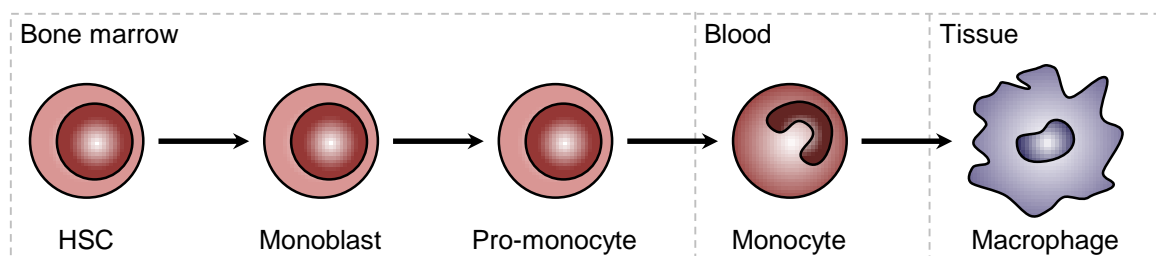


**Figure 2: Macrophage origin and development.**

Macrophages arise in the bone marrow from hematopoietic stem cells (HSC). HSC undergo differentiation steps during which they become monocytes, which exit the bone marrow and enter the bloodstream. Monocytes migrate to different tissues, where they differentiate into tissue-specific macrophages. Modified from [45].



Macrophages play a dual role in the host defense. They are a component of the innate immune response, but they also act as important accessory cells in the adaptive immune response. Macrophages are involved in the removal of erythrocytes and cellular debris generated during tissue remodeling and cells that have undergone apoptosis. The homeostatic clearance of apoptotic cells by macrophages through phagocytosis occurs independently of immune cell signaling and results in little production of immune mediators by unstimulated macrophages [46]. Necrosis also generates cellular debris which is cleared by macrophages. Phagocytosis of these components leads to alterations in the phenotype of macrophages with production of pro-inflammatory mediators [45]. Additionally, macrophages protect the host from infection through the recognition of PAMPs present on many microorganisms, the subsequent engulfment and degradation of the pathogens, and the secretion of cytokines and chemokines. The activation of macrophages in the absence of a specific antigen is classified as innate (antigen non-specific, T cell independent) immune activation of macrophages [29]. The receptors utilized in the innate situation include the family of scavenger receptors and C-type lectin receptors (dectin-1, mannose receptor) (Figure 3) [47]. Activation of these receptors leads to phagocytosis of apoptotic or necrotic cells, as well as exogenous ligands. Surface receptors that are not involved in phagocytosis, but are important in the recognition of bacteria, fungi and viruses are Toll-like receptors (TLRs) [48]. Activation of TLRs on macrophages by microbial stimuli like peptidoglycans and LPS induces the production of pro-inflammatory cytokines (TNF- $\alpha$ , IL-1, IL-6, IL-12), reactive oxygen species (ROS) and nitric oxide (NO), followed by a regulated immune response [48]. Macrophage activation leads to enhanced antigen presentation via up-regulation of surface MHC:peptide complexes underlying their importance as APCs.

The interaction of macrophages with activated T and B cells forms part of the antigen-specific immune response [29]. This adaptive macrophage activation is mediated by opsonic receptors including complement receptors and Fc receptors that are involved in phagocytosis of complement- or antibody-opsonized particles (Figure 3) [49, 50]. Besides phagocytosis, macrophage activation via Fc-receptors induces the secretion of cytokines and can thereby bias the subsequent immune responses [51]. Macrophages can be also

activated through their cytokine receptors by binding cytokines like IFN- $\gamma$  and IL-4 secreted from cells of the innate and adaptive immune system.

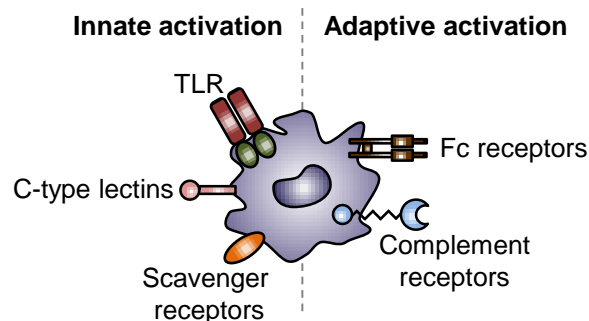


**Figure 3: Innate and adaptive immune activation of macrophages.**

Innate activation of macrophages is mediated by pattern recognition receptors, such as TLRs, scavenger receptors and lectins. The receptors utilized in the adaptive immune activation of macrophages include Fc and complement receptors.

The response of macrophages to environmental signals determines their functional properties at the site of inflammation. Among these signals, cytokines are responsible for the development of highly divergent macrophage phenotypes. In particular, IFN- $\gamma$  and IL-4/IL-13 activate distinct functional programs in macrophages which lead to macrophages being classified as “classically activated” or “alternatively activated”.

### 1.2.2 Classically activated macrophages (CAM)

Classical activation of macrophages was first described in the 1960s when studies on the infection of mice with *Listeria monocytogenes* showed antimicrobial activities of macrophages which were stimulus-dependent, but antigen-independent [29]. Further studies revealed that the classical activation of macrophages occurs in a Th1-type environment and is dependent on IFN- $\gamma$  and a second signal provided by PAMPs [52]. During an immune response IFN- $\gamma$  is first produced by innate immune cells, such as NK cells. As the immune response develops, antigen-specific Th1 cells become an important source of IFN- $\gamma$  [53]. The second signal is provided by pathogens that express one or more PAMPs, such as LPS, which stimulate macrophage activation through TLRs and induce the production of TNF- $\alpha$  by these cells [45]. Only the combination of two signals, IFN- $\gamma$

and TNF- $\alpha$ , results in full macrophage activation. These classically activated macrophages (CAM) become strongly microbicidal and are important immune effector cells in host defense against intracellular pathogens [54]. Studies with TNF-receptor-deficient mice have shown that lack of a second signal in macrophages results in ineffective elimination of *L. monocytogenes* [55]. The importance of TLR activation for TNF- $\alpha$  production for fully activated CAM has also been shown in *Leishmania* spp. infection studies. *Leishmania* species are parasites that survive and replicate intracellularly in macrophages. Stimulation of macrophages with IFN- $\gamma$  and TNF- $\alpha$  before infection with *Leishmania major* yields a population that efficiently kills the parasite. Macrophages stimulated with IFN- $\gamma$  alone result in ineffective parasite clearance because *Leishmania* does not express TLR ligands and therefore cannot trigger TNF- $\alpha$  production [56]. This impaired macrophage activation is consistent with gene expression studies showing limited responses in macrophages to *Leishmania* infection [57]. Genes that are expressed during the activation of CAM are controlled by Stat1 molecules. Stat1 molecules are activated following IFN- $\gamma$  receptor ligation, or ligand binding to the TLR or TNF receptor [58]. Activated CAM produce high levels of IL-12 and promoting thereby the differentiation of Th1 cells and the induction of pro-inflammatory Th1-type immune responses. In addition, CAM exert anti-proliferative and cytotoxic activities, resulting from their ability to activate the inducible nitric oxide synthase (iNOS), which leads to the synthesis of NO and ROS and the secretion of pro-inflammatory cytokines (TNF- $\alpha$ , IL-1 and IL-6) (Figure 4) [58, 59]. CAM promote strong pro-inflammatory immune responses to protect the host against pathogens, but their activation must be tightly controlled to prevent macrophage-mediated host-tissue injury.

### **1.2.3 Alternatively activated macrophages (AAM)**

The classification of IL-4 and/or IL-13-elicited macrophages as alternatively activated macrophages (AAM) was first described in 1992 by Gordon *et al.* [60]. Alternative activation of macrophages is associated with Th2-type immune responses and is important in responses to parasitic and extracellular pathogens as well as tissue remodeling [29]. IL-4 and IL-13 inhibit the differentiation of CAM and reduce the secretion of pro-inflammatory cytokines and induce the differentiation of AAM. AAM up-regulate the mannose receptor

(MR) which is important for endocytosis of mannosylated ligands as well as MHCII molecules on the cell surface (Figure 4) [60]. The differentiation of AAM after IL-4 and IL-13 stimulation is Stat6-dependent and requires the peroxisome proliferator-activated receptor  $\gamma$  (PPAR $\gamma$ ) to sustain this alternative phenotype [34, 61]. In addition to Stat6, PI3K signaling downstream of the IL-4R also plays an important role in alternative macrophage activation. Galectin-3, a membrane molecule that participates in a feedback loop resulting in sustained PI3K activation, seems to be important for optimal alternative macrophage activation [62]. SH2-containing inositol-5-phosphatase (SHIP) is a negative regulator of the PI3K pathway and mice lacking SHIP show increased generation of AAM, confirming the importance of PI3K pathway in IL-4/IL-13-mediated macrophage activation [63].

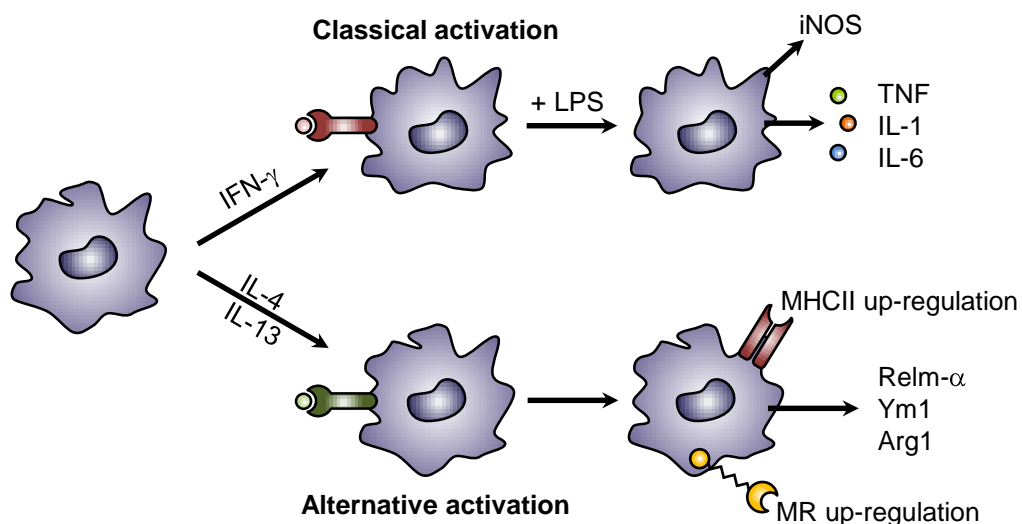


**Figure 4: Classical and alternative activation of macrophages.**

Classical activation is dependent on the priming stimulus IFN- $\gamma$  and a second signal provided by PAMPs (e.g. LPS). Alternative activation is mediated by IL-4 and IL-13 signaling via the common IL-4R $\alpha$  chain. Modified from [29].

IL-4/IL-13-mediated differentiation of AAM is associated with the production of characteristic markers like arginase1 (Arg1), resistin-like molecule alpha (Relm- $\alpha$ /Fizz1) and the chitinase-like protein Ym1 (Figure 4) [64]. Expression of these genes in AAM is induced in a Stat6-dependent fashion [65-67]. Arg1 in AAM has an important function in arginine metabolism and induces a shift from the IFN- $\gamma$ -induced production of NO via iNOS toward the production of ornithine and polyamines, which are important for wound healing [68]. Indeed, AAM have been shown to mediate tissue repair during an innate

response to injury, independently of adaptive immunity and infection [69]. Ym1 might also promote wound healing through the binding activity to carbohydrates and extracellular matrix [70].

AAM are observed in a variety of helminth infections, including Th2-type immune responses to *Nippostrongylus brasiliensis* and *Schistosoma mansoni* [71, 72]. The expression of signature markers for AAM like Relm- $\alpha$  and Ym1 identified in mouse lungs infected with *N. brasiliensis*, confirmed the alternative phenotype during this parasite infection [71]. Arg1 expression in macrophages from mice infected with *S. mansoni* egg antigens has been identified as an important mechanism to promote the shift from Th1-type toward Th2-type immune responses [68]. Studies with macrophage/neutrophil-specific IL-4R $\alpha$ -deficient mice have shown that a lack of macrophages with an alternative phenotype results in increased susceptibility to *S. mansoni* infection. These effect was due to increased Th1 cytokines, iNOS-activity and impaired egg expulsion, indicating that AAM are essential for immunoregulation and protection against tissue injury [72].

### **1.3 B7:CD28 family members: PD-1 and its ligands**

B7 molecules are crucial in regulating T cell activation and tolerance through the delivery of co-stimulatory signals. CD80 and CD86 are the best characterized B7 family members, both of which bind to the stimulatory receptor CD28 and the inhibitory receptor cytotoxic T-lymphocyte antigen-4 (CTLA-4) on the surface of T cells [73]. More recently, the interaction of the programmed death-1 (PD-1) receptor and its ligands programmed death-ligand 1 (PD-L1) and PD-L2 has been shown to promote co-stimulation to T cells as well (Figure 5) [74-76]. PD-1 was discovered in 1992 as a gene up-regulated in a T cell hybridoma undergoing cell death [74]. Further studies have shown that expression was associated with the negative regulatory function of PD-1, but not with cell death [77]. PD-1 is expressed on CD4<sup>+</sup> T cells, CD8<sup>+</sup> T cells, natural killer T cells (NKT cells) and B cells in an inducible way [77]. The receptor is a cell surface monomer consisting of an extracellular domain and a intracellular domain containing an immunoreceptor tyrosine-based inhibitory motif (ITIM) [78, 79]. PD-1 is phosphorylated on its intracellular

tyrosines upon ligand engagement, and then binds phosphatase that dephosphorylate effector molecules activated in the T cell receptor (TCR) or B cell receptor (BCR) signaling cascades [77, 79]. PD-1 may exert its effects on cell differentiation and survival directly, by inhibiting early activation events that are positively regulated by CD28, or indirectly through inhibition of IL-2 production, as well-known proliferation and survival factor for T cells [80]. The functional significance of PD-1-mediated inhibitory signals is demonstrated by the phenotype of PD-1-deficient mice: PD-1-deficient mice on the C57BL/6 background develop a lupus-like-disease, while PD-1-deficient mice on the BALB/c background develop a fatal cardiomyopathy [81, 82].

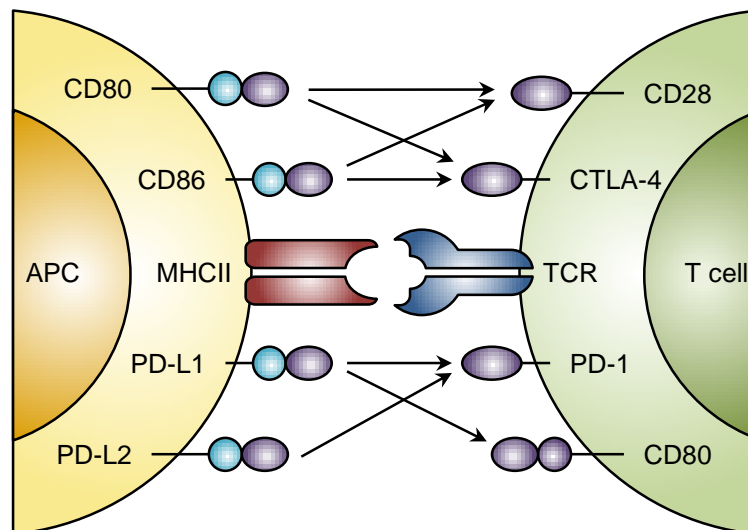


**Figure 5: B7:CD28 family members.**

The co-stimulatory molecules CD80 and CD86 on APCs have dual specificity for two receptors on T cells, the stimulatory receptor CD28 and the inhibitory receptor CTLA-4. PD-1 is a inhibitory receptor for both PD-L1 and PD-L2. Modified from [77].

Both PD-1-ligands, PD-L1 and PD-L2, exhibit distinct patterns of expression [83, 84]. PD-L1 is constitutively expressed on T cells, B cells, DCs, macrophages and cultured bone marrow-derived mast cells. PD-L1 is also expressed on non-hematopoietic cells, including epithelial cells and pancreatic islets cells, and is further up-regulated on a number of these cells after activation. In contrast to PD-L1, PD-L2 expression is much more restricted. PD-L2 is inducibly expressed on DCs, macrophages, cultured bone marrow-derived mast cells and peritoneal B-1 B cells. Although the phenotype of PD-1-deficient mice clearly suggests an inhibitory function for this receptor, the role of the ligands PD-L1 and PD-L2 in T cell activation is diverse and both stimulatory and inhibitory functions for these

ligands have been reported [76, 85, 86]. Recently, it was demonstrated that CD80 can bind to PD-L1, resulting in the inhibition of T cell responses (Figure 5) [87]. These findings suggest important roles for PD-1-ligands in regulating the balance between the stimulatory signals needed for effective immunity and the prevention of excessive inflammation. However, it remains unclear which PD-L1 and/or PD-L2 expressing cells are involved in certain infections and whether the two ligands have similar or distinct functions.

#### **1.4 Nematode infection: *Nippostrongylus brasiliensis* model**

Helminths are parasites that live inside their host. More than 25% of the human population is infected with parasitic helminths [88]. Infections with these pathogens cause marked morbidity, with chronic infection often leading to anemia and malnourishment. Helminths can be categorized into three groups: cestodes (tapeworms), nematodes (roundworms) and trematodes (flukes). Nematodes are colorless, unsegmented and lack appendages. Hookworms (e.g. *Necator americanus*, *Ancylostoma duodenale*) are parasitic nematodes of humans causing approximately 700 million infections worldwide, with the highest prevalence in South America, sub-Saharan Africa and East Asia [88].

The natural host of the hookworm *N. brasiliensis* is the rat and was adapted to the mouse in the 1970s for experimental purpose [89]. The infection of mice with this nematode is a well-characterized experimental system for the study of Th2-type immune responses. Infective third stage larvae (L3-larvae) are free-living. For experimental studies, L3 larvae are injected subcutaneously at the lower back of the mouse and 24-48 hours later, these larvae migrate via the bloodstream to the lungs. The larvae develop in the lung to L4 larvae before they are coughed up and swallowed 48-72 hours after inoculation, and mature in the small intestine into egg-laying adult worms by five to six days. Adult worms are expelled from the gut of mice nine to ten days after infection. During different stages of development, *N. brasiliensis* causes local inflammation first in the lung and subsequently in the small intestine with local and systemic basophilia, eosinophilia and accumulation of Th2 cells. These cells produce high levels of IL-4, IL-5 and IL-13 and induce the IgE and IgG1 synthesis by activated B cells [90]. *N. brasiliensis* can be used as a model for acute

infections that have a systemic as well as a gastrointestinal phase in which host defense mechanisms cause expulsion without killing the parasite. By employing this Th2-type immune response model in mice, whose IL-4 gene locus reports commitment to IL-4 production by simultaneous expression of green fluorescent protein (4get mice), it is possible to reliably quantify CD4<sup>+</sup> Th2 cell responses and other IL-4 producing cells in mice [91].

## 1.5 Aims of the work

The aim of this work was to characterize the phenotype and function of alternatively activated macrophages (AAM).

AAM accumulate in tissues during Th2-associated immune responses such as helminth infections and allergic disorders. These cells differentiate in response to IL-4- and IL-13-mediated activation of the transcription factor Stat6. Although AAM have immunoregulatory roles, the molecular mechanism that leads to the anti-inflammatory activity of AAM remains uncertain. A major aim of this work was to identify the mechanism through which AAM mediate immune alteration, by investigating the potential involvement of soluble factors or inhibitory ligands. The suppressive activity of AAM depends on IL-4/IL-13-mediated signals, although it is not clear whether these signals are mediated via Stat6 or activation of the MAPK or PI3K pathway. To clarify this question, macrophages from wild type and Stat6-deficient mice were phenotypically and functionally compared after *in vitro* exposure to IL-4. To study the physiological function of AAM *in vivo*, alveolar macrophages after infection with the helminth *Nippostrongylus brasiliensis* were analyzed. Additionally, conditional IL-4/IL-13-deficient mice were used to specifically delete both cytokines in CD4<sup>+</sup> T cells in order to identify the IL-4/IL-13 producing cell type required for AAM differentiation. There is currently limited information about how macrophage recruitment and mobilization in various tissues is regulated under homeostatic and inflammatory conditions. Therefore, the turnover and migration of AAM were assessed using BrdU incorporation experiments both in steady state as well as during *N. brasiliensis* infection.



## 2 MATERIAL

### 2.1 Equipment and consumable material

**Table 1: Equipment**

Equipment / Type	Manufacturer
Bacterial shaker	Infors-HT, Bottmingen, Switzerland
Camera / Olympus E330	Olympus, Tokio, Japan
Centrifuge / Eppendorf	Eppendorf, Hamburg, Germany
Centrifuge / Rotanta 460R	Hettich, Tuttlingen, Germany
Centrifuge / Sorvall Superspeed RC-5B	Thermo Scientific, Waltham, MA, USA
Cryostat / CM 1950	Leica Microsystems, Bensheim, Germany
Flow cytometer / Aria	BD Biosciences, San José, CA, USA
Flow cytometer / Calibur	BD Biosciences, San José, CA, USA
Flow cytometer / Canto II	BD Biosciences, San José, CA, USA
Gel chamber	Thermo Scientific, Waltham, MA, USA
Incubator (cell culture)	Heraeus, Kendro Laboratory, Osterode, Germany
Incubator (bacterial culture)	Ehret, Emmendingen, Germany
Laminar flow hood	Heraeus, Kendro Laboratory Products, Germany
LightCycler	Roche Diagnostics, Mannheim, Germany
Magnetic stirrer	IDL, Nidderau, Germany
Microscope / Laborlux O	Leica, Wetzlar, Germany
Microscope / SM-Lux	Leica, Wetzlar, Germany
Microscope	Zeiss, Oberkochen, Germany
PCR-machine / Robocycler Gradient 96	Stratagene Agilent Technologies, Sedar Creek, TX, USA
pH-meter	Inolab, Weilheim, Germany
Photometer / Ultraspec 3000	Pharmacia Biotech, Freiburg, Germany
Pipettes and multichannel pipettes	Eppendorf, Hamburg, Germany
Special accuracy weighing machine / PSR 620-3	Kern, Balingen-Frommern, Germany
Table vortex	Bender & Hobein, Zürich, Switzerland
UV-Transilluminator	Intas, Goettingen, Germany
Water bath	GFL, Burgwedel, Germany
Weighing machine / PL 1200	Mettler-Toledo, Greifensee, Switzerland

**Table 2: Computer software**

Software	Manufacturer
CellQuestPro 5.2.1	BD Biosciences, San José, CA, USA
FACS Diva 1.1.3	BD Biosciences, San José, CA, USA
FlowJo v. 6.4	Treestar, Ashland, OR, USA
SigmaPlot 2000	Systat Software Inc., San José, CA, USA

**Table 3: Consumable material**

Product	Manufacturer
Bottle top filter (0.22 µm)	VWR, Darmstadt, Germany
Cell culture flasks (75 cm <sup>2</sup> , 175 cm <sup>2</sup> )	Sarstedt, Nuembrecht, Germany
Cell scraper	Peske, Aindling-Amhofen, Germany
Cell strainer (70 µm)	BDFalcons, Franklin Lake, NJ, USA
Chromatography paper	Whatman, Kent, UK
Coverslips (18x18 mm)	Roth, Karlsruhe, Germany
Cryo conserving tubes (2 mL)	Roth, Karlsruhe, Germany
Erlenmeyer flasks	Brand, Wertheim, Germany
Falcon tubes (15 mL and 50 mL)	BDFalcons, Franklin Lake, NJ, USA
Filter membranes (40 µm and 70 µm)	VWR, Darmstadt, Germany
Glass pipettes (5 mL, 10 mL and 20 mL)	Roth, Karlsruhe, Germany
Hollow needles (0.45 x 12 mm and 0.40 x 20 mm)	Braun, Melsungen, Germany
ImmEdge Pen	Vector Laboratories, Burlingame, CA, USA
Injections (1 mL, 5 mL, 10 mL and 20 mL)	Braun, Melsungen, Germany
Introcan	Braun, Melsungen, Germany
Neubauer counting chamber	Roth, Karlsruhe, Germany
Omnican injections (1 mL syringes)	Braun, Melsungen, Germany
Pasteur pipettes, glass (150 mm and 230 mm)	Roth, Karlsruhe, Germany
Petri dishes (90 x 14 mm)	Roth, Karlsruhe, Germany
Petri dishes (150 x 20 mm)	Sarstedt, Nuembrecht, Germany
Pipette tips (1-200 µL and 100-1000 µL)	Sarstedt, Nuembrecht, Germany
Plastic pipettes (5 mL, 10 mL and 25 mL)	Sarstedt, Nuembrecht, Germany
Plates (flat bottom; 6-, 24-, 96-well)	Sarstedt, Nuembrecht, Germany
Round-bottom tubes (bacteria)	Greiner Bio-one, Frickausen, Germany
Sterile pipette tips (0.1-10 µL, 1-20 µL, 1-200 µL and 101-1000 µL)	Starlab, Ahrensburg, Germany
SuperFrost Plus Gold glass slides	Thermo Scientific, Braunschweig, Germany

Product	Manufacturer
Tissue-Tek-Cryomold (15x15x5 mm)	Sakura Finetek, Torrance, CA, USA
Tubes (PCR) 0.2 mL	Peske, Aindling-Arnhofen, Germany
Tubes 1.7 mL	Roth, Karlsruhe, Germany
Tubes (sterile) 1.5 mL	Brand, Wertheim, Germany
Tubes (flow cytometry)	Sarstedt, Nuembrecht, Germany

## 2.2 Reagents and chemicals

**Table 4: Reagents**

Product	Manufacturer
Acetic acid 100%	Roth, Karlsruhe, Germany
Acetone $\geq$ 99.8% p.a.	Roth, Karlsruhe, Germany
Agarose	Roth, Karlsruhe, Germany
Albumin Fraction V $\geq$ 98% biotin free (BSA)	Roth, Karlsruhe, Germany
Ammonium chloride	Roth, Karlsruhe, Germany
Ampicillin	Roth, Karlsruhe, Germany
Antifoam A	Fluka, St. Louis, MO, USA
N,N-Bis(2-hydroxyethyl)-2-aminoethanesulfonic acid (BES)	Roth, Karlsruhe, Germany
$\beta$ -Mercaptoethanol	Merck, Darmstadt, Germany
5-Bromo-2'-deoxyuridine (BrdU)	Sigma-Aldrich, St. Louis, MO, USA
Buffer for reverse transcription (10x)	Invitrogen, Carlsbad, CA, USA
Calcium phosphate	Roth, Karlsruhe, Germany
Carboxyfluorescein succinimidyl ester (CFSE)	Invitrogen, Carlsbad, CA, USA
Charcoal activated	Sigma-Aldrich, St. Louis, MO, USA
Chloroquine diphosphate salt	Sigma-Aldrich, St. Louis, MO, USA
4', 6' - Diamidino-2-phenylindol (DAPI)	Sigma-Aldrich, St. Louis, MO, USA
dATP	Roth, Karlsruhe, Germany
dCTP	Roth, Karlsruhe, Germany
DEPC-H <sub>2</sub> O	Sigma-Aldrich, St. Louis, MO, USA
dGTP	Roth, Karlsruhe, Germany
Dithiothreitol (DTT; 0.1 M)	Invitrogen, Carlsbad, CA, USA
DNase Digestion	Roche, Basel, Switzerland

## MATERIAL

<b>Product</b>	<b>Manufacturer</b>
dTTP	Roth, Karlsruhe, Germany
DyNAmo Cappillary Master Mix	Finnzymes, Espoo, Finland
Ethanol $\geq$ 99.8%	Roth, Karlsruhe, Germany
Ethidium bromide	Roth, Karlsruhe, Germany
Ethylenediaminetetraacetic acid (EDTA)	AppliChem, Darmstadt, Germany
Fetal Calf Serum (FCS)	Invitrogen, Carlsbad, CA, USA
Hematoxylin	Vector Laboratories, Burlingame, CA, USA
Heparin	Biochrom AG, Berlin, Germany
Isopropanol ( $\geq$ 99.8%)	Roth, Karlsruhe, Germany
Kaiser's glycerol gelatin	Merck, Darmstadt, Germany
LB-Agar	Roth, Karlsruhe, Germany
L-Glutamine	Biochrom AG, Berlin, Germany
Liberase	Roche, Basel, Switzerland
Lipopolysaccharide (LPS)	Sigma-Aldrich, St. Louis, MO, USA
LB-Medium	Roth, Karlsruhe, Germany
Magnesium chloride	Sigma-Aldrich, St. Louis, MO, USA
Neomycin sulfate	Roth, Karlsruhe, Germany
Oligonucleotides (dT) <sub>20</sub> (50 $\mu$ M)	Invitrogen, Carlsbad, CA, USA
Paraformaldehyde	Roth, Karlsruhe, Germany
pBR328 bp-DNA- ladder	Roth, Karlsruhe, Germany
Penicillin	Biochrom AG, Berlin, Germany
Phosphate buffered saline (PBS)	Biochrom AG, Berlin, Germany
Polybrene (Hexa-dimethrin bromide)	Sigma-Aldrich, St. Louis, MO, USA
Polymyxin B-sulfate	Roth, Karlsruhe, Germany
Potassium hydrogen carbonate	Roth, Karlsruhe, Germany
Rnase Zap <sup>®</sup> solution	Ambion, Austin, Texas, USA
Sodium azide	Roth, Karlsruhe, Germany
Sodium chloride	Roth, Karlsruhe, Germany
Sodium-ethylenediaminetetraacetic acid (EDTA)	Roth, Karlsruhe, Germany
Sodium hydrogen phosphate	Roth, Karlsruhe, Germany
Streptomycin	Biochrom AG, Berlin, Germany
Thioglycollate	Sigma-Aldrich, St. Louis, MO, USA
Tissue freezing medium	Jung, Nussloch, Germany
Tris chloride	Roth, Karlsruhe, Germany

<b>Product</b>	<b>Manufacturer</b>
Trypan blue solution	Sigma-Aldrich, St. Louis, MO, USA
Trypsin/EDTA 100x	Invitrogen, Carlsbad, CA, USA
Tween-20	AppliChem, Darmstadt, Germany

**Table 5: Commercial kits**

<b>Product</b>	<b>Manufacturer</b>
Alkaline Phosphatase Vectostain ABC kit	Vector Laboratories, Burlingame, CA, USA
Peroxidase Vectostain ABC kit	Vector Laboratories, Burlingame, CA, USA
Plasmid Maxi Kit (25)	Qiagen, Hilden, Germany
RNA isolation kit	Fluka, Buchs, Switzerland
RNeasy Mini Kit	Qiagen, Hilden, Germany
Streptavidin/Biotin blocking kit	Vector Laboratories, Burlingame, CA, USA
Qiaprep Spin Miniprep kit (250)	Qiagen, Hilden, Germany

**Table 6: Cytokines**

<b>Product</b>	<b>Manufacturer</b>
IL-2	ImmunoTools, Friesoythe, Germany
IL-4	R&D Systems, Minneapolis, MN, USA

**Table 7: Enzymes**

<b>Enzyme</b>	<b>Manufacturer</b>
DNase I	Sigma-Aldrich, St. Louis, MO, USA
EcoRI and Buffer 2	New England Biolabs, Ipswich, MA, USA
Superscript II reverse transcriptase	Invitrogen, Carlsbad, CA, USA
Taq-polymerase	Genecraft, Cologne, Germany

## 2.3 Buffer and cell culture media

**Table 8: Media**

Product	Manufacturer
Dulbecco's Modified Eagle's Medium (DMEM)	PanBiotech, Aidenbach, Germany
Dulbecco's Phosphate buffered saline (DPBS)	PanBiotech, Aidenbach, Germany
RPMI 1640	PanBiotech, Aidenbach, Germany
S.O.C. Medium	Invitrogen, Carlsbad, CA, USA

**Table 9: Buffer and cell culture media**

Solution	Composition
ACK buffer	8.29 g NH <sub>4</sub> Cl 1 g KHCO <sub>3</sub> 37.2 mg Na <sub>2</sub> EDTA H <sub>2</sub> O ad 1 L pH 7.2-7.4
2x BES/PO <sub>4</sub> solution	50 mM BES 280 mM NaCl 1.5 mM Na <sub>2</sub> HPO <sub>4</sub> pH 7.1
BrdU fixation buffer	DPBS without Ca <sup>2+</sup> and Mg <sup>2+</sup> 1% PFA, 0.01% Tween-20
CFSE buffer	PBS without Ca <sup>2+</sup> and Mg <sup>2+</sup> 0.1% BSA
DMEM medium	DMEM 10% FCS (v/v) 5 x 10 <sup>-5</sup> M β-Mercaptoethanol 2 mM L-Glutamine 100 µg/mL Penicillin/Streptomycin
DNase buffer	0.15 M NaCl 4.2 mM MgCl in H <sub>2</sub> O (pH 5)
Fluorescence activated cell sorter (FACS) blood buffer	DPBS without Ca <sup>2+</sup> and Mg <sup>2+</sup> 2% FCS 0.1% NaN <sub>3</sub> 2000 U/L Heparin
FACS buffer	DPBS without Ca <sup>2+</sup> and Mg <sup>2+</sup> 2% FCS 0.1% NaN <sub>3</sub>
FACS sort buffer	PBS without Ca <sup>2+</sup> and Mg <sup>2+</sup> , 4% FCS
PBS	9.55 g/L PBS without Ca <sup>2+</sup> and Mg <sup>2+</sup>
RPMI medium	RPMI 1640 10% FCS (v/v) 5 x 10 <sup>-5</sup> mM β-Mercaptoethanol 2 mM L-Glutamine 100 µg/mL Penicillin/Streptomycin
50x TAE buffer	242 g Tris 57.1 mL Acetic acid (100% (v/v)) 100 mL 0.5 M EDTA (pH 8.0), H <sub>2</sub> O ad 1 L

Solution	Composition
3% (w/v) Thioglycollate medium	Thioglycollate dissolved by heating in H <sub>2</sub> O and sterilized by autoclaving
0.1 M Tris buffer (pH 7.5)	12.1 g/L Tris pH 7.5 with fuming HCl
0.1 M Tris buffer (pH 8.4)	12.1 g/L Tris pH 8.4 with fuming HCl

All reagents, buffers and media were prepared with double distilled water.

## 2.4 Antibodies

**Table 10: Anti-mouse antibodies**

Anti-mouse	Species/Isotype	Clone	Conjugation	Manufacturer
BrdU	Mouse IgG1	3D4	FITC	BD Pharmingen, Heidelberg, Germany
B7-1	Armenian Hamster IgG	16-10A1	Biotinylated	eBioscience, San Diego, CA, USA
B7-2	Rat IgG2a	GL1	Biotinylated	eBioscience, San Diego, CA, USA
β TCR	Armenian Hamster IgG	H57-597	Purified	Biolegend, San Diego, CA, USA
CD3	Armenian Hamster IgG	145-2C11	PE	eBioscience, San Diego, CA, USA
CD4	Rat IgG2a	RM4-5	FITC, PE, PerCP-Cy5.5	eBioscience, San Diego, CA, USA
CD8	Rat IgG2a	53-6.7	APC	eBioscience, San Diego, CA, USA
CD11b	Rat IgG2b	M1/70	PE	eBioscience, San Diego, CA, USA
CD11c	Armenian Hamster IgG	N418	PE, PE-Cy5.5	eBioscience, San Diego, CA, USA
CD16/CD32	Rat IgG2b	2.4G2	Purified	BioXCell, West Lebanon, NH, USA
CD19	Rat IgG2a	eBio1D3	Alexa Fluor 647	eBioscience, San Diego, CA, USA
CD28	Golden Syrian Hamster IgG	37.51	Purified	eBioscience, San Diego, CA, USA
CD45.1	Mouse IgG2a	A20	Alexa Fluor 647	eBioscience, San Diego, CA, USA
CD45R	Rat IgG2a	RA3-6B2	FITC	eBioscience, San Diego, CA, USA
CD90.1	Mouse IgG2a	HIS51	PE-Cy5	eBioscience, San Diego, CA, USA
CD90.2	Rat IgG2a	53-2.1	PE	eBioscience, San Diego, CA, USA
CD115	Rat IgG2a	AFS98	Biotinylated	eBioscience, San Diego, CA, USA
F4/80	Rat IgG2a	BM8	PE, APC	eBioscience, San Diego, CA, USA
MHCII	Rat IgG2b	I-A/I-E; M5/114.15.2	APC, Biotinylated	eBioscience, San Diego, CA, USA
PD-1	Rat IgG2b	PMP1-30	Biotinylated	eBioscience, San Diego, CA, USA
PDCA-1	Rat IgG2b	eBio927	Alexa Fluor 647	eBioscience, San Diego, CA, USA
PD-L1	Rat IgG2a	1-111A	Biotinylated	eBioscience, San Diego, CA, USA

Anti-mouse	Species/Isotype	Clone	Conjugation	Manufacturer
PD-L2	Rat IgG2a	122	Biotinylated	eBioscience, San Diego, CA, USA
PD-L2	Rat IgG2a	TY25	Purified	BioXCell, West Lebanon, NH, USA
NK 1.1	Mouse IgG2a	PK136	APC	eBioscience, San Diego, CA, USA
SiglecF	Rat IgG2a	E50-2440	PE	BD Pharmingen, Heidelberg, Germany
Ym1	Rabbit	Polyclonal	Purified	StemCell Technologies, Sheffield, UK

**Table 11: Anti-rabbit antibodies**

Anti-rabbit	Species/Isotype	Clone	Conjugation	Manufacturer
IgG	Goat	Polyclonal	Biotinylated	Invitrogen, Carlsbad, CA, USA

**Table 12: Isotypes**

Species/Isotype	Conjugation	Manufacturer
Rat IgG2a	PE	eBioscience, San Diego, CA, USA
Rat IgG2a	Biotinylated	eBioscience, San Diego, CA, USA
Rat IgG2a	Purified	BioXCell, West Lebanon, NH, USA

**Table 13: Streptavidin**

Conjugation	Manufacturer
Pe-Cy7	BD Pharmingen, Heidelberg, Germany
APC	SouthernBiotech, Birmingham, AL, USA

## 2.5 Primer sequences

**Table 14: Primer sequences**

Primer	Sequence 5'-3'	Manufacturer
$\beta$ -actin: forward	ATGGATGACGATATCGCT	Metabion, Martinsried, Germany
$\beta$ -actin: reverse	ATGAGGTAGTCTGTCAGGT	Metabion, Martinsried, Germany
PD-L2: forward	GAGCCAGTTTGCAGAAGGTAG	Metabion, Martinsried, Germany
PD-L2: reverse	ATCCGACTCAGAGGGTCAATG	Metabion, Martinsried, Germany
Rentla: forward	CCATAGAGAGATTATCGTGGA	Metabion, Martinsried, Germany
Rentla: reverse	TGGTCGAGTCAACGAGTAAG	Metabion, Martinsried, Germany
Arginase1: forward	GTATGACGTGAGAGACCACG	Metabion, Martinsried, Germany
Arginase1: reverse	CTCGCAAGCCAATGTACACG	Metabion, Martinsried, Germany



Primer	Sequence 5'-3'	Manufacturer
Chi313: forward	TGGAATTGGTGCCCTACAA	Metabion, Martinsried, Germany
Chi313: reverse	AACTTGCACTGTGTATATTG	Metabion, Martinsried, Germany

## 2.6 Biological material

**Table 15: Mouse strains**

Mouse	Description	Source
BALB/c	BALB/c mice with the MHC haplotype H-2 <sup>d</sup> were used as wild type control mice.	The Jackson Laboratory, Bar Harbor, ME, USA
C57BL/6	C57BL/6 mice with the MHC haplotype H-2 <sup>b</sup> were used as wild type control mice.	The Jackson Laboratory, Bar Harbor, ME, USA
Stat6 <sup>-/-</sup>	The Stat6-deficient mice were generated by replacing the two exons of the Stat6 gene with the neomycin resistance gene [34].	The Jackson Laboratory, Bar Harbor, ME, USA
Ly5.1 (B6.SJL-Ptprc <sup>a</sup> Pepc <sup>b</sup> /BoyJ)	BALB/c Ly5.1 is a congenic mouse strain. Ly5.1 (CD45.1) and Ly5.2 (CD45.2) are congenic markers, used to distinguish hematopoietic cells from genetically identical mice.	Backcross from C57BL/6 Ly5.1 mice originally obtained from The Jackson Laboratory, Bar Harbor, ME, USA
Thy1.1 (CD90.1)	BALB/c/Thy1.1 is a congenic mouse strain. Thy1.1 (CD90.1) and Thy1.2 (CD90.2) are congenic markers, used to distinguish Thy1.1 <sup>+</sup> cells from genetically identical mice.	Trudeau Institute, Saranac Lake, NY, USA
CD4Cre	CD4Cre is a transgenic mouse strain in which the Cre recombinase is expressed under the control of the CD4 promoter [92].	Taconic Farms, Germantown, NY, USA
IL-4/eGFP reporter (4get mice)	These mice were generated by introducing an <i>internal ribosomal entry site</i> (IRES)-eGFP construct after the stop codon of IL-4 by homologous recombination, which leads to transcription of a bicistronic mRNA. eGFP is trapped inside the cell whereas IL-4 is secreted to the outside [91].	R. Locksley, SF, USA
IL-4/IL-13 <sup>F/F</sup> mice	The IL-4/IL-13 <sup>F/F</sup> mice were generated by insertion of two <i>loxP</i> sites flanking an exon in the IL-13 gene and downstream of the IL-4 gene [93].	D. Voehringer, Munich, Germany
IL-4/IL-13 <sup>-/-</sup>	This mouse strain was generated by targeted disruption of the mouse IL-13 and IL-4 genes in embryonic stem cells [94].	A. McKenzie, Cambridge, UK
CCR2 <sup>-/-</sup>	The CCR2-deficient mice were generated by replacing the coding exon 3 of the CCR2 gene with an eGFP construct [95].	B. Luckow, Munich Germany
CCR5 <sup>-/-</sup>	The CCR5-deficient mice were generated by replacing the coding region of CCR5 and a part of the non-coding region with the lacZ reporter gene [96].	B. Luckow, Munich Germany

Mouse	Description	Source
F4/80 <sup>-/-</sup>	The F4/80 mouse line expresses the Cre recombinase under the direct control of the F4/80 regulatory elements (F4/80-Cre knock-in) [97]. Mice were backcrossed for at least nine generations to C57BL/6 background.	K. Pfeffer, Düsseldorf, Germany

All mice were backcrossed for at least nine generations to BALB/c background, unless otherwise indicated, housed according to institutional guidelines, and used between 6 and 12 weeks of age. All animal experiments were approved by the Regierung von Oberbayern.

**Table 16: Rat strain**

Rat	Description	Source
Lewis	Lewis rats were used for maintenance of the <i>Nippostrongylus brasiliensis</i> life cycle	Janvier SAS, Le GenestSaint Isle, France

**Table 17: Cell lines**

Cell line	Origin	Source
L929	Mouse fibroblasts	R. Lang, Munich, Germany
Phoenix E	Based on 293 T cells. Packaging line for ecotropic retroviruses	T. Brocker, Munich, Germany
X63	Lymphoma cells transfected with the mouse GM-CSF gene	T. Brocker, Munich, Germany

**Table 18: Bacterial strain**

Bacterial strain	Manufacturer
One Shot <sup>®</sup> top10 competent <i>Escherichia coli</i>	Invitrogen, Carlsbad, CA, USA

## **3 METHODS**

### **3.1 Cellular and immunological methods**

#### **3.1.1 Removal of mouse organs and preparation of single cell suspensions**

Mice were killed by cervical dislocation between 6 and 12 weeks of age.

##### **Spleen and mesenteric lymph nodes**

Spleen and mesenteric lymph nodes were removed with sterile forceps and surrounding fat was removed. Organs were transferred to a 70  $\mu$ m cell strainer placed in Petri dishes containing 10 mL RPMI medium. Using a circular motion, spleen and mesenteric lymph nodes were pressed against the bottom of the Petri dish with the plunger of a 5 mL syringe until mostly fibrous tissue remained. Clumps in the cell suspension were removed by pipetting the suspension twice through the cell strainer before the suspension was transferred into a tube. To analyze tissue specific macrophages, spleen was digested using FCS-free RPMI medium containing liberase and DNase I followed by incubation at 37°C for 20 min. Single cell suspensions were centrifuged (1200 rpm, 5 min, 4°C) and supernatants were discarded. To remove red blood cells, pellets were resuspended in 1 mL ACK lysis buffer for 2 min at room temperature. Cells were washed in RPMI medium, centrifuged and pellets were resuspended in RPMI medium and stored on ice for further analysis.

##### **Bone marrow**

Femur and tibia were removed from mice and the muscles were removed from the bones using a sterile paper towel and placed in a Petri dish. Both ends of each bone were cut off with scissors and marrow was obtained by flushing out each of the shafts with RPMI medium using a syringe. Marrow was collected in a cell strainer placed on a 50 mL tube. Marrow plugs were disrupted with the plunger of a 5 mL syringe and were flushed with RPMI medium through the cell strainer into the 50 mL tube. The suspension was centrifuged (1200 rpm, 5 min, 4°C) and supernatant was discarded. Red blood cells were

lysed with ACK lysis buffer. Cells were washed in RPMI medium, centrifuged and the pellet was resuspended in RPMI medium.

### **Lungs**

After opening the thorax, lung lavage was performed by instillation of 10 mL PBS through the right ventricle of the heart after severing the aorta. Lungs were removed if they appeared pale white and free of blood leukocytes and transferred into RPMI medium. For single cell suspensions, lungs were placed into 70  $\mu$ m cell strainer with medium and were cut with scissors into small pieces. Using the plunger of a 5 mL syringe, single cells were then pressed through the cell strainer. The single cell suspension was transferred into a tube followed by centrifugation (1200 rpm, 5 min, 4°C) and lysis of red blood cells. To analyze tissue specific macrophages, lungs were digested using FCS-free RPMI medium containing liberase and DNase I as described above.

### **Bronchoalveolar lavage (BAL)**

To expose the trachea, tissue from the neck was dissected. A small incision in the trachea was made to allow passage of a 20-gauge needle into the trachea. A 1 mL syringe containing PBS was placed at the end of the needle and the PBS was injected into the mouse lung. BAL was aspirated by pulling the barrel of the syringe; the recovered lavage fluid was then transferred to a 15 mL tube on ice. This procedure was repeated twice per animal. Pooled lavage fluid was centrifuged (1200 rpm, 5 min, 4°C) and the pellet was resuspended in RPMI medium.

### **Peritoneal lavage**

Peritoneal lavage was collected by gentle insertion of a needle into the mouse lower abdominal area. Immediately after inserting the needle 8 mL RPMI medium was injected with a 10 mL syringe into the peritoneal cavity followed by massage of the peritoneum. Using the same syringe and a horizontal position of the needle inside the peritoneal cavity, the peritoneal lavage was collected by slow aspiration of medium containing cells. Cells were washed in RPMI medium, centrifuged (1200 rpm, 5 min, 4°C) and the pellet was resuspended in RPMI medium.

**Blood**

For blood collection an infrared lamp was placed over the cage. The resulting vasodilatation allowed the collection of blood through a cut at the end of the tail vein. Blood was collected directly in a 5 mL tube containing fluorescence activated cell sorter (FACS) blood buffer followed by centrifugation (1200 rpm, 5 min, 4°C) and red blood cell lysis.

**Cell counts**

To estimate the cell number of viable cells in the single cell suspension, trypan blue was used. The dye cannot penetrate intact cell membrane, but death cells absorb the dye and appear blue under the microscope. Cells were prepared for counting using a dilution of 1:10 in trypan blue and were then placed in a Neubauer counting chamber. Unstained cells were counted in at least two squares of 1 mm<sup>2</sup>. Given that a quadrant has an area of 1 mm<sup>2</sup> and the height between the chamber and the coverslip is 0.1 mm, the total volume is of 0.1 µL. The number of total cells was calculated using following equation:

$$\text{Number of total viable cells} = \frac{\text{number of cells}}{\text{number of squares}} \times 10^4 \times \text{dilution factor} \times \text{volume of cell suspension}$$

**3.1.2 *Nippostrongylus brasiliensis* infection**

Maintenance of the *Nippostrongylus brasiliensis* life cycle in rats allows production and preparation of a large number of parasites, sufficient to provide a good number of reproducible infections over several weeks. Lewis rats were infected with 2500 third-stage larvae (L3) of *N. brasiliensis* subcutaneously at the base of the tail. Rats were provided antibiotics-containing water (2 g/L neomycin sulfate, 100 mg/L polymyxin B-sulfate) for the first 5 days after infection. Between days 6 and 10 post-infection feces containing parasitic eggs were collected. The fecal pellets were softened with distilled water and then mixed with equal volumes of granulated charcoal to form a coarse paste. A dampened chromatography filter paper was placed into a 150 x 20 mm Petri dish and the fecal paste was distributed on top of the filter paper in the prepared dishes. The dishes were placed into a large plastic lidded container to ensure that sufficient humidity was maintained and incubated at room temperature in the dark for ≥ seven days. *N. brasiliensis* L3 larvae could

---

be harvested from the dishes 8 days after the start of the fecal culture. Using a pipette, 0.9% saline (37°C) was added to the periphery of the fecal culture dish and was swirled around the edges of the dish and edges of the filter paper, carefully avoiding the fecal culture material in the center of the filter. The L3 larvae were transferred to a 50 mL tube, were washed extensively in sterile 0.9% saline (37°C) and counted. 500 organisms were then injected into mice subcutaneously at the base of the tail. Mice were provided antibiotics-containing water for the first 5 days and were analyzed at the indicated time points after infection. Worm expulsion was determined by counting adult worms in the small intestine on day 9 after infection.

### 3.1.3 Flow cytometry and cell sorting

#### Surface staining

For staining of surface proteins  $1-3 \times 10^6$  single cells were washed once in FACS buffer and incubated with anti-CD16/CD32 blocking antibody (2.4G2) at room temperature for 5 min to block unspecific binding of antibodies to Fc receptors. 100  $\mu$ L of diluted antibodies were directly added to the cells, mixed and incubated in the dark on ice for 20 min. Cells were washed in FACS buffer (1200 rpm, 5 min, 4°C) to remove unbound antibodies. If biotinylated primary antibodies were used, cells were then stained for additional 20 min with 100  $\mu$ L diluted fluorophore-conjugated streptavidin antibodies. Finally, samples were washed, resuspended in 250  $\mu$ L FACS buffer and stained with DAPI to exclude dead cells. Acquisition was performed using a FACS-Calibur (CellQuest software) or FACS-Canto (FACSDiva software) instrument and analyzed with FlowJo software. Antibodies used in this work are listed in 2.4. Macrophages in lung and BAL were identified as autofluorescence<sup>hi</sup>SSC<sup>hi</sup>FSC<sup>hi</sup>F4/80<sup>+</sup>CD11c<sup>hi</sup> whereas macrophages in the spleen were detected as F4/80<sup>+</sup>CD11b<sup>hi</sup> and peritoneal macrophages as F4/80<sup>+</sup>.

#### Fluorescence activated cell sorter

To achieve pure cell populations, cells were stained with fluorophore-conjugated antibodies as described above and resuspended in FACS sort buffer. Cells were sorted using a high speed cell sorter (FACS Aria instrument and FACSDiva software). The purity of the sort ranged between 95-99%.

---

### 3.1.4 Generation of macrophages and dendritic cells

#### Generation of L929 and X63 supernatants

Vials of the M-CSF-producing fibroblast cell line L929 and the GM-CSF-producing X63 B lymphoma cell line were thawed, resuspended in complete medium and centrifuged before cells were transferred to 75 cm<sup>2</sup> cell culture flasks supplemented with 10 mL of complete medium and incubated at 37°C and 5% CO<sub>2</sub>. At the desired growth confluence, adherent cells were harvested by trypsin/EDTA treatment. Therefore, culture medium was removed and the cell layer was washed once in 5 mL PBS, followed by incubation with 1 mL of a 2x trypsin/EDTA solution in the cell culture incubator for 2 min. Fresh medium was added to the cells, which were then transferred to a tube and centrifuged (1200 rpm, 5 min, 4°C). The pellet was resuspended in 35 mL complete medium and transferred to 175 cm<sup>2</sup> cell culture flasks. The cells were split every 2-3 days until the cells were expanded to ten 175 cm<sup>2</sup> flasks. Then, the volume in the flasks was adjusted with medium to 90 mL and the cells were incubated for additional 3 days. The medium was then transferred to 50 mL tubes, centrifuged (1200 rpm, 10 min, 4°C) and the supernatants were collected in an Erlenmeyer flask, mixed, transferred into 50 mL tubes and stored at -80°C.

#### Peritoneal macrophages

Peritoneal macrophages were obtained by stimulation of macrophage recruitment in mice via injection of 3 mL 3% thioglycollate medium into the peritoneal cavity. Mice were killed after 4 days and macrophages were obtained by peritoneal lavage as described in 3.1.1.

#### Bone marrow-derived macrophages

Bone marrow cells were obtained as described in 3.1.1 and resuspended in RPMI medium in the presence of 10% supernatant from the M-CSF-producing fibroblast cell line L929. 5x10<sup>6</sup> cells/10 mL were cultured in a Petri dish and incubated at 37°C, 5% CO<sub>2</sub> for 7 days. At the second day 5 mL fresh RPMI medium with 10% L929 supernatant was added to the culture. Three days later 7.5 mL culture medium was removed and replaced with 7.5 mL fresh medium. After removal of non-adherent cells on day 7, macrophages were detached from Petri dishes using 5 mM EDTA in PBS. Macrophages were washed, counted and used for further experiments. We generated F4/80<sup>+</sup> macrophages with purity > 90%.

**Bone marrow-derived dendritic cells**

Bone marrow cells were obtained as described in 3.1.1 and resuspended in RPMI medium in the presence of 3% supernatant from the GM-CSF-producing X63 B lymphoma cell line.  $2 \times 10^6$  cells/10 mL were cultured in Petri dishes and incubated at 37°C, 5% CO<sub>2</sub> for 10 days. On day 4 10 mL fresh RPMI medium containing GM-CSF was added to the culture. On day 6 10 mL of cultured medium was transferred into a 15 mL tube, centrifuged (1200 rpm, 5 min, 4°C) and the cell pellet was resuspended in fresh RPMI medium supplemented with GM-CSF and replated. The procedure was repeated on day 8. On day 10 non-adherent dendritic cells were collected and used for further experiments. We generated CD11c<sup>+</sup> dendritic cells with purity > 90%.

**3.1.5 Cell culture****Stimulation of macrophages and dendritic cells**

Peritoneal macrophages, bone marrow-derived macrophages and dendritic cells were cultured at a density of  $10^6$  cells/mL in Petri dishes. Cells were incubated for 24 h in RPMI medium (control) or RPMI medium supplemented with IL-4 (10 ng/mL) or LPS (1 µg/mL).

**Co-culture of splenocytes with macrophages**

Splenocytes from BALB/c mice were washed once in CFSE buffer, counted and resuspended at a density of  $2 \times 10^7$  cells/mL in pre-warmed CFSE buffer. Cells were filtered through a cell strainer into a 50 mL tube. 2 µL of 5 mM CFSE per mL cell suspension was added while vortexing to give a final concentration of 10 µM CFSE, followed by an incubation at 37°C for 10 min. After incubation, the cell suspension was underlaid with the same volume of pre-warmed FCS and centrifuged (5 min, 1500 rpm, 4°C) followed by two additional washing steps in RPMI medium.

CFSE-labeled splenocytes were then cultured either alone or at the indicated ratios with bone marrow-derived macrophages from BALB/c or Stat6<sup>-/-</sup> mice or with supernatant of cultured macrophages in 96-well flat bottom plates, which had been pre-coated with 0.5



---

$\mu\text{g/mL}$  anti- $\beta$  TCR and  $0.2 \mu\text{g/mL}$  anti-CD28 antibodies. Cells were cultured at a density of  $5 \times 10^5$  cells/well in RPMI medium and  $20 \text{ ng/mL}$  recombinant IL-2. After 4 days, non-adherent cells were collected, stained for CD4 and CD8, and analyzed by flow cytometry.

### ***In vitro* blockade of PD-L2 on alternatively activated macrophages**

Splenocytes from BALB/c mice were labeled with  $10 \mu\text{M}$  CFSE and were either cultured alone or with IL-4- ( $10 \text{ ng/mL}$ ) treated bone marrow-derived macrophages from BALB/c mice. Anti-PD-L2 (clone 122;  $5 \mu\text{g/mL}$ ) blocking antibody or isotype control antibody ( $5 \mu\text{g/mL}$ ) was added to the culture. After 4 days, non-adherent cells were collected, stained for CD4 and CD8, and analyzed by flow cytometry.

### **Co-culture with retrovirally transfected macrophages**

Stat6<sup>-/-</sup> bone marrow-derived macrophages were retrovirally transfected as described in 3.2.3. GFP<sup>+</sup>, F4/80<sup>+</sup> macrophages were sorted and co-cultured with CFSE-labeled BALB/c splenocytes at a ratio of 1:3 as indicated in 3.1.5. Non-adherent cells were collected after 4 days, stained for CD4 and CD8, and analyzed by flow cytometry.

### **3.1.6 *In vivo* blockade of PD-L2**

4get/Thy1.1 mice received intraperitoneal injections of  $500 \mu\text{g}$  anti-mouse PD-L2 mAb (clone TY25, isotype rat IgG2a) or control rat IgG2a (clone 2A3) diluted in PBS on day 5 after *N. brasiliensis* infection, followed by  $250 \mu\text{g}$  on day 8.

### **3.1.7 Mixed bone marrow chimeras**

Bone marrow cells were prepared from tibia and femur of BALB/c/Ly5.1 and Stat6<sup>-/-</sup>/Ly5.2 mice or 4get/Thy1.1 and Stat6<sup>-/-</sup>/Thy1.2 mice, mixed at equal ratios, and washed in PBS. Recipient mice (BALB/c/Ly5.1 or 4get/Thy1.1) were lethally irradiated with two doses of  $550 \text{ rad}$  given 5 h apart followed by reconstitution with  $5 \times 10^6$  mixed bone marrow cells i.v. Mice were treated for 8 weeks with antibiotics in the drinking water ( $2 \text{ g/L}$  neomycin sulfate,  $100 \text{ mg/L}$  polymyxin B sulfate).

---

### 3.1.8 5-Bromo-2'-deoxyuridine (BrdU)-staining

1 mg 5-bromo-2'-deoxyuridine (BrdU) dissolved in 100  $\mu$ L PBS was injected intraperitoneally at 0, 12, 24, 36 hours before *N. brasiliensis*-infected mixed bone marrow chimeras were analyzed. Single-cell suspensions from total lung tissue, spleen, peritoneum and bronchoalveolar lavage (BAL) were stained for F4/80, CD11c or CD11b and Ly5.1 (CD45.1), and washed twice in PBS. Cells were resuspended in 0.15 M NaCl, fixed by adding dropwise  $-20^{\circ}\text{C}$  ethanol to a final concentration of 70% and incubated on ice for 30 min. After additional washing in PBS, cells were permeabilized with 1% paraformaldehyde and 0.01% Tween-20 in PBS for 30 min at  $20^{\circ}\text{C}$ , followed by 30 min at  $4^{\circ}\text{C}$ . Cells were washed in PBS and resuspended in 0.15 M NaCl and 4.2 mM  $\text{MgCl}_2$  (pH 5.0). Genomic DNA was fragmented by adding 50 Kunitz units of DNase I and incubated for 10 min at  $20^{\circ}\text{C}$ , followed by 30 min on ice and an additional washing step. Finally, cells were stained with FITC-labeled anti-BrdU antibody at  $20^{\circ}\text{C}$  for 30 min. Cells were washed and analyzed by flow cytometry. Macrophages were identified as described above.

### 3.1.9 Immunohistochemistry

To prepare lungs for microscopy, a small incision in the trachea of BALB/c and *Stat6*<sup>-/-</sup> mice, which had been infected with *N. brasiliensis* 13 days before, was made to allow a passage of a 20-gauge needle (Introcan) into the trachea. A 1 mL syringe was placed at the end of the needle which had been loaded with an equal mixture of PBS and tissue freezing medium. The lungs were removed, washed once in PBS and were then transferred into tissue freezing medium to form a tissue-cryomedium-block. Lungs were frozen in liquid nitrogen and stored at  $-80^{\circ}\text{C}$ .

For immunohistochemistry analysis the lung-cryomedium-block was fixed in the object holder of a cryostat and sections (6  $\mu\text{m}$  thick) were cut and stretched on the surface of a SuperFrost Plus Gold glass slide. The cryostat sections were fixed in  $-20^{\circ}\text{C}$  cold acetone for 10 min at  $-20^{\circ}\text{C}$  and were air-dried for 30 min. Each lung section was surrounded with a fat pen to create a hydrophobic border that allows the aqueous reagent solution to stay on the tissue section. The tissue was treated with 100  $\mu\text{L}$  1% mouse serum, 1% rat serum and

---

2.5% 2.4G2 Fc-block diluted in 0.1 M Tris buffer (pH 7.5) for 30 min. Sections were washed for 10 min in 0.1 M Tris buffer (pH 7.5) and were blocked with 2 drops of streptavidin blocking kit for 20 min. After additional washing in Tris buffer, 2 drops of biotin blocking kit were added for 20 min. The tissues were washed and stained with 100  $\mu$ L biotinylated anti-PD-L2 (clone TY25) or purified rabbit anti-mouse Ym1 diluted in 0.1 M Tris buffer (pH 7.5) supplemented with 1% mouse and rat serum. After incubation of 1 h sections were washed and the Ym1 stained tissue was incubated for 45 min with a biotinylated goat anti-rabbit IgG secondary antibody. For detection avidin-horseradish peroxidase or avidin-horseradish phosphatase were used, which had been prepared according to the manufacturer's instructions 30 min before, in 0.1 M Tris buffer (pH 7.5) at room temperature. Sections were incubated for 30 min and washed in Tris buffer. The peroxidase or phosphatase substrates were diluted in 0.1 M Tris buffer pH 8.4 according to the manufacturer's instructions and sections were incubated with the related substrate in the dark for 20-30 min. Sections were washed in water and the nuclei were stained with hematoxylin solution for 30-60 sec followed by an additional washing step in water. Slides were covered with a drop of pre-warmed (50°C) Kaiser's glycerol gelatin and sealed with a coverslip. Pictures were acquired on a Leitz Laborlux O microscope equipped with an Olympus E330 camera. Original magnification of the objective was 40x.

## **3.2 Molecular biology methods**

### **3.2.1 RNA isolation and polymerase chain reaction (PCR)**

#### **RNA Isolation**

Total cellular RNA was isolated from sorted macrophages.

RNA for microarray analysis was isolated using the Fluka Isolation kit. Sorted macrophages were resuspended in 300  $\mu$ L solution D (100  $\mu$ L  $\beta$ -mercaptoethanol + 14 mL denaturing solution). 30  $\mu$ L of 2 M sodium acetate solution was added and samples were mixed thoroughly by inversion, followed by direct application of 300  $\mu$ L water-saturated phenol and 50  $\mu$ L chloroform:isoamylalcohol mixture. Samples were shaken vigorously for 10 sec and the suspension was incubated for 15 min before centrifugation (14000 rpm,

20 min, 4°C). RNA was present in the upper aqueous layer, which was transferred to a fresh tube. An equal volume of isopropanol was added, mixed and RNA was precipitated by placing the sample at -80°C for at least 1 h. After precipitation samples were centrifuged (14000 rpm, 20 min, 4°C) and the supernatant was discarded. The RNA pellet was dissolved in 300 µL solution D and 300 µL isopropanol and precipitated for at least 1 h at -80°C. Samples were centrifuged (14000 rpm, 20 min, 4°C), supernatant was removed and the RNA pellet was washed in 1 mL 70% pre-cooled ethanol followed by centrifugation (14000 rpm, 20 min, 4°C). The supernatant was carefully removed and the RNA was air-dried until the pellet turned transparent. Pellets were resuspended in 20 µL DEPC-H<sub>2</sub>O and the RNA concentration and purity (A260:A280 ratio) was determined by photometric analysis.

RNA for quantitative RT-PCR was isolated using the RNeasy Mini Kit according to the manufacturer's recommendations. Briefly, sorted macrophages were resuspended in 350 µL RLT buffer, mixed with 350 µL 70% ethanol and applied to the RNeasy columns. After 3 centrifugation steps (10000 rpm, 15 sec) with one application of 350 µL of RW1 buffer and two applications of 500 µL RPE buffer, samples were centrifuged again (14000 rpm, 1 min) followed by the addition of 50 µL RNase-free H<sub>2</sub>O and centrifugation (10000 rpm, 1 min). The RNA concentration and purity (A260:A280 ratio) was determined by photometric analysis.

### **Reverse transcription (RT)**

For first-strand cDNA synthesis 2 µg total RNA was adjusted to 11 µL with DEPC-H<sub>2</sub>O and was incubated for 10 min at 72°C with 1 µL oligo(dT). 7 µL of a solution containing 4 µL 5x buffer, 2 µL 0.1 M DTT and 1 µL 10 mM dNTP was mixed with the sample and 1 µL Superscript II reverse transcriptase was added. For cDNA synthesis, samples were incubated for at least 50 min at 42°C followed by 15 min at 72°C. 80 µL DEPC-H<sub>2</sub>O was added and samples were stored at -80°C.

### **Quantitative real-time RT-PCR**

Alternative activation markers were analyzed using the LightCycler system. PCR amplification was performed in 20 µL volume containing 1 mM forward and reverse

primers, 5  $\mu$ L H<sub>2</sub>O, 3  $\mu$ L cDNA and 10  $\mu$ L of the DyNAmo Cappillary Master Mix under the following conditions: 30 sec denaturation at 94°C, 30 sec annealing of primers at 56°C and 60 sec elongation at 72°C, for 40 cycles. Expression of  $\beta$ -actin was used for normalization. Primer sequences are listed in 2.5.

### **3.2.2 Microarrays**

Gene expression profiling was performed on Affymetrix Mouse Gene ST 1.0 high-density oligonucleotide arrays in collaboration with Dr. Reinhard Hoffmann, Institute for Medical Microbiology, Immunology & Hygiene at the Technical University Munich. Total cellular RNA was isolated from sorted macrophages using a RNA isolation kit as described in 3.2.1, labeled, fragmented, and hybridized to the arrays according to the manufacturer's recommendations. Raw data analysis was performed with Affymetrix Expression Console software, using RMA-sketch for normalization as implemented. Data were exported to Microsoft Excel for differential gene expression analysis. Microarray data have been submitted to the GEO database and have the accession number GSE20030.

### **3.2.3 Retroviral transduction of macrophages**

#### **Transformation of plasmid DNA into bacteria**

The retroviral vector encoding murine PD-L2 was kindly provided by H. Kuipers [98]. This vector contains an *internal ribosomal entry site* (IRES) which allows the simultaneous expression of PD-L2 and the green fluorescence protein (GFP) (Figure 6). 3  $\mu$ L of DNA was incubated with competent *Escherichia coli* bacteria on ice for 20 min, followed by incubation in a 42°C water bath for 30 sec and on ice for 1 min. S.O.C. medium was added to the transformed bacteria sample, mixed carefully and incubated at 37°C for 30 min. After incubation the bacteria were plated on LB-Agar plates supplemented with ampicillin (100  $\mu$ g/mL) in the appropriate dilution and incubated at 37°C overnight.

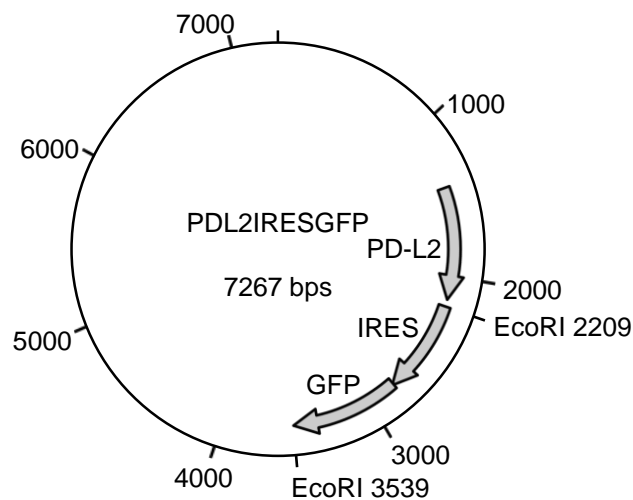


**Figure 6: Schematic of the PD-L2 IRES GFP vector used for the transduction of PD-L2 into macrophages.**

Arrows indicate coding regions for the plasmid. Numbers give the position of the corresponding cDNA in the plasmid and the insert size achieved by digestion with the restriction enzyme EcoRI.

### Plasmid DNA mini preparation

A single bacterial colony per round-bottom tube was picked the next day and used to inoculate a starter culture of 3 mL LB-Medium containing ampicillin (100 µg/mL). The starter culture was incubated overnight at 37°C with vigorous shaking (approximately 300 rpm).

Plasmid DNA mini preparation was performed using a Qiagen kit according to the manufacturer's instructions. 1.2 mL of bacteria were transferred to a 2 mL tube and centrifuged (14000 rpm, 2 min) at room temperature. The supernatant was decanted and the pellet was resuspended with 250 µL buffer P1. 250 µL buffer P2 were added to the sample and mixed by inverting the tube followed by 350 µL buffer N3 and centrifugation (13000 rpm, 10 min). The supernatant was applied to the spin column and was centrifuged (13000 rpm, 30-60 sec). The flow-through was discarded and the spin column was washed by adding 750 µL buffer PE followed by centrifugation (13000 rpm, 30-60 sec). The flow-through was discarded and the spin column centrifuged again before the DNA was eluted from the column with 50 µL 10 mM TrisCl, pH 8.5 and stored at -20°C for further analysis.

**Plasmid DNA maxi preparation**

100 mL LB-Medium supplemented with ampicillin (100 µg/mL) was inoculated with 100 µL of the starter culture. The culture was grown at 37°C 12-16 h in an Erlenmeyer flask with vigorous shaking (approximately 300 rpm). The bacterial cells were then harvested by centrifugation (Sorvall Superspeed; 8000 rpm, 15 min, 4°C) and the pellet was resuspended in 10 mL buffer P1 until no clumps remained. Following resuspension, 10 mL buffer P2 were added, mixed thoroughly by vigorously inverting the tube and incubated at room temperature for 5 min. 10 mL of buffer P3 were added to the lysate and mixed immediately by vigorously inverting followed by centrifugation (13000 rpm, 30 min, 4°C). During the centrifugation the Qiagen-tip 500 was equilibrated by applying 10 mL buffer QBT. The supernatant was applied to the Qiagen-tip and allowed to enter the resin by gravity flow. The Qiagen-tip was washed with 2 x 30 mL buffer QC followed by DNA elution with 15 mL buffer QF. DNA was precipitated by adding 10.5 mL isopropanol to the eluted DNA. The mixture was centrifuged immediately (11000 rpm, 30 min, 4°C) and the supernatant was decanted carefully. After an additional washing step in 5 mL 70% ethanol and centrifugation (11000 rpm, 10 min, 4°C), the obtained pellet was air-dried for 5-10 min and re-dissolved in 250 µL 10 mM TrisCl, pH 8.5. The plasmid DNA was stored at -20°C.

**Restriction analysis of plasmid DNA**

The PD-L2-IRES-GFP plasmid recovered from bacteria was controlled for insert size by digestion with the restriction enzyme EcoRI. Restriction analysis was performed using 2 µL buffer 2, 1 µL restriction enzyme and 1 µg DNA adjusted with H<sub>2</sub>O to a volume of 20 µL followed by incubation for 2 h at 37°C. The digested products were visualized on an agarose gel.

**Insert PCR**

PD-L2 positive clones were confirmed by insert PCR. PCR amplification was performed in 20 µL volume containing 2 µL 10x PCR-buffer, 1 µL 20 mM forward and reverse primers, 0.7 µL dNTPs, 0.25 µL Taq-polymerase, 12.05 µL H<sub>2</sub>O and 3 µL plasmid DNA under the following conditions: 30 sec denaturation at 94°C, 30 sec annealing of primers at 56°C and 60 sec elongation at 72°C, 38 cycles. PD-L2 primer sequences are listed in 2.5.

---

**DNA electrophoresis**

A 1.5% agarose gel was prepared with 1x TAE buffer and 0.3 µg/mL ethidium bromide. 20 µL digested DNA was mixed with loading dye and loaded onto the gel. Running conditions were 45 min at 110 volts.

**Generation of PD-L2 encoding retrovirus vector particles**

Phoenix E cells were used as the packaging cell line to generate retroviral particles encoding cDNAs of interest. The retroviral vector with the desired coding sequence was transiently introduced, together with the packaging vector, into the Phoenix E cells by calcium phosphate precipitation. Phoenix E cells were seeded ( $5 \times 10^6$  cells per 75 cm<sup>2</sup> flask) in DMEM medium and cultured overnight at 37°C and 5% CO<sub>2</sub>. The next day, cells were adherent and formed a 70% confluent layer. 5 min prior to transfection, the medium was removed from the cells and replaced with 8 mL DMEM medium supplemented with 16 µL 12.5 mM chloroquine diphosphate salt. Cells were again incubated. Plasmid DNA solution was prepared as followed; 20 µg plasmid DNA (PD-L2-IRES-GFP or PMXpie-IRES-GFP), 5 µg pCL-eco packaging vector and 920 µL CaCl<sub>2</sub> were added to a 15 mL tube containing H<sub>2</sub>O to a final volume of 1 mL. 1 mL 2x BES/PO<sub>4</sub> solution was added to the plasmid DNA solution and bubbled vigorously for 15-20 sec with an automatic pipettor. 2 mL of the transfection solution was added drop-wise to the media of the Phoenix E cells. After 24 h, the transfection medium was replaced with 5 mL fresh RPMI medium and the cells were incubated for another 24 h. The supernatant containing retrovirus vector particles was collected and stored at -80°C (Figure 7).

**Retroviral transduction of Stat6<sup>-/-</sup> bone marrow-derived macrophages**

Bone marrow cells from Stat6<sup>-/-</sup> mice were seeded at  $1 \times 10^6$  cells/mL in a 24 well plate and cultured in RPMI medium in the presence of L929 supernatant at 37°C and 5% CO<sub>2</sub>. Two days later 500 µL medium were replaced with retroviral supernatant containing 2 µg/mL polybrene (Figure 7). Cells were transduced by spin infection at 2450 rpm, 2 h, 32°C followed by incubation for 2 h at 37°C, 5% CO<sub>2</sub>. After retroviral transduction, medium was removed and 1 mL fresh RPMI medium supplemented with L929 supernatant was added. Transduced bone marrow cells were cultured for 7 days before GFP<sup>+</sup>F4/80<sup>+</sup> cells were sorted.



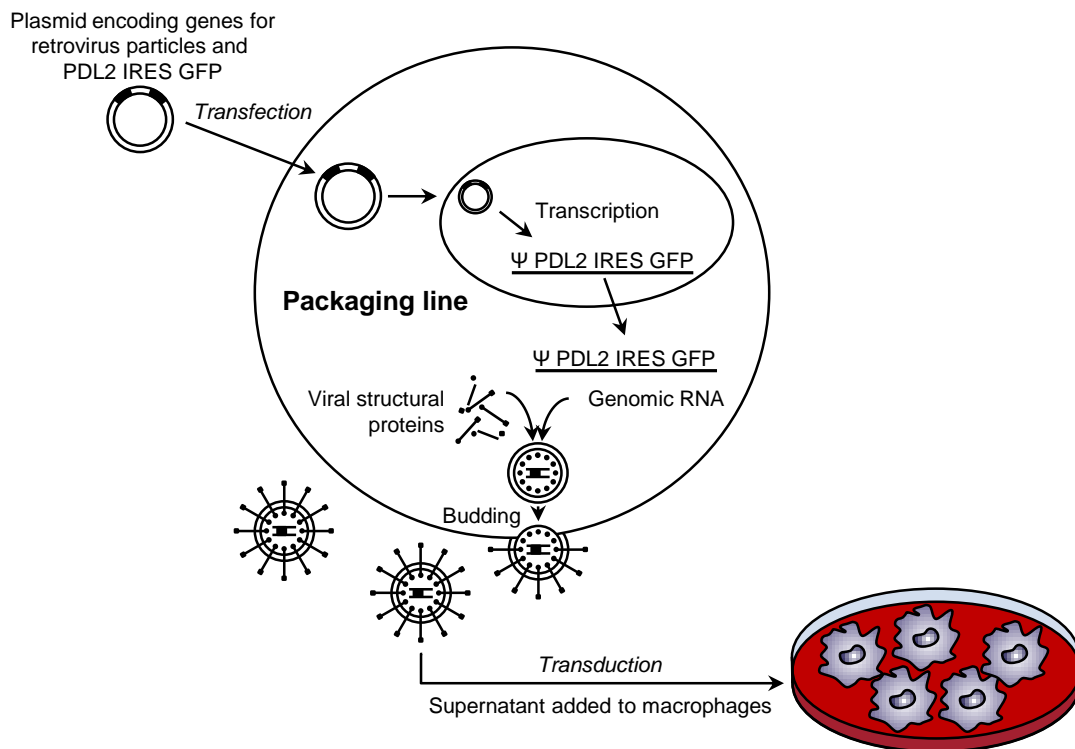


**Figure 7: Transfection of Phoenix E cells for virus production and transduction of macrophages.**

A vector encoding PD-L2 and a vector encoding the retrovirus genes pCL-eco were introduced via calcium phosphate transfection into the packaging line Phoenix E cells. The viral transcript contains the packaging sequence  $\Psi$ , which is recognized by the capsid proteins and allows it to be packaged into viral particles. A fully infectious viral particle containing the PD-L2 vector is budded from the packaging cell. The culture supernatant is removed from the cells and used as the source of virus for transduction of macrophages. Modified from [99].

### 3.3 Statistics

P-values were calculated by Student's t test using SigmaPlot software.

---

## 4 RESULTS

### 4.1 The inhibitory effect of AAM on T cell proliferation

#### 4.1.1 IL-4-exposed macrophages suppress T cell proliferation in a Stat6-dependent manner

Cells of the mononuclear phagocyte system develop from precursors in the bone marrow. When cultured in the presence of the growth factor M-CSF bone marrow cells differentiate into a population of adherent macrophages. We cultured bone marrow cells from wild type mice for seven days in the presence of 10% supernatant from the M-CSF producing fibroblast cell line L929. Bone marrow-derived macrophages (BMDM) highly up-regulated surface expression of the macrophage specific antigen F4/80 (Figure 8). Surface F4/80 on mouse macrophages is a useful marker to define macrophages *in vitro*. We achieved > 95% purity of F4/80<sup>+</sup> macrophages differentiated from the bone marrow.

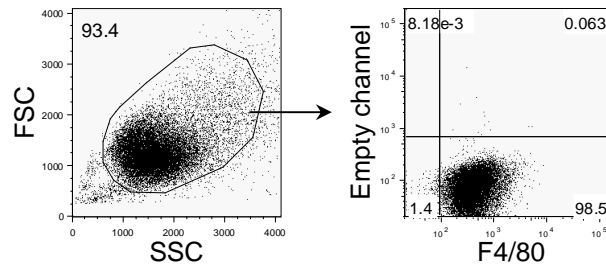


**Figure 8: Surface expression of F4/80 on bone marrow-derived macrophages.**

Macrophages were differentiated from wild type bone marrow cells in RPMI medium for seven days in the presence of 10% supernatant from the M-CSF producing fibroblast cell line L929. After removal of non-adherent cells, macrophages were detached from Petri dishes, stained for F4/80 and analyzed by flow cytometry. Dot plots shown are an example of the gating strategy for F4/80<sup>+</sup> bone marrow-derived macrophages (purity > 90%).

The macrophage phenotype can be directed by additional stimuli to fulfill specific functional roles during inflammation. Macrophages undergo alternative activation in the presence of IL-4 or IL-13 and acquire an inhibitory activity against T cells. Since the signaling pathway shared by IL-4 and IL-13 can activate Stat6 phosphorylation and other pathways, including the MAPK/ERK or PI3K pathway, we determined the requirement of Stat6 for the anti-inflammatory activity of AAM. Macrophages were differentiated from

the bone marrow of wild type or Stat6-deficient (Stat6<sup>-/-</sup>) mice and were pre-cultured for 24 hours in the presence or absence (control) of IL-4. IL-4-treated or control macrophages were then cultured with CFSE-labeled splenocytes from naïve wild type mice on anti-TCR/anti-CD28 monoclonal antibody (mAb) coated plates. Non-adherent cells were collected after four days and analyzed by flow cytometry. Lymphocytes were selected based on the light scatter characteristics of T cells (forward scatter; FSC and side scatter; SSC) (Figure 9 left). Staining with anti-CD4 and anti-CD8 antibodies distinguished both T cell subtypes. Then CD4<sup>+</sup> and CD8<sup>+</sup> T cells were gated for analysis of the CFSE proliferation profile (Figure 9). When control wild type macrophages were cultured with splenocytes at a ratio of 1:3 (macrophage:splenocyte), we observed 49.8% proliferation of CD4<sup>+</sup> and 94% proliferation of CD8<sup>+</sup> T cells (Figure 9, Figure 10A). T cells exhibited equal levels of proliferation in the presence of control Stat6<sup>-/-</sup> macrophages. Proliferation of T cells co-cultured with wild type or Stat6<sup>-/-</sup> macrophages was comparable to the proliferation of T cells cultured alone (T cells only, Figure 10A).

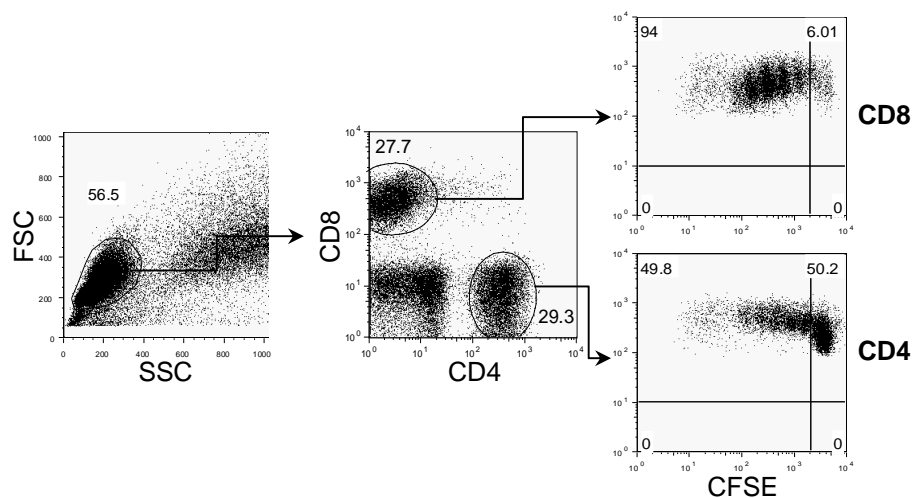


**Figure 9: T cell proliferation in the presence of control wild type bone marrow-derived macrophages.** CFSE-labeled wild type (WT) splenocytes were stimulated with plate-bound anti-TCR/anti-CD28 mAb and were co-cultured with BMDM from WT mice at a ratio of 1:3 (BMDM:splenocyte). Cells were collected after four days, stained for CD4 and CD8 and analyzed by flow cytometry. Dot plots show a representative gating strategy for the analysis of CD4<sup>+</sup> and CD8<sup>+</sup> T cell proliferation.

In contrast, IL-4-exposed macrophages from wild type but not from Stat6<sup>-/-</sup> mice markedly suppressed proliferation of CD4<sup>+</sup> and CD8<sup>+</sup> T cells. Especially at a macrophage:splenocyte ratio of 1:3, we detected highly significant inhibition of CD4<sup>+</sup> and CD8<sup>+</sup> T cell proliferation mediated by IL-4-exposed wild type macrophages ( $p < 0.001$ ; Figure 10A, B).

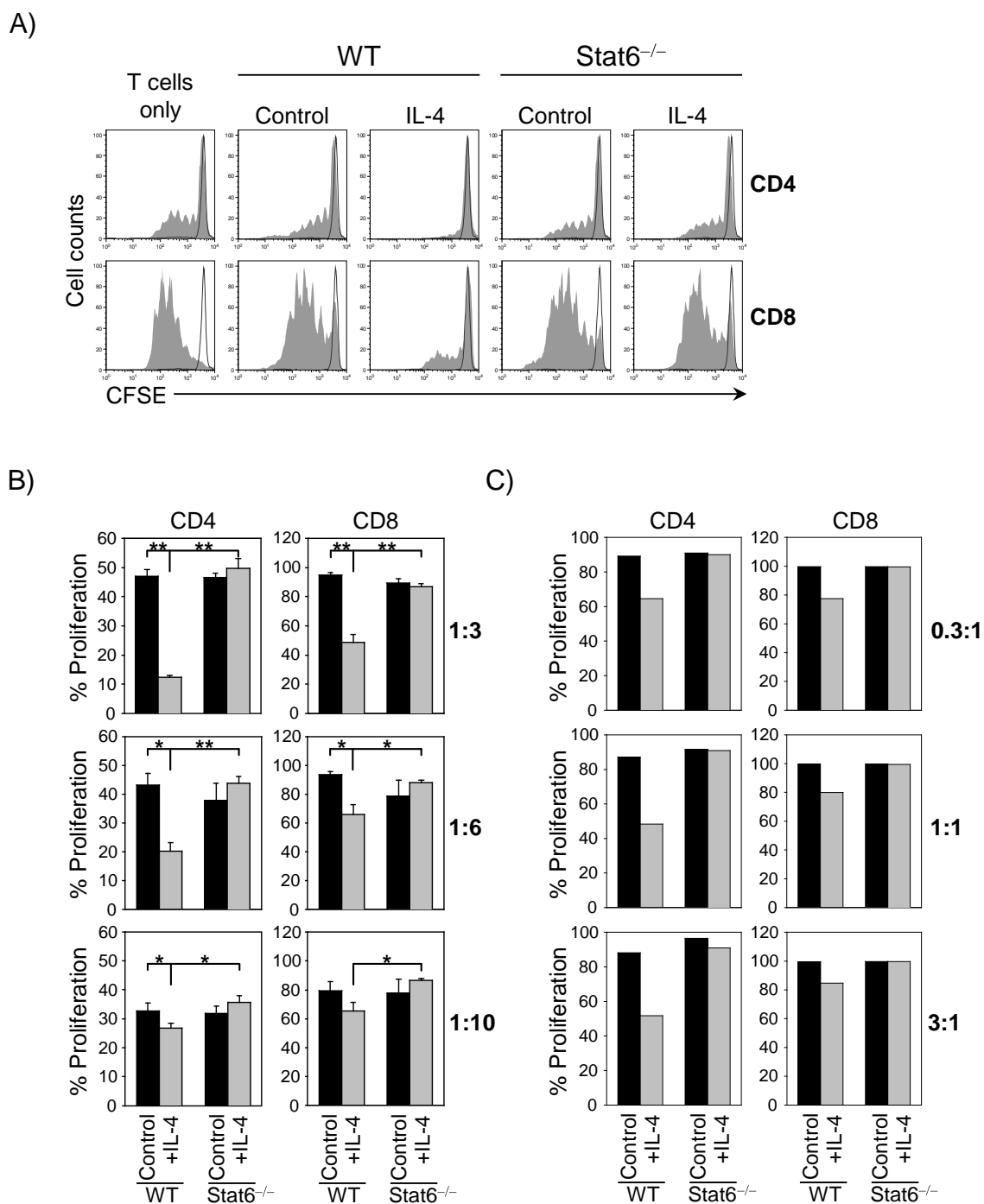


**Figure 10: Suppression of T cell proliferation by IL-4-exposed macrophages.**

**A)** CFSE-labeled wild type (WT) splenocytes were left untreated (black line) or stimulated with plate-bound anti-TCR/anti-CD28 mAb (filled) and either cultured alone (T cells only) or co-cultured with control or IL-4 (10 ng/mL) BMDM from WT or Stat6<sup>-/-</sup> mice at ratio of 1:3 (BMDM:splenocyte). Cells were collected after four days, stained for CD4 and CD8 and analyzed by flow cytometry. Histograms show the CFSE profiles of gated CD4<sup>+</sup> and CD8<sup>+</sup> T cells. **B)** CFSE-labeled WT splenocytes were cultured with untreated BMDM (black bars) or IL-4-treated BMDM (grey bars) from WT or Stat6<sup>-/-</sup> mice at ratios of 1:3, 1:6 and 1:10 (BMDM:splenocyte). Bars show means + SD from three separate cultures per condition (\*\*  $P < 0.001$ , \*  $P < 0.05$ ). **C)** CFSE-labeled WT splenocytes were cultured with untreated BMDM (black bars) or IL-4-treated BMDM (grey bars) from WT or Stat6<sup>-/-</sup> mice at ratios of 0.3:1, 1:1 and 3:1 (BMDM:splenocyte). Bars show means of two independent experiments.

The suppressive activity of IL-4-treated wild type macrophages on T cell proliferation was observed in cultures with increased numbers of T cells (macrophage:splenocyte ratio 1:3, 1:6, 1:10) (Figure 10A, B) and in cultures with constant T cell numbers (macrophage:splenocyte ratio 0.3:1, 1:1, 3:1) (Figure 10C). This result indicates that AAM inhibit T cell proliferation in a Stat6-dependent manner.

#### 4.1.2 T cell suppression is dependent on cell-cell contact

To further address whether AAM act directly on T cells to modulate T cell proliferation or whether this effect is mediated by soluble factors, we stimulated T cells in the presence of supernatants from Stat6<sup>-/-</sup> or wild type macrophages. BMDM from Stat6<sup>-/-</sup> or wild type mice were cultured for 24 hours in the presence or absence (control) of IL-4 and supernatants were collected. Supernatants were then incubated with CFSE-labeled splenocytes from naïve wild type mice which were stimulated with plate-bound anti-TCR/anti-CD28 mAb. Non-adherent cells were collected after four days, stained for CD4 and CD8 and were analyzed by flow cytometry. No inhibition of T cell activation could be detected following incubation with supernatants from control or IL-4-exposed Stat6<sup>-/-</sup> or wild type macrophages (Figure 11).

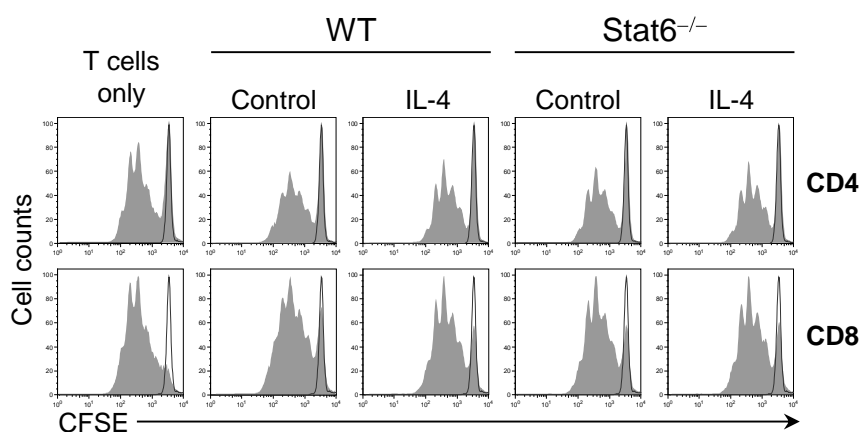


**Figure 11: Cell-cell contact-dependent T cell suppression by IL-4-exposed macrophages.**

Supernatants of untreated (control) or IL-4-treated WT and Stat6<sup>-/-</sup> BMDM were collected and added to CFSE-labeled WT splenocytes which were left untreated (black line) or were stimulated with plate-bound anti-TCR/anti-CD28 mAb (filled). “T cells only” indicates cultures without addition of supernatant. The data are representative of three independent experiments.

T cell proliferation from all culture conditions was comparable to cultures without addition of supernatant (T cells only, Figure 11). This result demonstrates that AAM-mediated suppression of T cell proliferation requires expression of Stat6 in macrophages and depends on cell-cell contact.

## 4.2 PD-L2 expression on AAM

### 4.2.1 PD-L2 is expressed on AAM in a Stat6-dependent manner

The activity of T cells can be regulated by a number of inhibitory receptors including CTLA-4 and PD-1. A gene expression profiling approach was used to identify expression of potential inhibitory ligands for these receptors on AAM which could be involved in mediating T cell inhibition. Macrophages were differentiated from Stat6<sup>-/-</sup> or wild type bone marrow cells and treated with or without IL-4 for 24 hours. Macrophages were stained for F4/80 and F4/80<sup>+</sup> cells were sorted. Figure 12 shows purity > 99% of sorted F4/80<sup>+</sup> wild type macrophages. Similar purity was obtained for Stat6<sup>-/-</sup> macrophages (data not shown).

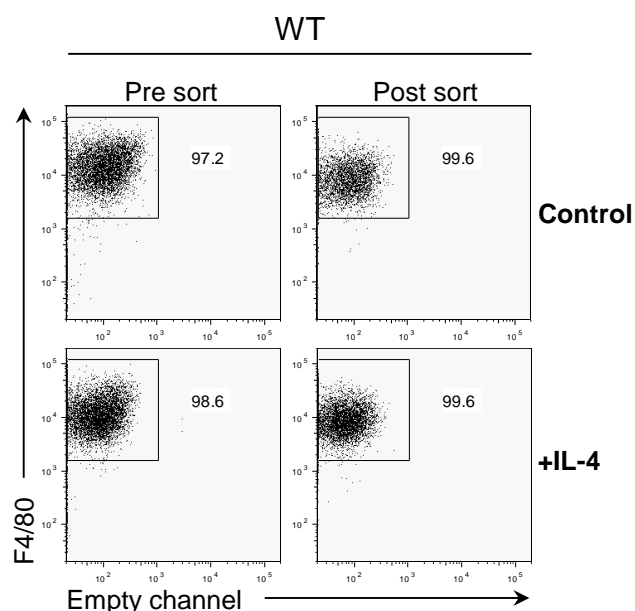


**Figure 12: High purity of control or IL-4-treated BMDM.**

BMDM were either left untreated (control) or were stimulated for 24 hours with IL-4 (10 ng/mL). After removal of non-adherent cells, macrophages were detached from Petri dishes and stained for F4/80. F4/80<sup>+</sup> cells were sorted with purity > 99% and RNA was isolated for microarray analysis. The experiment was repeated with similar results for Stat6<sup>-/-</sup> bone marrow-derived macrophages.

Sorted BMDM were analyzed using high-density oligonucleotide arrays. Direct comparison of macrophages from wild type and *Stat6*<sup>-/-</sup> mice before IL-4 treatment revealed that 17 genes showed > 3-fold higher expression and 13 genes showed > 3-fold lower expression in wild type as compared to *Stat6*<sup>-/-</sup> macrophages (Figure 13). The gene encoding for *Stat6* was 6.9-fold up-regulated. There were no major differences detectable in gene expression of IL-4-treated *Stat6*<sup>-/-</sup> macrophages compared to untreated control *Stat6*<sup>-/-</sup> macrophages (Figure 13).

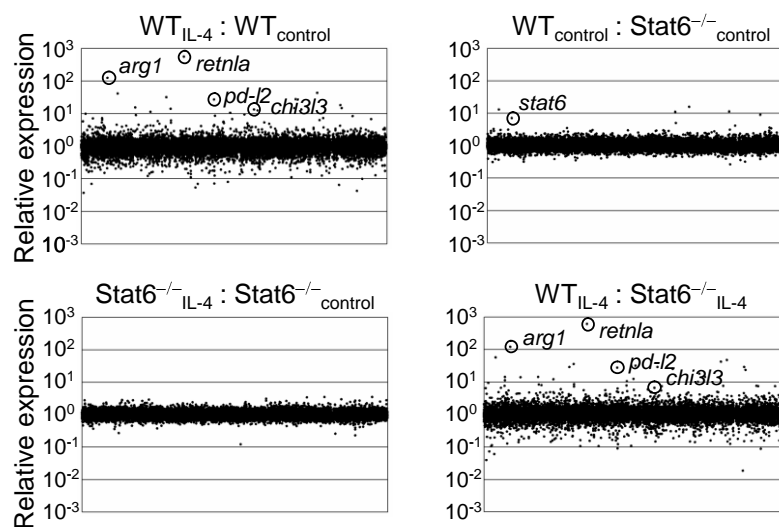


**Figure 13: Stat6-regulated gene expression profile of macrophages.**

RNA was isolated from sorted (purity 99%) untreated (control) or IL-4-(10 ng/mL) treated WT and *Stat6*<sup>-/-</sup> F4/80<sup>+</sup> BMDM. Gene expression profiling was performed on high-density oligonucleotide arrays (Affymetrix).

Wild type macrophages exposed to IL-4 exhibited 394 genes that were > 3-fold repressed in comparison to control wild type macrophages. 53% of the down-regulated genes were controlled by *Stat6*. Among the *Stat6*-dependent down-regulated genes were genes encoding for proteins with typical functions of classical activated macrophages. These include the IFN-responsive chemokine CXCL10 (9-fold down-regulated), TLR2 (7.7-fold down-regulated) and the integrins alpha 4 (*Itga4*; 6.7-fold down-regulated) and alpha9 (*Itga9*; 11.1-fold down-regulated), both important for mediating cell adhesion. The low affinity Fc gamma receptor IV (*FcγRIV*) was 6-fold down-regulated and activated *FcγRIV* is important in promoting macrophage-mediated phagocytosis and the production of pro-inflammatory cytokines (Table 19) [100]. IL-4 treatment of wild type macrophages showed

113 genes that were > 3-fold induced in comparison to control wild type macrophages. 79% of the up-regulated genes were controlled by Stat6, which include genes encoding for proteins like lectins, chemokines, amino acid transporter and proteins involved in lipid metabolism (Table 19). Among these were the enzymes squalene epoxidase (*Sqle*; 6.1-fold up-regulated) and stearoyl-coenzyme A desaturase 2 (*Scd2*; 8.4-fold up-regulated). *Sqle* plays a key role in the biosynthesis of sterol, whereas *Scd2* is involved in the induction of PPAR- $\gamma$ , which is required for the maintenance of AAM [61]. We further observed the up-regulation of genes which are typical signature genes for AAM like *retnla* (558-fold up-regulated, encodes for Relm- $\alpha$ /Fizz1), *arg1* (124-fold up-regulated, encodes for arginase1) and *chi3l3* (13-fold up-regulated, encodes for Ym1) (Table 19, Figure 13; WT<sub>IL-4</sub> : WT<sub>control</sub>). Expression of these genes was Stat6-dependent and confirms previous reports (Table 19, Figure 13; WT<sub>IL-4</sub>: Stat6<sup>-/-</sup> IL-4) [65, 66]. Interestingly, *pd-l2*, an inhibitory ligand for PD-1, was strongly (27-fold) induced by IL-4 in a Stat6-dependent manner in AAM (Table 19, Figure 13; WT<sub>IL-4</sub>: Stat6<sup>-/-</sup> IL-4).

We performed quantitative RT-PCR analysis to verify the Stat6-dependent expression of the AAM markers *retnla*, *arg1*, *chi3l3* and expression of *pd-l2* as a potential inhibitory ligand (Figure 14). IL-4-exposed wild type macrophages showed 2-4-fold higher expression levels of the AAM markers *retnla*, *arg1*, *chi3l3* and also 2-fold higher expression level of *pd-l2* compared to control wild type or Stat6<sup>-/-</sup> macrophages treated with or without IL-4. These quantitative RT-PCR results confirmed the microarray data.

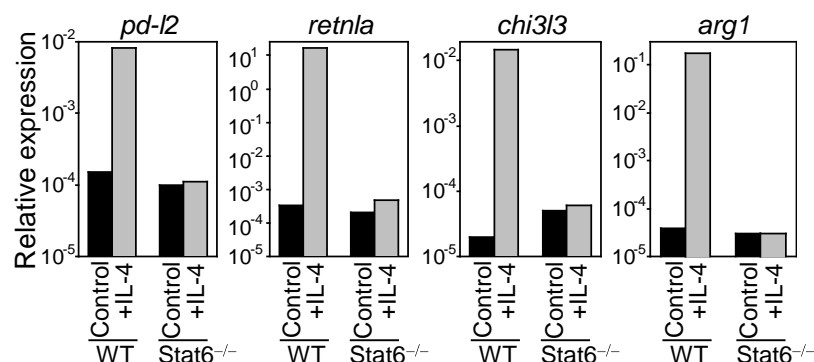


**Figure 14: Quantitative RT-PCR analysis of selected genes based on the microarray analysis.** Selected genes from the microarray experiment that appeared differently expressed in untreated (black bars) or IL-4-treated (grey bars) WT and Stat6<sup>-/-</sup> BMDM were analyzed by quantitative RT-PCR. Samples were normalized to  $\beta$ -actin expression.



**Table 19: Gene expression analysis of control and IL-4-treated BMDM.**

RNA was isolated from sorted untreated (control) or IL-4 (10 ng/mL) treated WT and Stat6<sup>-/-</sup> F4/80<sup>+</sup> BMDM. Gene expression profiling was performed on high-density oligonucleotide arrays. Shown are **A)** IL-4-induced genes (> 6-fold up-regulated) and **B)** IL-4-repressed genes (> 6-fold down-regulated) of WT<sub>IL-4</sub>: WT<sub>Control</sub> BMDM which are expressed in a Stat6-dependent fashion.

**A) IL-4-induced genes**

Gene name	Gene Accession number	Gene expression		Description
		WT <sub>IL-4</sub> : WT <sub>Control</sub>	WT <sub>IL-4</sub> : Stat6 <sup>-/-</sup> <sub>IL-4</sub>	
<i>Retnla</i>	NM_020509	558.049	608.343	Resistin like alpha (Fizz1/Relm $\alpha$ )
<i>Arg1</i>	NM_007482	124.191	119.962	Arginase1
<i>IL-4i1</i>	NM_010215	42.576	41.983	Interleukin 4 induced 1
<i>Mgl2</i>	NM_145137	41.395	13.742	Macrophage galactose N-acetyl-galactosamine specific lectin 2
<i>Ear11</i>	NM_053113	31.593	28.787	Eosinophil-associated ribonuclease A family member 11
<i>Flt1</i>	NM_010228	27.218	17.945	FMS-like tyrosine kinase 1
<i>Pdcd1lg2</i>	NM_021396	27.036	27.457	Programmed cell death 1 ligand 2 (PD-L2)
<i>F10</i>	NM_007972	18.021	28.612	Coagulation factor X
<i>Ccl24</i>	NM_019577	14.678	10.022	Chemokine (C-C motif) ligand 24
<i>Slc7a2</i>	NM_007514	14.625	23.206	Solute carrier family 7
<i>Tm7sf</i>	NM_029422	13.967	35.932	Transmembrane 7 superfamily member 4 (DC-STAMP)
<i>Bhlhb2</i>	NM_011498	13.195	14.292	Basic helix-loop-helix domain containing, class B2
<i>Slc7a11</i>	NM_011990	13.178	28.694	Solute carrier family 7 member 11
<i>Chi3l3</i>	NM_009892	12.350	5.472	Chitinase 3-like 3 (Ym1)
<i>Ankrd55</i>	NM_029898	11.141	12.094	Ankyrin repeat domain 55
<i>Cst7</i>	NM_009977	10.504	12.482	Cystatin F (leukocystatin)
<i>Gpc1</i>	NM_016696	9.726	9.337	Glypican 1
<i>Mboat2</i>	NM_026037	8.888	8.267	Membrane bound O-acyltransferase domain containing 2
<i>Scd2</i>	NM_009128	8.413	4.801	Stearoyl-Coenzyme A desaturase 2
<i>Nqo1</i>	NM_008706	8.190	7.484	NAD(P)H dehydrogenase, quinone 1
<i>Tmem26</i>	NM_177794	7.273	11.262	Transmembrane protein 26
<i>Itgax</i>	NM_021334	7.159	47.223	Integrin alpha X
<i>Fn1</i>	NM_010233	6.989	56.484	Fibronectin 1
<i>Mmp9</i>	NM_013599	6.642	31.308	Matrix metalloproteinase 9
<i>Lrrc32</i>	NM_001113379	6.275	7.593	Leucine rich repeat containing 32
<i>Sqle</i>	NM_009270	6.119	7.262	Squalene epoxidase

## B) IL-4-repressed genes

Gene name	Gene Accession number	Gene expression		Description
		WT <sub>IL-4</sub> : WT <sub>Control</sub>	WT <sub>IL-4</sub> : Stat6 <sup>-/-</sup> <sub>IL-4</sub>	
<i>Wwp1</i>	NM_177327	0.164	0.185	WW domain containing E3 ubiquitin protein ligase 1
<i>Rcbtb2</i>	NM_134083	0.163	0.238	Regulator of chromosome condensation (RCC1) and BTB (POZ) domain containing protein 2
<i>F13a1</i>	NM_028784	0.161	0.187	Coagulation factor XIII, A1 subunit
<i>Fcgr4</i>	NM_144559	0.160	0.106	Fc receptor, IgG, low affinity IV
<i>Gpr162</i>	NM_013533	0.157	0.248	G protein-coupled receptor 162
<i>Cd93</i>	NM_010740	0.156	0.198	CD93 antigen
<i>Gpr141</i>	NM_181754	0.155	0.173	G protein-coupled receptor 141
<i>Itga4</i>	NM_010576	0.151	0.228	Integrin alpha 4
<i>Hal</i>	NM_010401	0.150	0.139	Histidine ammonia lyase
<i>Cd14</i>	NM_009841	0.150	0.165	CD14 antigen
<i>Siglece</i>	NM_031181	0.148	–	Sialic acid binding Ig-like lectin E
<i>Nfkbiz</i>	NM_030612	0.146	0.235	Nuclear factor of kappa light polypeptide gene enhancer in B-cells inhibitor, zeta
<i>Arrdc3</i>	NM_001042591	0.141	0.162	Arrestin domain containing 3
<i>Tlr2</i>	NM_011905	0.135	0.197	Toll-like receptor 2
<i>Pde3b</i>	NM_011055	0.125	0.228	Phosphodiesterase 3B, cGMP-inhibited
<i>Entpd1</i>	NM_009848	0.123	0.125	Ectonucleoside triphosphate diphosphohydrolase 1
<i>Rnf144b</i>	NM_146042	0.119	0.145	Ring finger protein 144B
<i>Cxcl10</i>	NM_021274	0.111	0.140	Chemokine (C-X-C motif) ligand 10
<i>Itga9</i>	NM_133721	0.097	0.243	Integrin alpha 9
<i>Thbs1</i>	NM_011580	0.079	0.112	Thrombospondin 1
<i>Ifit3</i>	NM_010501	0.070	0.104	Interferon-induced protein with tetratricopeptide repeats 3
<i>Fpr1</i>	NM_013521	0.069	0.189	Formyl peptide receptor 1
<i>Slc40a1</i>	NM_016917	0.068	0.071	Solute carrier family 40 (iron-regulated transporter), member 1
<i>Ifitm6</i>	NM_001033632	0.063	0.018	Interferon induced transmembrane protein 6
<i>Emr4</i>	NM_139138	0.053	0.108	EGF-like module containing, mucin-like, hormone receptor-like sequence 4
<i>Cd28</i>	NM_007642	0.036	0.039	CD28 antigen

#### 4.2.2 PD-L2 is the only B7 family member which is induced by IL-4 on macrophages in a Stat6-dependent manner

Since *pd-l2* gene expression in IL-4-treated wild type macrophages was up-regulated in the Microarray experiments, we were interested to examine whether PD-L2 is also expressed on the cell surface of macrophages. Macrophages were differentiated from bone marrow cells of wild type and Stat6<sup>-/-</sup> mice and either left untreated (control) or exposed to IL-4. BMDM were double stained for F4/80 and PD-L2 and analyzed by flow cytometry (Figure 15). No PD-L2 staining could be detected on control wild type or control Stat6<sup>-/-</sup> F4/80<sup>+</sup> macrophages. In contrast, IL-4-exposed macrophages from wild type but not from Stat6<sup>-/-</sup> mice strongly up-regulated surface PD-L2 expression (Figure 15).

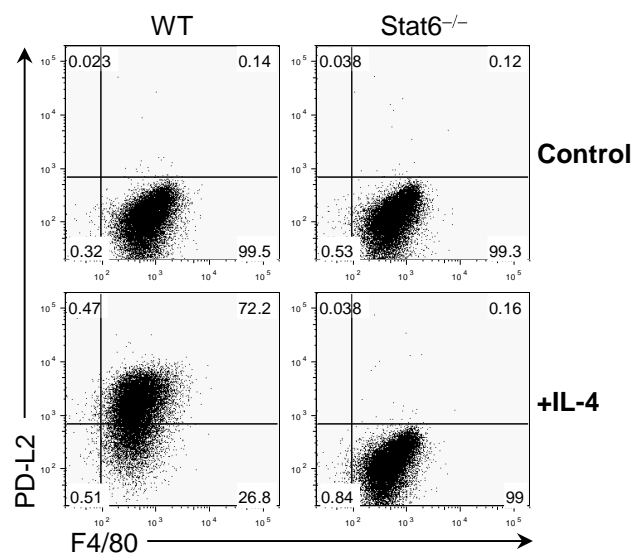


**Figure 15: Stat6-dependent expression of PD-L2 on the surface of IL-4-exposed BMDM.**

BMDM from WT or Stat6<sup>-/-</sup> mice were either left untreated (control) or stimulated with IL-4 (10 ng/mL). Macrophages were stained for F4/80 and PD-L2 and analyzed by flow cytometry.

PD-L2 is a member of the B7 family, which includes the ligands PD-L1, CD80 and CD86. Therefore, it was of further interest to compare the IL-4 induced expression of PD-L2 on macrophages to other potentially inhibitory ligands of the B7 family by flow cytometry. BMDM from wild type and Stat6<sup>-/-</sup> mice were either left untreated or cultured for 24 hours with LPS (to induce CAM) or IL-4 (to induce AAM). Untreated wild type and Stat6<sup>-/-</sup> macrophages showed no major difference in expression of PD-L1, PD-L2 and CD80 (Figure 16). Only a slight Stat6-dependent up-regulation of CD86 on wild type control

macrophages was observed. The expression level of MHCII, which is known to be regulated by Stat6 in macrophages, was also comparable between untreated wild type and Stat6<sup>-/-</sup> macrophages [101]. In addition to the IL-4-induced up-regulation of PD-L2 on wild type macrophages, MHCII was also highly expressed on IL-4-treated wild type, but not on IL-4-exposed Stat6<sup>-/-</sup> macrophages. Wild type macrophages slightly increased PD-L1 expression upon IL-4 treatment. After exposure to LPS macrophages from both mouse strains strongly up-regulated PD-L1 expression. Furthermore, CD86 was down-regulated on LPS-exposed wild type but not Stat6<sup>-/-</sup> macrophages (Figure 16).

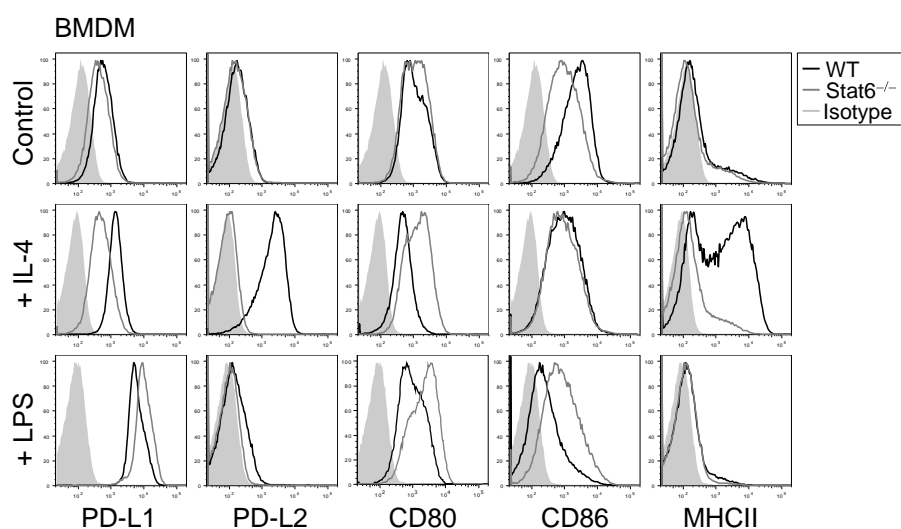


**Figure 16: Comparison of IL-4-induced expression of PD-L2 on BMDM to other B7 family members.** BMDM from WT mice (black line) and Stat6<sup>-/-</sup> mice (grey line) were cultured in medium alone (control) or were activated with IL-4 (10 ng/mL) or LPS (1  $\mu$ g/mL). The cells were double-stained for F4/80 and PD-L1, PD-L2, CD80, CD86 or MHCII. Histograms are gated on F4/80<sup>+</sup> macrophages. Filled histograms show isotype control staining. Data shown are representative of three independent experiments.

Next, we determined whether this differential regulation of B7 family members and MHCII expression by classical versus alternative activation was restricted to BMDM or was common to other macrophage populations, such as thioglycollate-elicited macrophages from the peritoneal cavity. Peritoneal macrophages were obtained by stimulation of macrophage recruitment in mice through injection of thioglycollate medium into the peritoneal cavity. After four days macrophages were obtained by peritoneal lavage (> 90% purity) and double stained for F4/80, the B7 family members and MHCII. No differences were observed in the expression of PD-L1, CD80, CD86 and MHCII on

untreated peritoneal macrophages from both mouse strains (Figure 17). PD-L2 staining was comparable to isotype control staining on untreated macrophages from wild type and Stat6<sup>-/-</sup> mice. After IL-4 treatment, peritoneal wild type macrophages showed the same pattern of Stat6-dependent inducible PD-L2 expression compared to BMDM (Figure 16, Figure 17). However, only a slight Stat6-dependent up-regulation of MHCII was detected. The LPS-induced up-regulation of PD-L1 on wild type and Stat6<sup>-/-</sup> macrophages was comparable to that of BMDM. In contrast, up-regulation of CD86 was observed after LPS treatment on peritoneal macrophages of both mice strains, but not on BMDM (Figure 16, Figure 17).

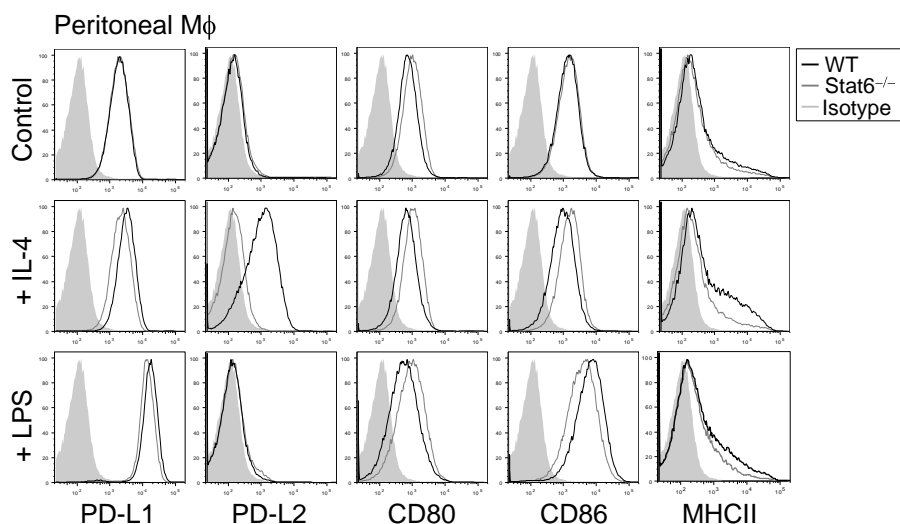


**Figure 17: Comparison of IL-4-induced expression of PD-L2 on peritoneal macrophages to other B7 family members.**

Peritoneal macrophages (M $\phi$ ) from WT mice (black line) and Stat6<sup>-/-</sup> mice (grey line) were cultured in medium alone (control) or activated with IL-4 (10 ng/mL) or LPS (1  $\mu$ g/mL). The cells were double-stained for F4/80 and PD-L1, PD-L2, CD80, CD86 or MHCII. Histograms are gated on F4/80<sup>+</sup> macrophages. Filled histograms show isotype control staining. Data shown are representative of three independent experiments.

Having determined that classical versus alternative activation differentially regulates PD-L2 expression on both, bone marrow-derived and peritoneal macrophages, it was of further interest to determine whether DCs express PD-L2 after IL-4 treatment. DCs were differentiated from bone marrow of wild type and Stat6<sup>-/-</sup> mice in the presence of supernatant from the GM-CSF-producing X63 B cell lymphoma cell line. We obtained CD11c<sup>+</sup> DCs at a purity of > 90%. Bone marrow-derived DCs were then either left untreated or cultured for 24 hours with IL-4. Expression of B7 family members and

MHCII on CD11c<sup>+</sup> DCs was analyzed by flow cytometry (Figure 18). Untreated DCs showed no major difference in expression of PD-L1, CD80 and CD86 between wild type and Stat6<sup>-/-</sup> DCs. However, PD-L2 was constitutively expressed on control DCs of both mouse strains, with an increased expression upon IL-4 activation on wild type DCs, which was dependent on Stat6. These results clearly demonstrate that PD-L2 is the only B7 family member, which is induced on macrophages by IL-4 in a Stat6-dependent manner.

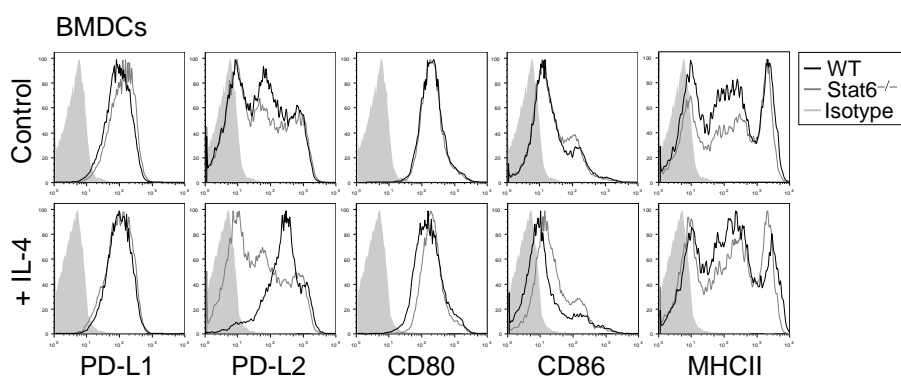


**Figure 18: Comparison of B7 family members on control and IL-4-exposed bone marrow-derived DCs.** Bone marrow-derived DCs (BMDCs) from WT mice (black line) and Stat6<sup>-/-</sup> mice (grey line) were cultured in medium alone (control) or activated with IL-4 (10 ng/mL). The cells were double-stained for CD11c and PD-L1, PD-L2, CD80, CD86 or MHCII. Histograms are gated on CD11c<sup>+</sup> DCs. Filled histograms show isotype control staining. Data shown are representative of three independent experiments.

#### 4.2.3 PD-L2 expression correlates with other established AAM markers

To further characterize surface expression of PD-L2 on AAM, we measured PD-L2 expression by flow cytometry at various time points after IL-4 stimulation of BMDM. PD-L2 was induced two hours after stimulation and reached a maximum of 97% PD-L2 positive cells at 24 hours (Figure 19A). These results indicate a rapid up-regulation of PD-L2 on macrophages after IL-4 activation and show that over a longer period of stimulation almost all macrophages up-regulate PD-L2 surface expression.

To determine whether PD-L2 surface expression correlates with established markers for AAM, we stimulated BMDM with IL-4 for six hours, sorted PD-L2<sup>+</sup> and PD-L2<sup>-</sup> macrophages and performed quantitative RT-PCR analysis (Figure 19B, C). Sorted PD-L2<sup>+</sup> cells showed 2-4-fold higher expression levels of the AAM markers *retnla*, *chi3l3* and

*arg1* as compared to PD-L2<sup>-</sup> cells (Figure 19C). These results demonstrate that PD-L2 can serve as a reliable surface marker for AAM.

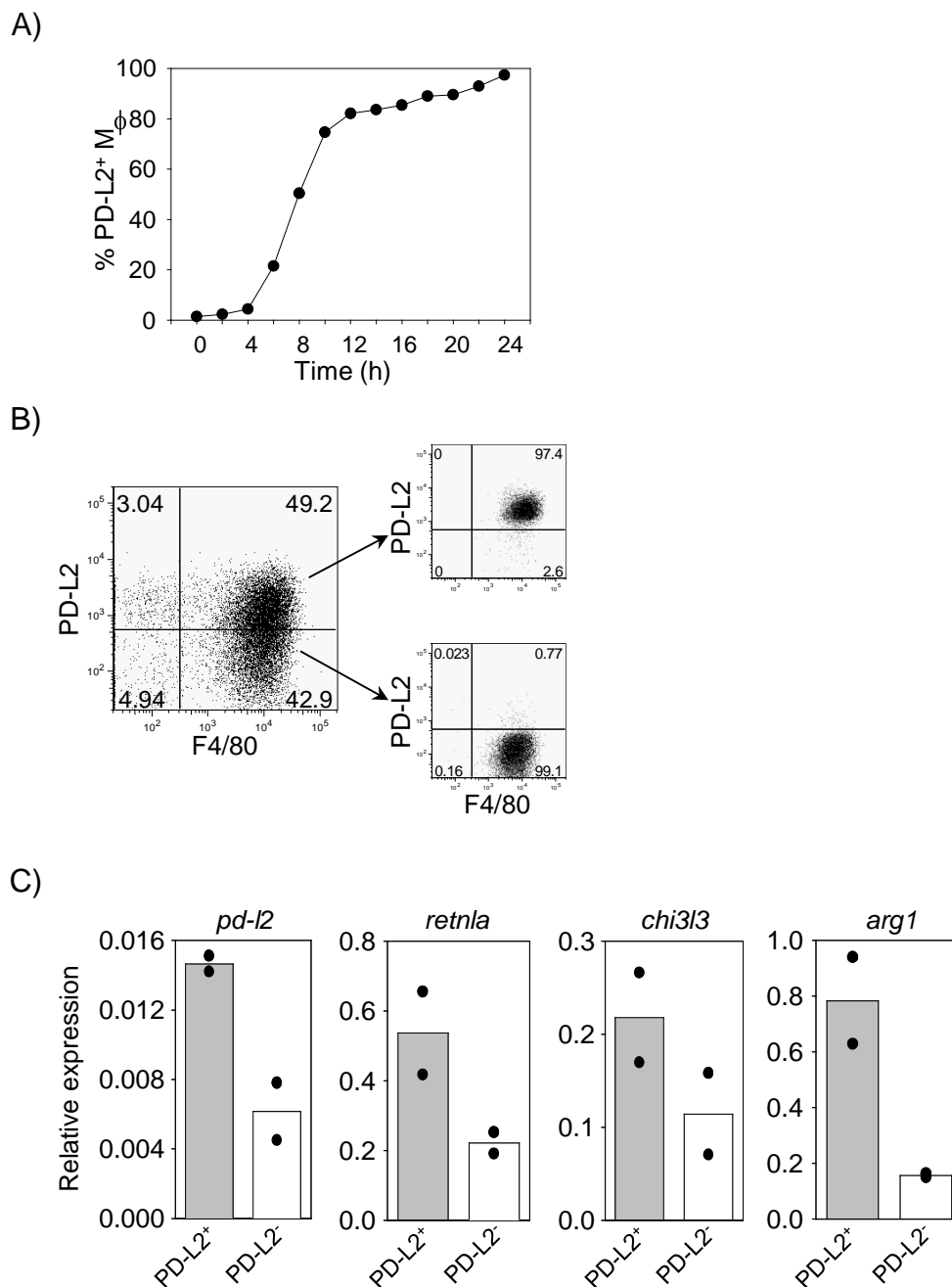


**Figure 19: PD-L2 surface expression: kinetics and correlations with AAM markers.**

**A)** Time course of PD-L2 up-regulation on BMDM from WT mice. Macrophages (Mφ) were activated with IL-4 (10 ng/mL), collected at different time points after activation, stained for F4/80, PD-L2 and analyzed by flow cytometry. The experiment has been repeated with similar results. **B)** BMDM from WT mice were cultured for six hours with IL-4 and sorted into PD-L2<sup>+</sup> and PD-L2<sup>-</sup> populations (purity > 97%). **C)** RNA was isolated from PD-L2<sup>+</sup> (solid bars) or PD-L2<sup>-</sup> (open bars) sorted BMDM and *pd-l2*, *retna*, *chi3l3* and *arg1* expression was analyzed by quantitative RT-PCR. Bars show means of two independent experiments (black circles), normalized to β-actin expression.

### 4.3 Stat6 dependence and plasticity of PD-L2 expression

Stat6 appears to be required for IL-4-mediated PD-L2 up-regulation in AAM, although there are no Stat6-binding sites present in the PD-L2 promoter [80]. Therefore, it remains unclear whether Stat6-mediated signaling is directly required in PD-L2-expressing macrophages or if Stat6-induced factors mediate PD-L2 expression on bystander macrophages. To distinguish between these two possibilities, we co-cultured congenic wild type (Ly5.1<sup>+</sup>) and Stat6<sup>-/-</sup> (Ly5.1<sup>-</sup>) BMDM in the presence of IL-4. Cells were stained for F4/80, Ly5.1 and PD-L2 and were analyzed by flow cytometry. PD-L2 was only induced on wild type F4/80<sup>+</sup> macrophages, clearly demonstrating the cell-intrinsic requirement of Stat6 for PD-L2 expression (Figure 20).

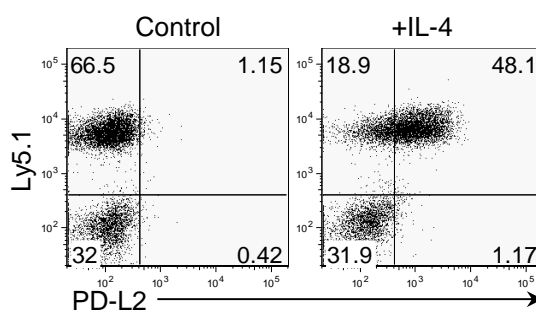


**Figure 20: Cell intrinsic requirement of Stat6 for PD-L2 expression.**

Bone marrow cells from WT (Ly5.1<sup>+</sup>) and Stat6<sup>-/-</sup> (Ly5.1<sup>-</sup>) mice were co-cultured in medium alone (control) or in the presence of IL-4 (10 ng/mL). Dot plots are gated on F4/80<sup>+</sup> macrophages and show expression of Ly5.1 and PD-L2.

It was of further interest to address the plasticity of PD-L2 and PD-L1 expression on AAM and CAM. Macrophages were differentiated from wild type bone marrow cells and were either cultured for 24 hours with LPS (to induce CAM) or IL-4 (to induce AAM). CAM were double stained for F4/80 and PD-L1, while AAM were double stained for F4/80 and PD-L2 (Figure 21A). PD-L1<sup>high</sup> CAM were sorted with purity of > 97% and PD-L2<sup>+</sup> AAM with purity > 95% (Figure 21A). Sorted cells were then cultured for 24 hours under opposite polarizing conditions, i.e. CAM were treated with IL-4 and AAM were treated with LPS. IL-4 induced expression of PD-L2 on CAM while LPS induced expression of PD-L1 on AAM (Figure 21B). These results demonstrate that the differentiation state of macrophages is flexible and cells can rapidly respond to environmental changes.



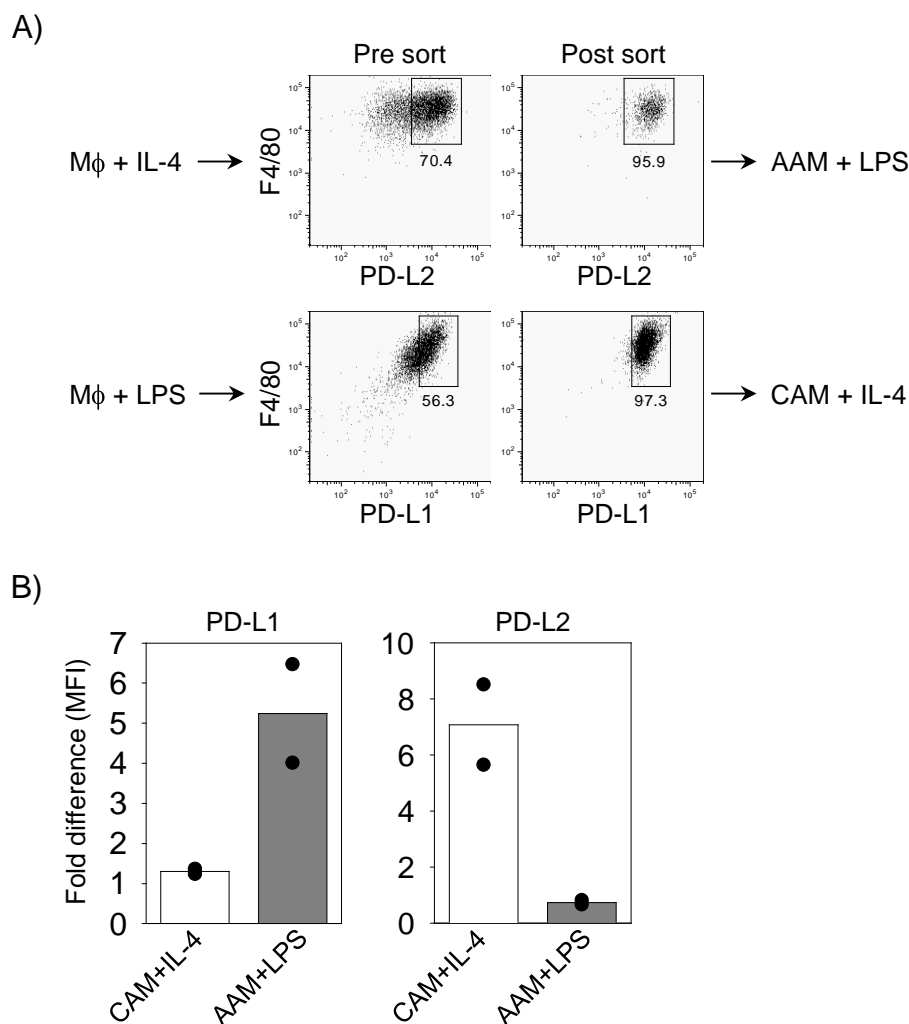


**Figure 21: Plasticity of PD-L1 and PD-L2 surface expression on AAM and CAM.**

(A) BMDM from WT mice were treated for 24 hours with either LPS (1  $\mu\text{g}/\text{mL}$ ) or IL-4 (10 ng/mL). The cells were recovered, double-stained for F4/80 and PD-L1 or PD-L2 and analyzed by flow cytometry. (B) PD-L1<sup>hi</sup> sorted CAM were cultured with IL-4 (open bars) whereas PD-L2<sup>+</sup> AAM were sorted and cultured for 24 hours with LPS (solid bars). The cells were collected and double-stained for F4/80 and PD-L1/PD-L2. The graph shows the fold difference of mean fluorescence intensity (MFI) for PD-L1 or PD-L2 expression on macrophages (M $\phi$ ). Bars show means of two independent experiments (black circles).

## 4.4 Inhibitory activity of PD-L2 on AAM

### 4.4.1 PD-L2 is required to mediate the inhibitory activity of AAM

To explore whether PD-L2 expression mediates the inhibitory activity of AAM through binding to the inhibitory receptor PD-1 on T cells, PD-L2 blocking experiments were performed. CFSE-labeled wild type splenocytes were cultured with IL-4-treated BMDM from wild type mice in the absence (control) or presence of an anti-PD-L2 blocking antibody or isotype control. CD4<sup>+</sup> T cells were stimulated with plate bound anti-TCR/anti-CD28 mAb and cell proliferation was analyzed after four days. Greater T cell proliferation was observed in anti-PD-L2-treated co-cultures than in untreated cultures (66.3% versus 23.1%; Figure 22). This effect was specific for PD-L2, as cultures treated with isotype control antibodies showed proliferation profiles comparable to those of control cultures (35.9%; Figure 22).

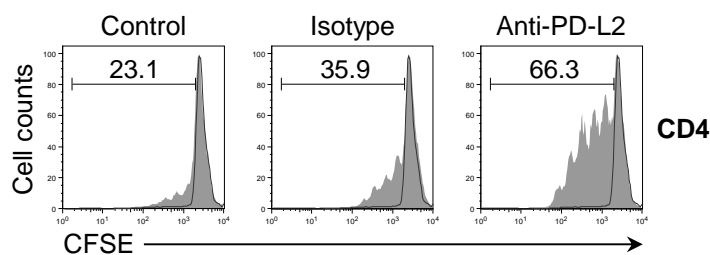


**Figure 22: PD-L2-mediated inhibition of CD4<sup>+</sup> T cell proliferation.**

Untreated (black line) or anti-TCR/anti-CD28 mAb stimulated (filled) CFSE-labeled WT splenocytes were cultured with IL-4-(10 ng/mL) treated BMDM from WT mice in the absence (control) or presence of anti-PD-L2 (clone 122; 5 µg/mL) or isotype control mAb (rat IgG2a; 5 µg/mL) and analyzed after four days. Histograms show the CFSE profile of gated CD4<sup>+</sup> T cells. The experiment was repeated with similar results.

It is possible that besides AAM other cells in the spleen express PD-L2. Therefore, different cell types in the spleen of naïve wild type mice were stained for PD-L2 expression. PD-L2 was not detectable by flow cytometry on CD4<sup>+</sup> T cells, B cells, eosinophils, conventional DCs (cDCs), plasmacytoid DCs (pDCs) or macrophages (Figure 23A). To verify that PD-L2 on AAM is required for T cell inhibition and to ensure that other PD-L2 expressing cells in the spleen are not involved, the effect of anti-PD-L2 antibody treatment in the absence of AAM was analyzed. CFSE-labeled wild type splenocytes were stimulated with anti-TCR/anti-CD28 mAb for four days in the presence of blocking antibodies against PD-L2. Anti-PD-L2 administration in the absence of AAM

did not enhance proliferation of CD4<sup>+</sup> and CD8<sup>+</sup> T cells (Figure 23B). These results suggest that other PD-L2 expressing cells in the spleen do not contribute to inhibition of T cell proliferation and PD-L2 on AAM is responsible for this effect.

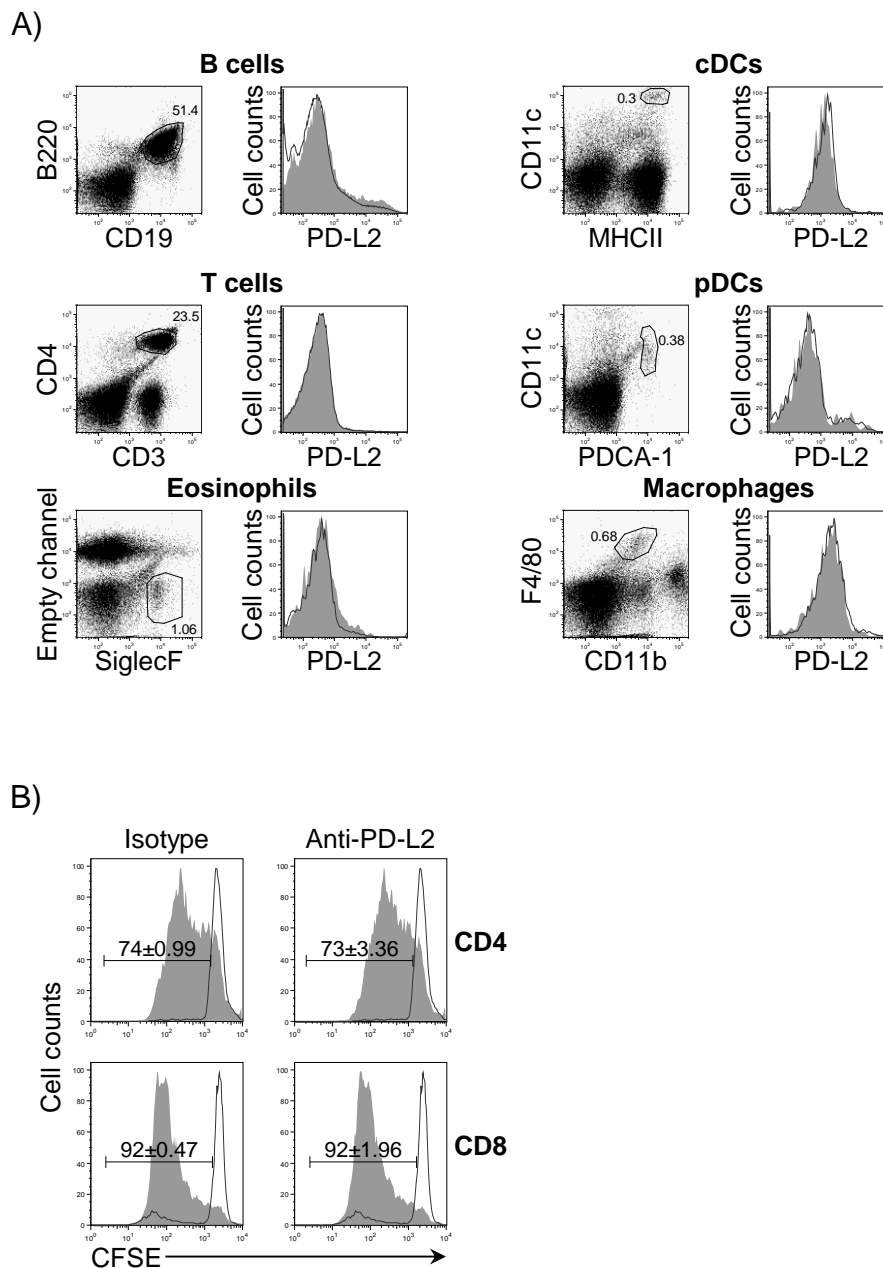


**Figure 23: Analysis of PD-L2 expression on WT naïve splenocytes.**

**A)** Staining of PD-L2 on WT splenocytes. Dot plots show staining for B cells (B220<sup>+</sup>CD19<sup>+</sup>), T cells (CD4<sup>+</sup>CD3<sup>+</sup>), eosinophils (SiglecF<sup>+</sup>), cDC (CD11c<sup>+</sup>MHCII<sup>+</sup>), pDCs (CD11c<sup>+</sup>PDCA-1<sup>+</sup>) and macrophages (F4/80<sup>+</sup>CD11b<sup>+</sup>) on single cell suspensions from the spleen of WT mice. Histogram overlay show PD-L2 expression on indicated cell types (black line) and isotype control staining (filled histogram). **B)** Splenocytes from WT mice were labeled with CFSE and were left untreated (black line) or were stimulated with plate-bound anti-TCR/anti-CD28 mAb (filled). Anti-PD-L2 (clone 122; 5 µg/mL) blocking antibody or isotype control (IgG2a; 5 µg/mL) were added to the culture. After four days, cells were collected, stained for CD4 and CD8 and analyzed by flow cytometry. Results show % of proliferated cells as means ± SD of four experiments.

#### 4.4.2 PD-L2 is sufficient to mediate the inhibitory activity of AAM

Having determined that Stat6-dependent PD-L2 expression in AAM is required for the inhibitory effect of AAM on T cells, we examined whether retroviral transduction of PD-L2 in Stat6<sup>-/-</sup> macrophages would be sufficient to mediate T cell suppression or whether other Stat6-dependent molecules are involved in this process. Therefore, a retroviral vector encoding murine PD-L2 IRES GFP was used [98]. The insert size of the retroviral vector was checked by digestion with the restriction enzyme EcoRI (Figure 24A). PD-L2<sup>+</sup> clones were further confirmed by insert PCR analysis (Figure 24B).

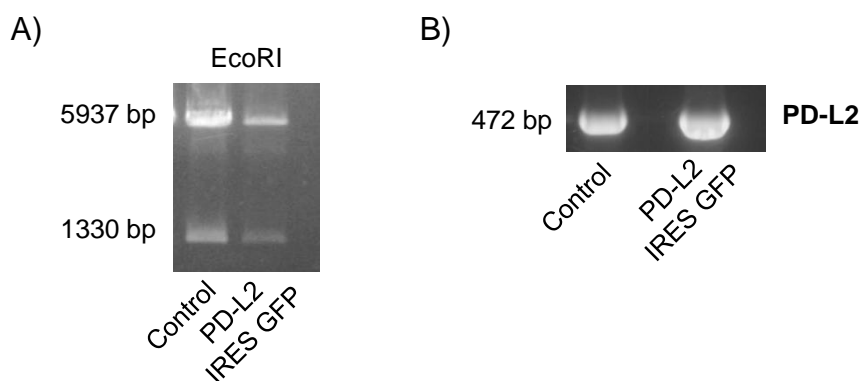


**Figure 24: Retroviral vector encoding murine PD-L2.**

**A)** The retroviral vector encoding murine PD-L2 (PD-L2 IRES GFP) recovered from bacteria was controlled for the insert size by digestion with the restriction enzyme EcoRI. The original PD-L2 IRES GFP plasmid provided by H. Kuipers was used as control [98]. Digested products were visualized on an agarose gel after electrophoresis. **B)** PD-L2<sup>+</sup> colonies were confirmed by insert PCR analysis.

BMDM from Stat6<sup>-/-</sup> mice were then transduced either with the bicistronic retroviral PD-L2 GFP expression vector or with an empty GFP control vector (Figure 25A). Control macrophages (F4/80<sup>+</sup>GFP<sup>+</sup>PD-L2<sup>-</sup>) were transduced with efficiency of 34.2% and PD-L2 macrophages (F4/80<sup>+</sup>GFP<sup>+</sup>PD-L2<sup>+</sup>) with a transduction efficiency of 45% (Figure 25A). GFP<sup>+</sup> macrophages were sorted to obtain a pure population of Stat6<sup>-/-</sup> GFP<sup>+</sup>PD-L2<sup>+</sup> macrophages or GFP<sup>+</sup> control macrophages. Sorted GFP<sup>+</sup> macrophages were cultured with CFSE-labeled splenocytes from naïve wild type mice on anti-TCR/anti-CD28 mAb coated plates. Non-adherent cells were collected after four days, stained for CD4 and CD8 and proliferation of these T cells was analyzed by flow cytometry. PD-L2-transduced macrophages efficiently blocked the proliferation of CD4<sup>+</sup> and CD8<sup>+</sup> T cells, whereas control macrophages had no suppressive activity (Figure 25B). This result indicates that

the interaction between PD-1 and PD-L2 is a relevant inhibitory mechanism by which AAM suppress T cells. Other Stat6-dependent proteins, such as Arg1, Ym1 or Relm- $\alpha$ , are not required for this effect.

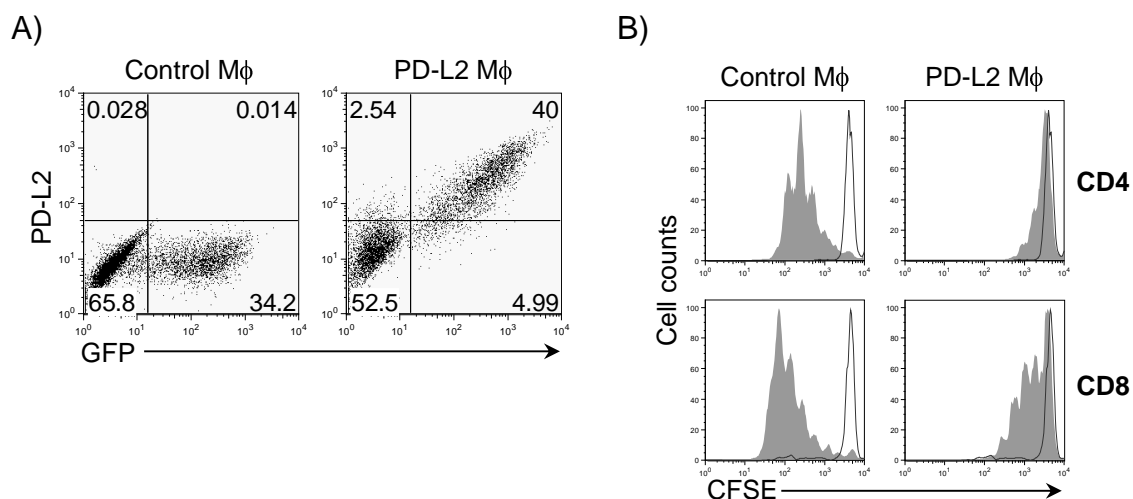


**Figure 25: Retroviral expression of PD-L2 in Stat6<sup>-/-</sup> macrophages.**

**A)** BMDM from Stat6<sup>-/-</sup> mice were transduced with the bicistronic retroviral PD-L2 IRES GFP expression vector (PD-L2 Mφ) or empty GFP control vector (control Mφ). Cells were stained for F4/80 and PD-L2. Dot plots are gated on F4/80<sup>+</sup> cells. F4/80<sup>+</sup>GFP<sup>+</sup> macrophages were sorted (purity 94%). **B)** CFSE-labeled WT splenocytes were left untreated (black line) or were stimulated with plate-bound anti-TCR/anti-CD28 mAb (filled) and were cultured in the presence of GFP<sup>+</sup> sorted macrophages. After four days, cells were collected, stained for CD4 and CD8 and analyzed by flow cytometry. Histograms are gated on CD4<sup>+</sup> or CD8<sup>+</sup> cells as indicated. The data are representative of three independent experiments.

---

## 4.5 PD-L2 expression on macrophages *in vivo*

### 4.5.1 PD-L2 is induced on alveolar macrophages during *N. brasiliensis* infection

It was of further interest to investigate whether expression of PD-L2 on AAM determined *in vitro*, also has physiological functions *in vivo*. Therefore, we investigated the phenotype of alveolar macrophages *in vivo* after infection with the helminth *N. brasiliensis*, which induces a strong type 2 immune response in the lung. Wild type mice were infected with *N. brasiliensis* and PD-L2 expression on macrophages in the lung 13 days after infection was analyzed. The gating strategy used to identify macrophages in the lung is depicted in Figure 26A. Dead cells were excluded by staining with DAPI and macrophages were selected based on the morphology (FFC<sup>hi</sup>/SSC<sup>hi</sup>) and expression of CD11c and F4/80. PD-L2 was found to be highly expressed on lung macrophages 13 days after infection (Figure 26A, B).

To assess potential phenotypic changes on macrophages induced by the passage of *N. brasiliensis* through the lung and to analyze whether these changes might be Stat6-dependent, wild type and Stat6<sup>-/-</sup> mice were infected with *N. brasiliensis*. PD-L2 expression on macrophages in the lung and bronchoalveolar lavage (BAL) was analyzed on different days after infection. Macrophages were isolated from lungs by tissue digestion with liberase and DNase, while alveolar macrophages were collected by lung lavage. Isolated macrophages were stained for CD11c, F4/80 and PD-L2 and were analyzed by flow cytometry. During infection PD-L2 was induced on macrophages from wild type mice with the highest frequency and absolute number of PD-L2<sup>+</sup> macrophages between day 13 and 16 in lung and BAL (Figure 26B, C). In contrast, Stat6<sup>-/-</sup> macrophages showed no specific staining in either lung or BAL (Figure 26B, C). The expression of PD-L2 on macrophages was specific, as isotype control antibody showed no staining.

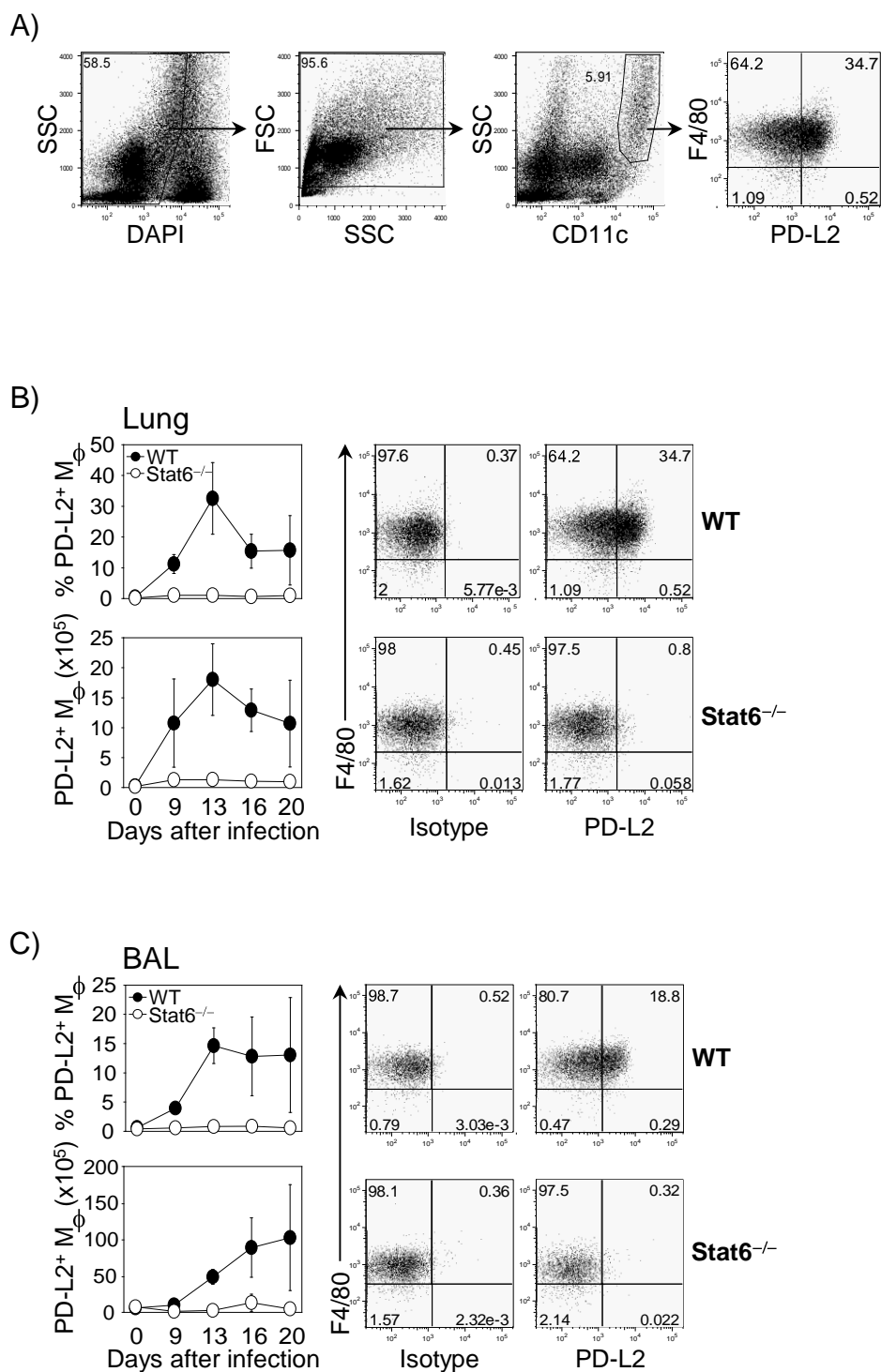


**Figure 26: PD-L2 expression on macrophages *in vivo* during *N. brasiliensis* infection.**

A) Lungs from WT mice were analyzed 13 days after *N. brasiliensis* infection. Dot plots show a representative gating strategy for staining of F4/80 and PD-L2 on DAPI<sup>+</sup>CD11c<sup>+</sup>SSC<sup>hi</sup> gated cells. Lung (B) and bronchoalveolar lavage (BAL) (C) from WT and Stat6<sup>-/-</sup> mice were analyzed before and at the indicated time points after *N. brasiliensis* infection for PD-L2 expression by flow cytometry. Dot plots show staining of F4/80 and PD-L2 or isotype control on DAPI<sup>+</sup>CD11c<sup>+</sup>SSC<sup>hi</sup> gated cells 13 days after *N. brasiliensis* infection. Graphs show the frequency and absolute number of PD-L2<sup>+</sup> macrophages (Mφ) in WT (filled circles) and Stat6<sup>-/-</sup> (open circles) mice as mean ± SE with three individual mice from two independent experiments.

To examine whether PD-L1 in addition to PD-L2 could be induced on macrophages after *N. brasiliensis* infection, we infected wild type and Stat6<sup>-/-</sup> mice with *N. brasiliensis* and analyzed PD-L1 expression on macrophages in the lung and BAL. PD-L1 was constitutively expressed on naïve alveolar macrophages and expression levels remained unchanged after 9 or 13 days of infection (Figure 27). Expression of PD-L1 on macrophages was independent of Stat6 (Figure 27). These *in vivo* results indicate that PD-L1 expression on alveolar macrophages is not regulated during Th2 immune responses, whereas PD-L2 expression is induced on macrophages in infected lungs. Expression of PD-L2 is controlled by Stat6 and is up-regulated at later time points after infection.

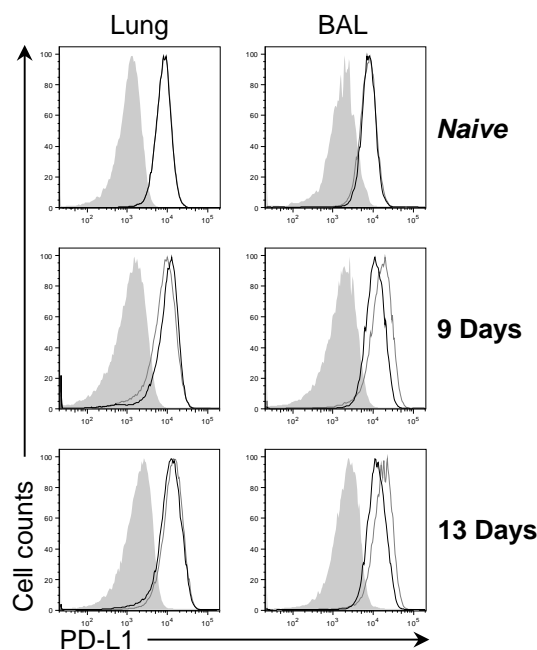


**Figure 27: PD-L1 expression on macrophages *in vivo* after *N. brasiliensis* infection.**

Lung and BAL from WT (black line) and Stat6<sup>-/-</sup> mice (grey line) were analyzed before infection (naïve) and on day nine and 13 after *N. brasiliensis* infection for PD-L1 expression by flow cytometry. Histograms are gated on F4/80<sup>+</sup>DAPI<sup>-</sup>CD11c<sup>+</sup>SSC<sup>hi</sup> macrophages. Filled histograms show isotype control staining. The experiment shown is one representative of three experiments.

We further characterized the alternative phenotype of lung macrophages from wild type and Stat6<sup>-/-</sup> mice after *N. brasiliensis* infection using immunohistochemical analysis. In histological sections of the lung, AAM were identified by staining with anti-PD-L2 and anti-Ym1 antibodies. We detected PD-L2 and Ym1 expression in alveolar macrophages from wild type, but not from Stat6<sup>-/-</sup> mice 13 days after infection (Figure 28). These results



demonstrate that PD-L2 is induced on macrophages *in vivo* after *N. brasiliensis* infection and expression of PD-L2 correlates with the AAM marker Ym1, confirming that PD-L2 serves as surface marker for AAM *in vitro* and *in vivo*.

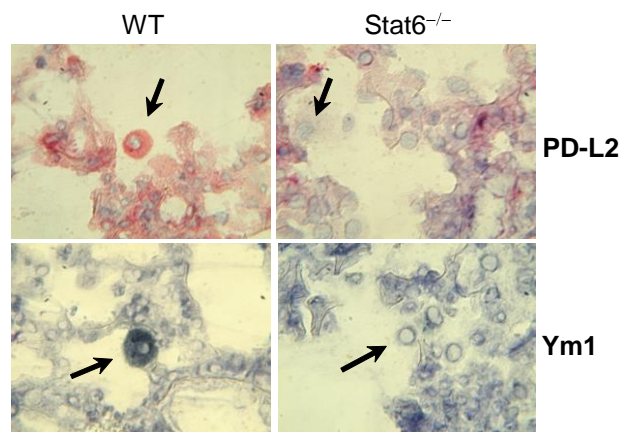


**Figure 28: Stat6-dependent PD-L2 expression in lung tissue of *N. brasiliensis* infected mice.** Detection of Ym1 (blue) and PD-L2 (red) expression in alveolar macrophages (arrows) of WT mice that had been infected with *N. brasiliensis* 13 days before. Acquired with magnification of 40x.

#### 4.5.2 T cell derived IL-4/IL-13 is required for PD-L2 expression on AAM *in vivo*

IL-4/IL-13 has been shown to be required for the differentiation of AAM, although the cellular source of these cytokines *in vivo* has not been determined [60]. Therefore, we analyzed whether expression of IL-4/IL-13 from T cells or non-T cells, including eosinophils, basophils and mast cells, is required for AAM differentiation. We used complete IL-4/IL-13-deficient mice (IL-4/IL-13<sup>-/-</sup>), mice which lack IL-4/IL-13 only in T cells (CD4Cre x IL-4/IL-13<sup>F/F</sup>) and control mice with normal expression of both cytokines (IL-4/IL-13<sup>F/F</sup>). When lung and BAL were analyzed 13 days after *N. brasiliensis* infection, IL-4/IL-13<sup>F/F</sup> control mice showed abundant expression of PD-L2 on macrophages (Figure 29). However, both IL-4/IL-13<sup>-/-</sup> and CD4Cre/IL-4/IL-13<sup>F/F</sup> mice lacked PD-L2 expression (Figure 29). This indicates that PD-L2 expression on macrophages requires IL-4/IL-13 from CD4<sup>+</sup> T cells.

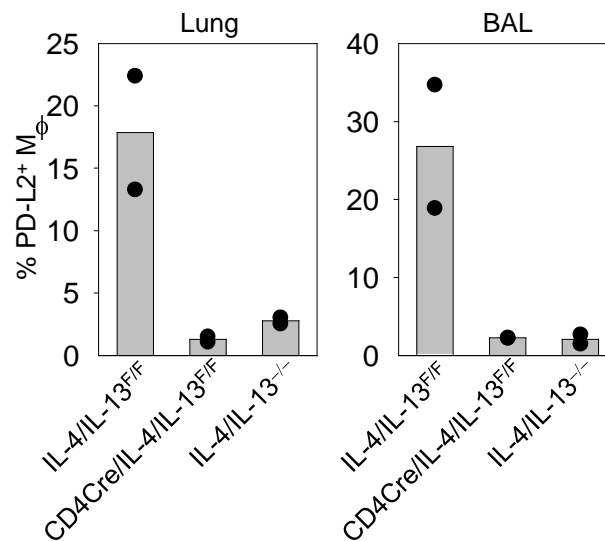


**Figure 29: Analysis of T cell derived IL-4/IL-13 for PD-L2 expression on AAM *in vivo*.**

Analysis of PD-L2 expression on macrophages (M $\phi$ ) in lung and BAL (F4/80<sup>+</sup> CD11c<sup>+</sup> SSC<sup>hi</sup>) in complete IL-4/IL-13-deficient mice (IL-4/IL-13<sup>-/-</sup>), mice deficient in IL-4/IL-13 only in T cells (CD4Cre/IL-4/IL-13<sup>F/F</sup>) and control mice (IL-4/IL-13<sup>F/F</sup>) 13 days after *N. brasiliensis* infection. Bars show the mean frequency of PD-L2<sup>+</sup> macrophages of two mice (dots).

## 4.6 Macrophage recruitment during *N. brasiliensis* infection

### 4.6.1 Accumulation of macrophages in the lung after *N. brasiliensis* infection is independent of Stat6

Stat6 is required for T cell proliferation and differentiation into Th2 cells, as well as the induction of IgE synthesis [34]. It was of further interest to investigate whether the lack of PD-L2<sup>+</sup> macrophages in the lungs of infected Stat6<sup>-/-</sup> mice shown in Figure 26 was due to Stat6-dependent functions, the reduced proliferation of resident macrophages or impaired monocyte recruitment to the lung compartment. To address these possibilities we generated congenic mixed bone marrow chimeras in which bone marrow from wild type (Ly5.1<sup>+</sup>) and Stat6<sup>-/-</sup> (Ly5.1<sup>-</sup>) mice were transferred into lethally irradiated wild type recipient mice, allowing to analyze wild type and Stat6<sup>-/-</sup> macrophages side-by-side in the same animal (Figure 30). Eight weeks after reconstitution equal frequencies of bone marrow-derived cells from wild type and Stat6<sup>-/-</sup> donors were observed (Figure 31A). To analyze the turnover of wild type and Stat6<sup>-/-</sup> macrophages, chimeras were analyzed nine days after

infection with *N. brasiliensis* that had been treated with BrdU for the previous 36 hours (Figure 30). BrdU that incorporated into the DNA was visualized by staining with an anti-BrdU antibody.

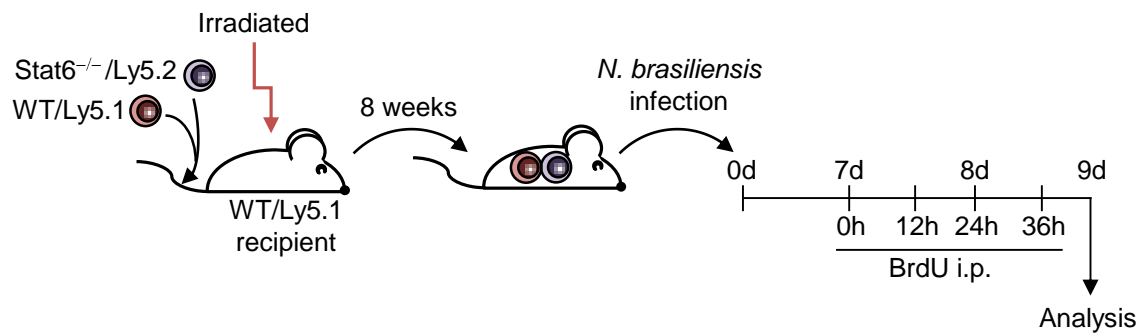


**Figure 30: Overview of BrdU treatment in *N. brasiliensis* infected mixed bone marrow chimeras.**

Bone marrow cells from WT (Ly5.1<sup>+</sup>) and Stat6<sup>-/-</sup> (Ly5.1<sup>-</sup>) mice were transferred into lethally irradiated wild type recipient mice. Eight weeks after reconstitution congenic mixed bone marrow chimeras were infected with *N. brasiliensis*. Seven days after infection chimeras were treated with BrdU every twelve hours before they were analyzed nine days after infection.

Peritoneal exudate cells (PEC) were stained for F4/80 to identify macrophages and for Ly5.1 to distinguish wild type and Stat6<sup>-/-</sup> donors. We could clearly distinguish populations of BrdU<sup>+</sup> and BrdU<sup>-</sup> F4/80<sup>+</sup>SSC<sup>hi</sup> wild type (Ly5.1<sup>+</sup>) and Stat6<sup>-/-</sup> (Ly5.1<sup>-</sup>) macrophages in the peritoneal cavity nine days after *N. brasiliensis* infection (Figure 31B). Direct comparison of BrdU incorporation in naïve and infected chimeric mice revealed that in naïve mice BrdU was incorporated in about 10% of peritoneal macrophages and the incorporation rate increased 5-fold after infection (Figure 31C). We observed no differences in BrdU incorporation between wild type and Stat6<sup>-/-</sup> peritoneal macrophages before or after infection (Figure 31C). To determine the turnover of wild type and Stat6<sup>-/-</sup> macrophages in other tissues within the same animal, chimeric mice were left untreated or were infected with *N. brasiliensis*. Seven days after infection mixed bone marrow chimeras were treated with BrdU every twelve hours before they were analyzed nine days after infection by flow cytometry for incorporation of BrdU. Macrophages in different tissues were identified by staining for F4/80 and CD11c (lung and BAL), F4/80 and CD11b (spleen) or F4/80 (PEC). Besides peritoneal macrophages we observed 10% BrdU incorporation also in spleen, BAL and lung in naïve mice (Figure 32A).

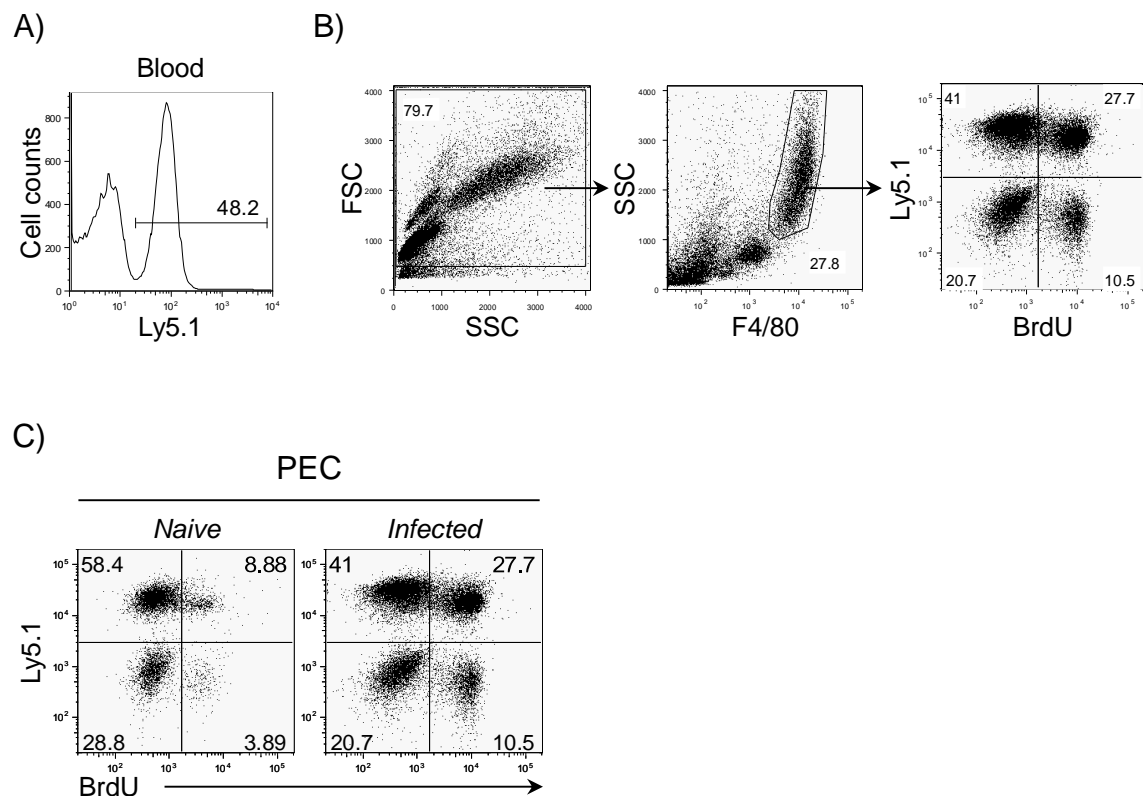


**Figure 31: BrdU staining of macrophages in mixed bone marrow chimeras after *N. brasiliensis* infection.**

Congenetic mixed bone marrow chimeras were generated with bone marrow cells from WT (Ly5.1<sup>+</sup>) and Stat6<sup>-/-</sup> (Ly5.1<sup>-</sup>) donor mice **A**) The histogram shows frequency of Ly5.1<sup>+</sup> cells in the peripheral blood. **B**) Dot plots show a representative gating strategy of peritoneal cells from chimeras nine days after infection with *N. brasiliensis* that had been treated with BrdU for the previous 36 hours. Macrophages were identified as F4/80<sup>+</sup>SSC<sup>hi</sup> and were stained for BrdU and Ly5.1 to distinguish WT and Stat6<sup>-/-</sup> macrophages. **C**) Peritoneal cells (PEC) of naïve mice (left dot plot) or of day nine *N. brasiliensis* infected mice (right dot plot) that had been given BrdU for the last 36 hours. Dot plots are gated on F4/80<sup>+</sup>SSC<sup>hi</sup> and show staining for Ly5.1 and BrdU.

Infection with *N. brasiliensis* increased BrdU incorporation 2-fold in splenic macrophages, but did not affect BrdU incorporation rates in the lung and BAL. The incorporation rate was independent of Stat6 in naïve and infected mice in all tissues analyzed (Figure 32A). In naïve mice significantly more wild type macrophages as compared to Stat6<sup>-/-</sup> macrophages were observed in the peritoneum ( $p \leq 0.05$ ) and lung ( $p \leq 0.001$ ) but not in spleen and BAL (Figure 32B). Stat6-dependent accumulation of macrophages after infection was significant in the peritoneum ( $p \leq 0.05$ ; Figure 32B). These results suggest that macrophage turnover after infection is independent of Stat6, although Stat6 seems to promote recruitment and prolong the lifespan of macrophages in selected tissues.

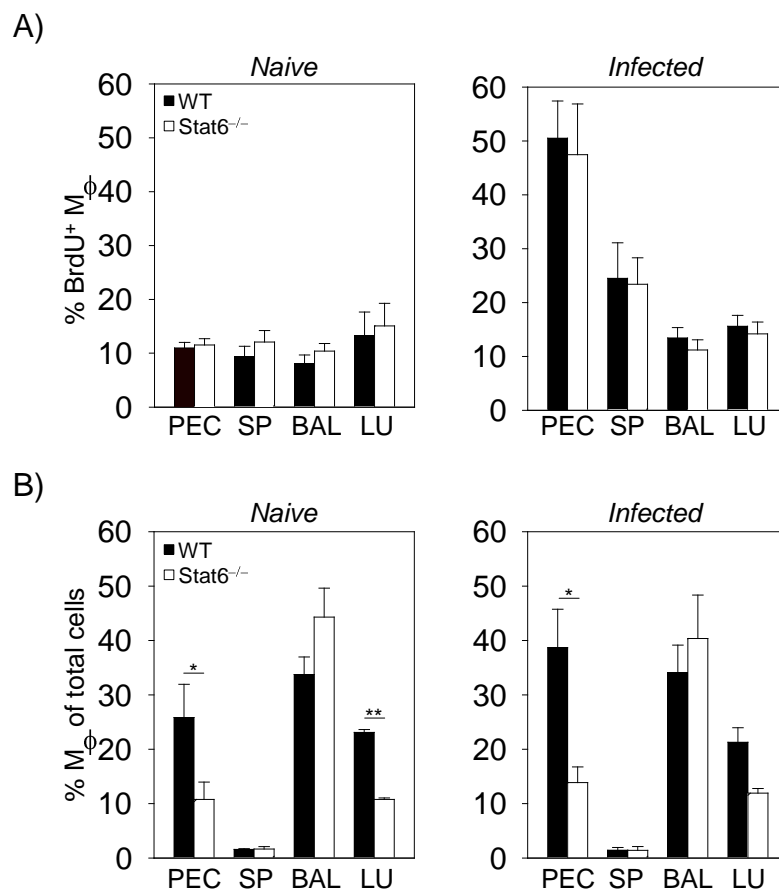


**Figure 32: Analysis of Stat6 requirement for accumulation of macrophages after infection.**

**A, B)** Congenic mixed bone marrow chimeras were generated with bone marrow cells from WT (Ly5.1<sup>+</sup>) and Stat6<sup>-/-</sup> (Ly5.1<sup>-</sup>) donor mice. Macrophages (M $\phi$ ) in peritoneum (PEC), spleen (SP), bronchoalveolar lavage (BAL) and lung (LU) of wild type (WT) (filled bars) and Stat6<sup>-/-</sup> (open bars) mice that had been infected with *N. brasiliensis* nine days before (infected) or were left untreated (naïve) were analyzed 36 hours after BrdU administration. **A)** Shows the frequency of BrdU<sup>+</sup> cells among total macrophages and **B)** shows the frequency of macrophages among total cells. Macrophages were identified by staining for F4/80 and CD11c (lung and BAL), F4/80 and CD11b (spleen) or F4/80 (PEC). The bars show mean + SE of seven individual mice from four independent experiments. \*\*  $P \leq 0.001$ , \*  $P \leq 0.05$ .

#### 4.6.2 Recruitment of macrophages in the lung after *N. brasiliensis* infection is independent of CCR2, CCR5 and F4/80

The chemokine receptor CCR2 is expressed abundantly on a subset of blood monocytes and has been associated with monocyte and macrophage recruitment [102-104]. Therefore, we further analyzed CCR2-dependent macrophage trafficking nine days after helminth infection using CCR2<sup>-/-</sup> mice. No significant differences were observed in the frequency of

macrophages in spleen and lung of  $CCR2^{-/-}$  compared to control mice ( $CCR2^{+/-}$ ; Figure 33A, B). However,  $CCR2^{-/-}$  mice showed significantly more recruitment of macrophages in the peritoneal cavity ( $p \leq 0.05$ ) but less accumulation in BAL compared to the heterozygous strain (Figure 33B).

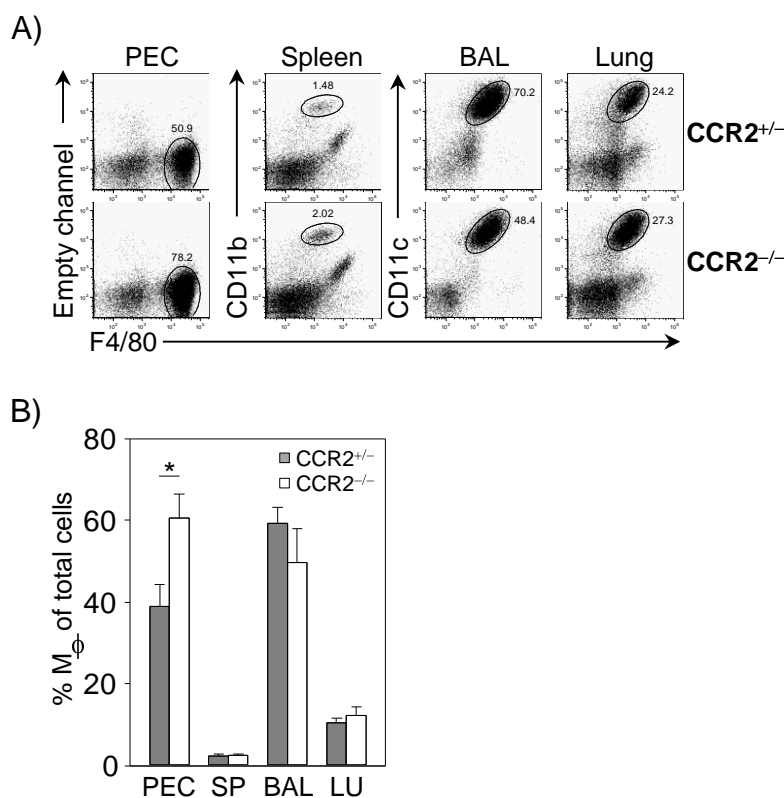


**Figure 33: Analysis of CCR2 requirement for recruitment of macrophages after infection.**

**A)** Control  $CCR2$ -heterozygous ( $CCR2^{+/-}$ ) and  $CCR2^{-/-}$  mice were analyzed nine days after *N. brasiliensis* infection. Macrophages in peritoneum (PEC), spleen (SP), bronchoalveolar lavage (BAL) and lung (LU) were stained for F4/80 and CD11c or CD11b. **B)** Graphs show the frequency of macrophages among total cells of  $CCR2^{+/-}$  mice (grey bars) and  $CCR2^{-/-}$  mice (open bars) as mean + SD of three individual mice from two independent experiments. \*  $P \leq 0.05$ .

$CCR5$  is expressed predominantly on macrophages differentiated from blood monocytes [105]. Recently published data showed an induction of alternative macrophage activation in  $CCR5^{-/-}$  mice [106]. Nine days after *N. brasiliensis* infection we observed preferential accumulation of macrophages in the peritoneum, but not in spleen, BAL or lung of control mice compared to the  $CCR5^{-/-}$  mice (Figure 34A, B). These findings suggest that  $CCR2$  and  $CCR5$  differentially regulate mobilization of macrophages to the peritoneum but seem not to be required for recruitment of macrophages to the site of infection.

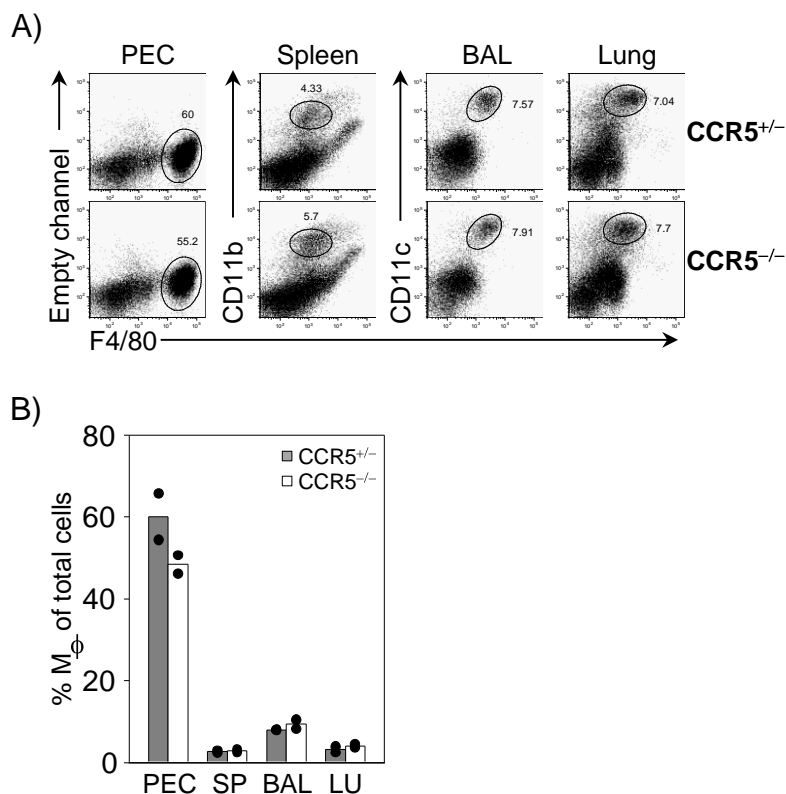


**Figure 34: Analysis of CCR5 requirement for recruitment of macrophages after infection.**

A) Control CCR5-heterozygous (CCR5<sup>+/-</sup>) and CCR5<sup>-/-</sup> mice were analyzed nine days after *N. brasiliensis* infection. Macrophages in peritoneum (PEC), spleen (SP), bronchoalveolar lavage (BAL) and lung (LU) were stained for F4/80 and CD11c or CD11b. B) Graphs show the frequency of macrophages among total cells of CCR5<sup>+/-</sup> (grey bars) and CCR5<sup>-/-</sup> mice (open bars) as mean values from two mice (dots).

F4/80 is expressed on a variety of macrophage subsets but the function of this molecule is not well defined. We hypothesized that a lack of F4/80 expression might alter macrophage recruitment after *N. brasiliensis* infection. Nine days after infection, F4/80<sup>-/-</sup> mice demonstrated only a slight increase in macrophage recruitment to the lung and BAL and significantly less accumulation in the peritoneum ( $P \leq 0.05$ ; Figure 35). These results provide no evidence for a role of F4/80 in recruitment of macrophage to infected tissues during *N. brasiliensis* infection.

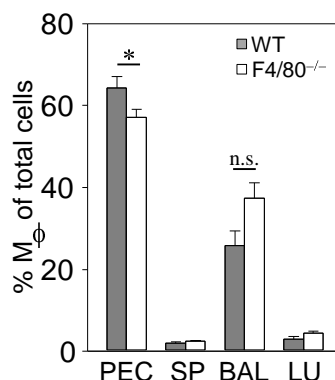


**Figure 35: Analysis of F4/80 requirement for recruitment of macrophages after infection.**

F4/80<sup>-/-</sup> mice (open bars) and WT (grey bars) were analyzed nine days after *N. brasiliensis* infection. Macrophages in peritoneum (PEC), spleen (SP), bronchoalveolar lavage (BAL) and lung (LU) were stained for CD115 and CD11c or CD11b. Graphs show the frequency of macrophages among total cells. Bars show mean + SD of three individual mice from two independent experiments. \*  $P \leq 0.05$ , n.s. = not significant.

## 4.7 PD-1 expression on Th2 cells during *N. brasiliensis* infection

### 4.7.1 PD-L2 expression on macrophages correlates inversely with PD-1 expression on T cells

Since PD-L2 binds to PD-1 on T cells we thought that the lack of PD-L2 expression on macrophages in Stat6<sup>-/-</sup> mice could modulate PD-1 expression on T cells. To address this possibility, we analyzed PD-1 expression on CD4<sup>+</sup> T cells in lungs and mesenteric lymph nodes (MLN) from wild type and Stat6<sup>-/-</sup> mice at different time points after *N. brasiliensis* infection. We used mice that had been crossed to IL-4/eGFP reporter mice (4get mice) to visualize Th2 cells. These mice were generated by introducing an eGFP construct directly behind the IL-4 gene, which leads to the transcription of a bicistronic mRNA [91]. eGFP is trapped inside the cell whereas IL-4 is secreted to the outside. Figure 36 shows the gating of DAPI<sup>+</sup> lymphocytes in the lung 13 days after infection. Lymphocytes were further gated on CD4<sup>+</sup> T cells to identify PD-1 expression on Th2 cells (CD4<sup>+</sup>/IL-4/eGFP<sup>+</sup> cells).



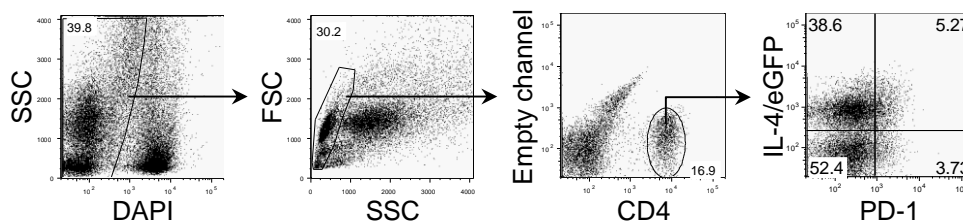


**Figure 36: Analysis of PD-1 expression on Th2 cells after *N. brasiliensis* infection.**

Lungs of 4get mice were analyzed 13 days after *N. brasiliensis* infection. Dot plots show a representative gating strategy for staining of PD-1 on IL-4/eGFP<sup>+</sup> cells. Dead cells were excluded using DAPI.

The frequency of Th2 cells in wild type mice 13 days after *N. brasiliensis* infection was 2.4-fold higher in the lung and 2-fold higher in the MLN as compared to Stat6<sup>-/-</sup> mice (dot plot, Figure 37) reflecting the requirement of Stat6 for T cell proliferation and differentiation into Th2 cells. The frequency of PD-1<sup>+</sup> IL-4/eGFP<sup>+</sup> cells among all CD4<sup>+</sup> T cells was comparable between wild type and Stat6<sup>-/-</sup> mice in the lung (5.27% WT versus 5.3% Stat6<sup>-/-</sup>) and in the MLN (3.15% WT versus 4.5% Stat6<sup>-/-</sup>) (dot plot, Figure 37). However, due to the lower frequency of Th2 cells in Stat6<sup>-/-</sup> mice we observed significantly more PD-1<sup>+</sup> cells among Th2 cells in the lung from Stat6<sup>-/-</sup> mice, with maximal expression of PD-1 on day nine after infection ( $p \leq 0.05$ ; Figure 37). This difference was even more pronounced in the lymph nodes with significantly more PD-1<sup>+</sup> cells among Th2 cells in Stat6<sup>-/-</sup> mice compared to wild type mice on day nine ( $p \leq 0.001$ ) and maximal expression on day 13 after infection ( $p \leq 0.05$ ; Figure 37). Given that Stat6<sup>-/-</sup> mice recruited fewer CD4<sup>+</sup> T cells to the lung and the MLN as compared to wild type mice, we also observed higher total numbers of PD-1<sup>+</sup> Th2 cells in Stat6<sup>-/-</sup> mice. We observed significant differences in the total numbers of PD-1<sup>+</sup> cells among Th2 cells in the lung from Stat6<sup>-/-</sup> mice on day nine ( $p \leq 0.005$ ) and in the lymph nodes on day 13 ( $p \leq 0.01$ ) after infection (Figure 37). Interestingly, wild type Th2 cells down-regulated PD-1 expression in the lymph nodes after the peak on day 13, whereas Th2 cells from Stat6<sup>-/-</sup> mice maintained PD-1 expression for several days (Figure 37). These results suggest that the lack of PD-L2 or other Stat6-dependent factors limit the accumulation of Th2 cells at the site of infection in Stat6<sup>-/-</sup> mice via up-regulation of PD-1 expression.

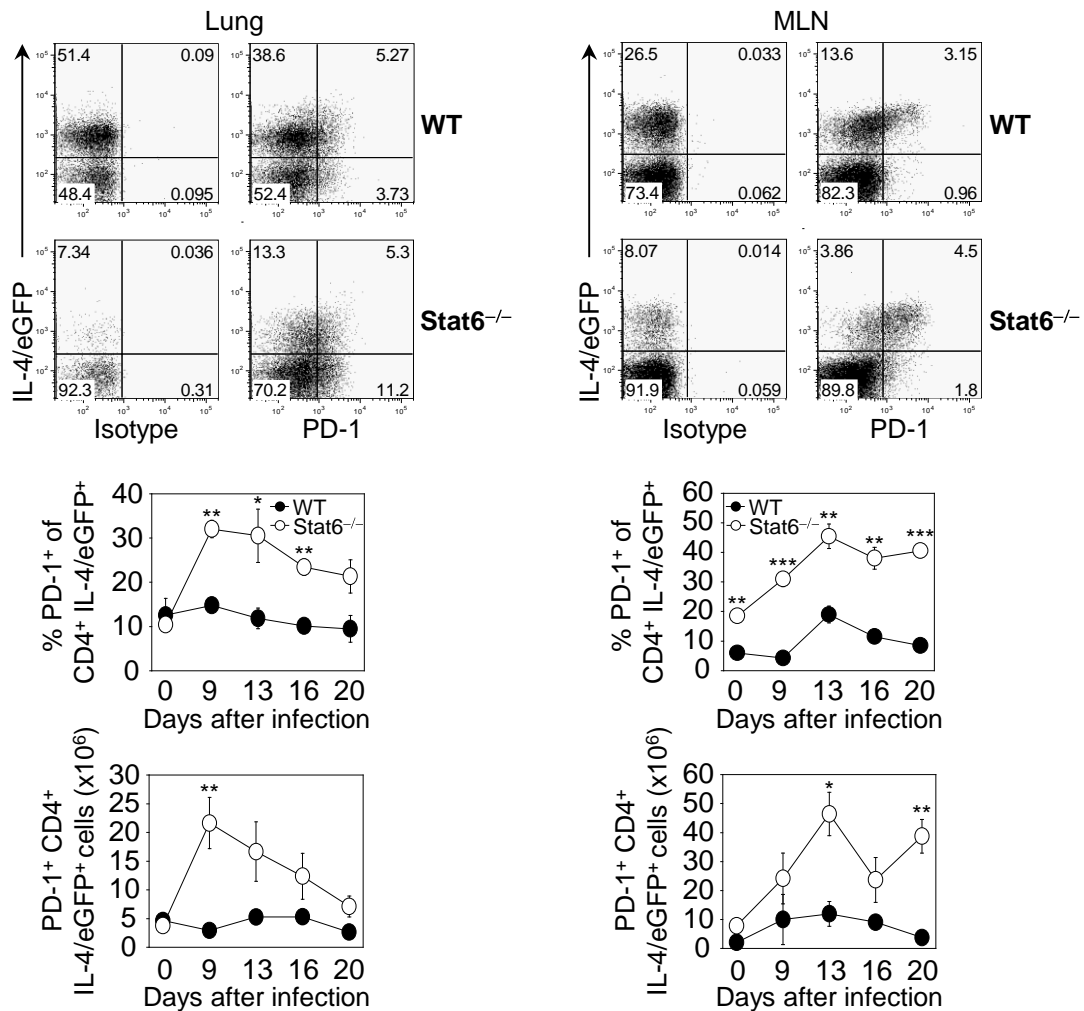


**Figure 37: PD-1 expression on Th2 cells during *N. brasiliensis* infection.**

Lungs and mesenteric lymph nodes (MLN) of 4get (WT) and 4get/Stat6<sup>-/-</sup> (Stat6<sup>-/-</sup>) mice were analyzed before or at indicated time points after *N. brasiliensis* infection. Dot plots are gated on CD4<sup>+</sup> cells and show staining for PD-1 or isotype control versus expression of IL-4/eGFP 13 days after *N. brasiliensis* infection. The graphs show the frequency and absolute number of PD-1<sup>+</sup> cells among Th2 cells (CD4<sup>+</sup> IL-4/eGFP<sup>+</sup> T cells) from WT (filled circles) or Stat6<sup>-/-</sup> (open circles) mice as mean  $\pm$  SE of three individual mice from two independent experiments. \*\*\*  $P \leq 0.001$ , \*\*  $P \leq 0.01$ , \*  $P \leq 0.05$ .

### 4.7.2 PD-1 expression is partly directly regulated by Stat6 in a cell-intrinsic manner

To better define the correlation between PD-L2 expression on AAM and PD-1 expression on T cells, mixed bone marrow chimeras were generated by reconstituting lethally irradiated 4get/Thy1.1 mice with a mixture of bone marrow cells from 4get/Thy1.1 mice and 4get/Stat6<sup>-/-</sup> Thy1.2 mice (Figure 38). Mice were infected with *N. brasiliensis* eight weeks after reconstitution and were analyzed nine days later for PD-1 expression on Th2 cells derived from wild type and Stat6<sup>-/-</sup> donor cells in the lungs and MLN. Dot plots of a representative experiment from lung tissue are shown in Figure 39A. DAPI<sup>-</sup> lymphocytes were gated on CD4<sup>+</sup> T cells and the two donors were distinguished by gating on wild type Thy1.1<sup>+</sup> or Stat6<sup>-/-</sup> Thy1.2<sup>+</sup> CD4<sup>+</sup> T cells. The PD-1 expression on Th2 cells (IL-4/eGFP<sup>+</sup> cells) of both donor cells was analyzed.

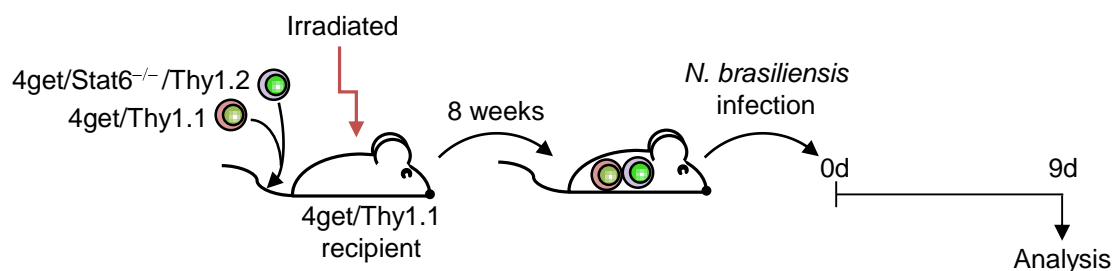


**Figure 38: Overview of the generation of mixed bone marrow chimeras.**

Bone marrow cells from WT (4get/Thy1.1<sup>+</sup>) and Stat6<sup>-/-</sup> (4get/Thy1.2<sup>+</sup>) donor mice were transferred into lethally irradiated WT 4get/Thy1.1 recipient mice. Eight weeks after reconstitution congenic mixed bone marrow chimeras were infected with *N. brasiliensis* and analyzed nine days later.

The frequency of PD-1<sup>+</sup> Th2 cells among all CD4<sup>+</sup> T cells was 1.4-fold higher in the lung ( $p \leq 0.05$ ) and 1.6-fold higher in the MLN ( $p \leq 0.01$ ) in the Stat6<sup>-/-</sup> population compared to the wild type population (Figure 39B). These results indicate that PD-1 expression is to some extent directly regulated by Stat6 in a cell-intrinsic manner. However, the results could not completely account for the large accumulation of PD-1<sup>+</sup> Th2 cells nine days after *N. brasiliensis* infection in lung (3-fold) and MLN (6.4-fold) in Stat6<sup>-/-</sup> compared to wild type mice shown in Figure 37. The results obtained from the infected chimeric mice study indicate that the increased up-regulation of PD-1 on Th2 cells in the absence of Stat6 seems to be additionally regulated by PD-L2 or other Stat6-dependent factors.

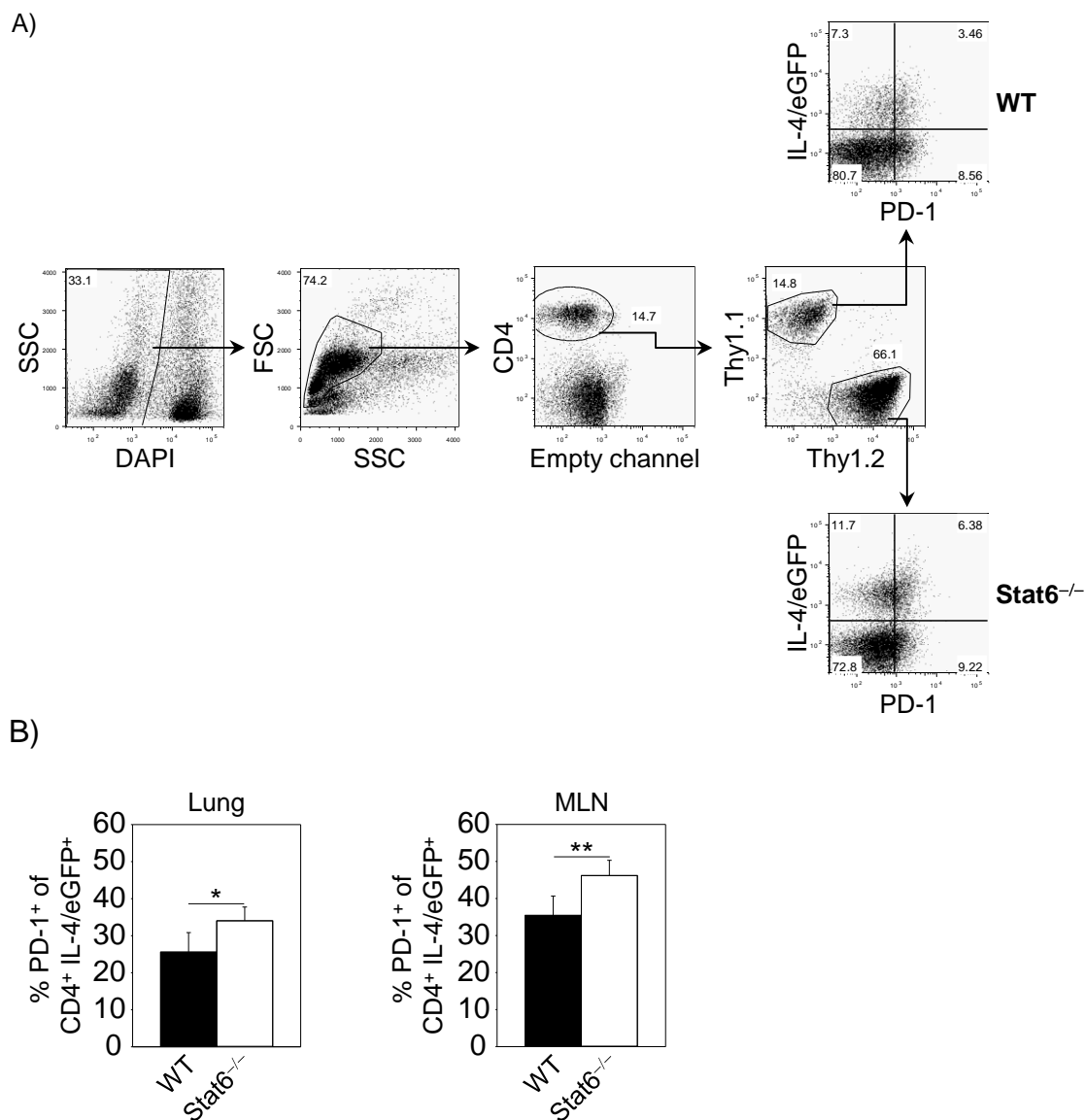


**Figure 39: PD-1 expression on Th2 cells in mixed bone marrow chimeras.**

Congenic mixed bone marrow chimeras were generated with bone marrow cells from WT (4get/Thy1.1<sup>+</sup>) and Stat6<sup>-/-</sup> (4get/Thy1.2<sup>+</sup>) donor mice in 4get/Thy1.1 recipient mice. **A)** Dot plots show a representative gating strategy of lung cells from chimeras nine days after infection with *N. brasiliensis*. Cells were stained for CD4, Thy1.1, Thy1.2 and PD-1. Th2 cells were identified as DAPI<sup>-</sup>CD4<sup>+</sup>IL-4/eGFP<sup>+</sup>. **B)** Bar graphs show the frequency of PD-1<sup>+</sup> cells among CD4<sup>+</sup>IL-4/eGFP<sup>+</sup> cells in lung and MLN from WT (black bars) and Stat6<sup>-/-</sup> (open bars) mice as mean + SE of five individual mice from two independent experiments. \*  $P \leq 0.05$ , \*\* $P \leq 0.01$ .

## 4.8 Anti-PD-L2 treatment during *N. brasiliensis* infection

To directly address the possibility that PD-L2 might interfere with Th2 accumulation via regulation of PD-1 in the lung, we blocked PD-L2 in wild type mice during *N. brasiliensis* infection by injection of an anti-PD-L2 antibody. 4get mice received anti-PD-L2 antibody (clone Ty25) or control rat IgG five days after *N. brasiliensis* infection and an additional injection on day eight. Lungs of anti-PD-L2- or control IgG antibody-treated mice were analyzed nine days after infection by flow cytometry for binding of an APC-labeled donkey anti-rat antibody to detect bound anti-PD-L2 antibody on the cell surface of F4/80<sup>+</sup> AAM. Cells were also stained with biotinylated anti-PD-L2 antibody (clone 122) followed by PE-Cy7-labeled streptavidin to demonstrate that the clone TY25 interferes with binding of clone 122 to PD-L2 (Figure 40). We efficiently blocked PD-L2 in wild type mice treated with an anti-PD-L2 antibody, as PD-L2 could be detected on lung macrophages from control rat IgG-treated mice but not on macrophages from mice which had been given anti-PD-L2 blocking antibody (Figure 40).

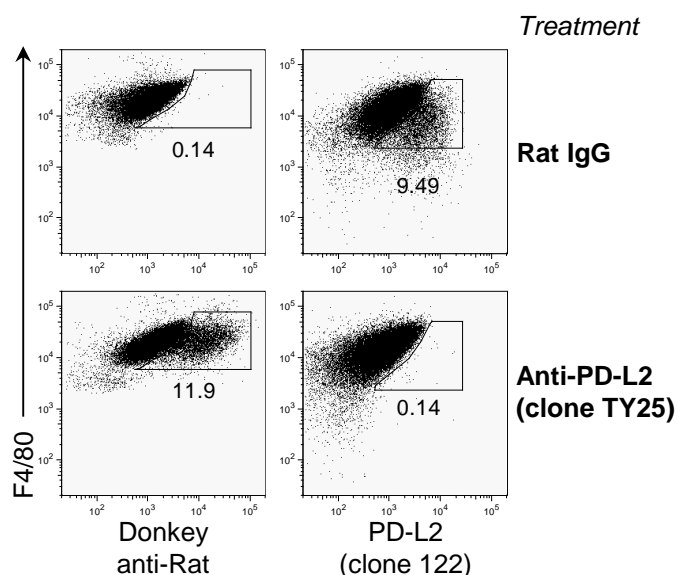


**Figure 40: Efficiency of anti-PD-L2 treatment *in vivo*.**

4get mice received i.p. injections with 500 µg/animal of anti-PD-L2 mAb (clone TY25) or control rat IgG five days after *N. brasiliensis* infection and an additional 250 µg/animal on day eight. Lungs of anti-PD-L2 or control IgG mAb-treated mice were analyzed nine days after infection by flow cytometry. Dot plots are gated on CD11c<sup>+</sup>SSC<sup>hi</sup> macrophages and show staining of F4/80 and binding of donkey anti-rat mAb or of anti-PD-L2 mAb (clone 122).

---

Staining with donkey anti-rat antibody showed almost no unspecific binding of the control rat IgG, but binding could be observed on isolated macrophages from mice treated with anti-PD-L2 antibody, indicating that this blocking antibody did not deplete AAM (Figure 40). Recent studies have shown that depletion of AAM in mice infected with *N. brasiliensis* results in impaired worm expulsion, indicating that AAM play a role in eliminating worms after infection [107]. To investigate whether PD-L2 on AAM is involved in this process, we determined adult worm numbers in the small intestine from mice treated with anti-PD-L2 antibody or with rat IgG control. On day nine after infection, almost all worms were expelled from the small intestine of mice treated with isotype control, whereas significantly more worms ( $p \leq 0.01$ ) were detected in mice treated with anti-PD-L2 antibody (Figure 41A). This observation indicates that treatment with anti-PD-L2 antibody impaired the protective responses against *N. brasiliensis* infection in the intestine.

We further analyzed PD-1 expression on CD4<sup>+</sup> T cells nine days after infection in mice treated with anti-PD-L2 antibody or with control rat IgG. Significantly more PD-1<sup>+</sup> T cells were present in the lung of anti-PD-L2-treated as compared to isotype control-treated mice ( $P \leq 0.05$ ; Figure 41B, C). Interestingly, the frequency of Th2 cells was also higher in anti-PD-L2-treated as compared to control mice, suggesting that PD-L2 on AAM attenuates the Th2 response in the lung by engaging the inhibitory receptor PD-1 on T cells ( $P \leq 0.05$ ; Figure 41B, C).

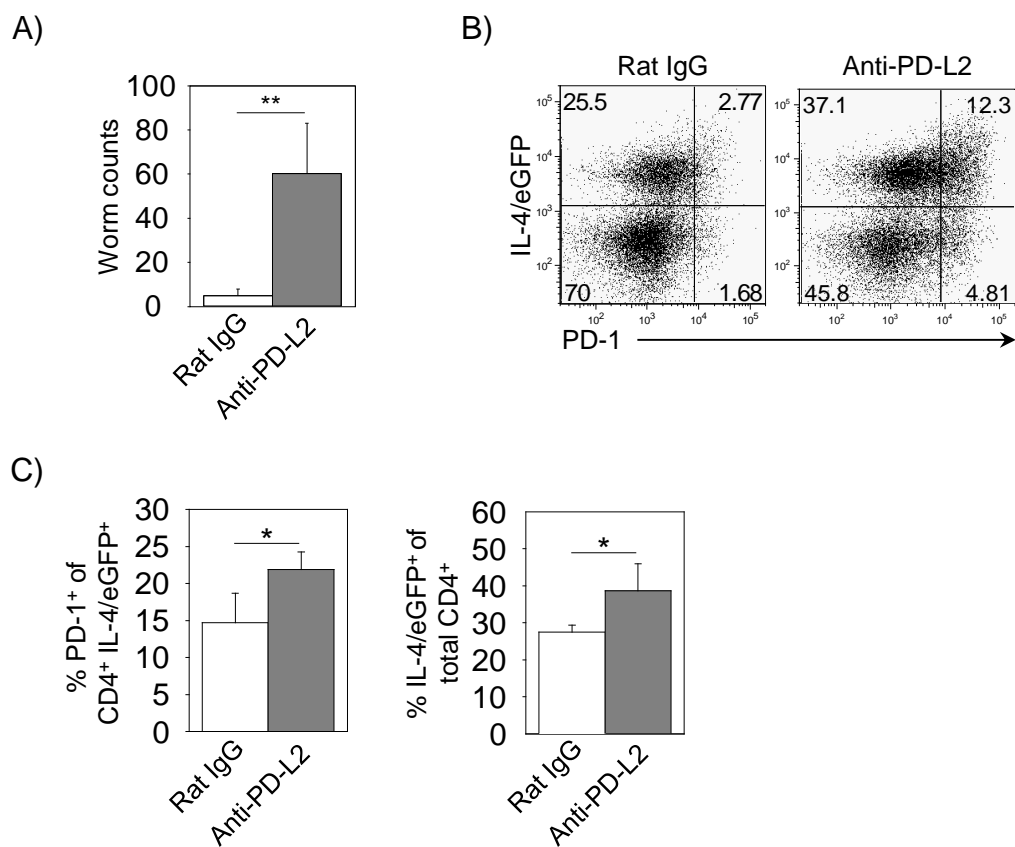


**Figure 41: Effect of anti-PD-L2 treatment after *N. brasiliensis* infection.**

Anti-PD-L2- (grey bars) treated or rat IgG- (open bar) treated 4get mice were analyzed nine days after infection. **A)** Number of adult worms in the small intestine of 4get mice that had been treated with anti-PD-L2 or rat IgG. Bar graphs show the mean + SD of four mice from two independent experiments. \*\*  $P \leq 0.01$ . **B)** Dot plots are gated on CD4<sup>+</sup> cells and show staining for PD-1 versus expression of IL-4/eGFP in the lung. **C)** Bar graphs show the frequency of PD-1<sup>+</sup> cells among CD4<sup>+</sup>IL-4/eGFP<sup>+</sup> cells (left) and the frequency of IL-4/eGFP<sup>+</sup> cells among all CD4<sup>+</sup> cells (right) as mean + SE of four individual mice from two independent experiments. \*  $P \leq 0.05$ .

---

## 5 DISCUSSION

The aim of the present thesis was to characterize the phenotype and function of AAM. Therefore, macrophages from wild type and Stat6<sup>-/-</sup> mice were compared after *in vitro* exposure to IL-4 or infection with the helminth *N. brasiliensis*. We defined expression of PD-L2 on AAM as an important mechanism by which AAM mediate immune alteration. PD-L2 is Stat6-dependent expressed on AAM *in vitro* after exposure to IL-4 and *in vivo* on lung macrophages during *N. brasiliensis* infection. Expression of PD-L2 on AAM requires IL-4 and/or IL-13 secretion from CD4<sup>+</sup> T cells. Furthermore, retroviral transduction of PD-L2 in Stat6<sup>-/-</sup> macrophages was sufficient to inhibit T cell proliferation and *in vivo* blockade of PD-L2 during *N. brasiliensis* infection caused an enhanced Th2-type immune response. Therefore, PD-L2 expression on AAM appears to provide a non-redundant inhibitory signal against T cells.

Suppression of T cell proliferation by *ex vivo* isolated macrophages was first described in mice infected with the parasitic nematode *B. malayi* [108]. The induction of these suppressive macrophages was dependent on host production of the Th2 cytokine IL-4, but independent of IL-10 [109]. Expression of Arg1, Ym1 and Relm- $\alpha$  confirmed the alternative phenotype of this nematode-elicited macrophages [110]. Further experiments revealed that the anti-proliferative effect of *B. malayi*-elicited AAM was mediated by cell-cell contact [102]. In contrast, immune regulation by macrophages recruited during *Litomosoides sigmodontis* infection was partially mediated by soluble factors, in particular TGF- $\beta$  [111]. Chronic *Taenia crassiceps* infection revealed a Stat6-dependent mechanism of T cell suppression [112]. However, since Stat6 controls many genes in different cell types it remained unclear whether Stat6 was required in macrophages themselves or in other cells to generate suppressive macrophages. We showed that macrophages exposed to IL-4 inhibited T cell proliferation in a Stat6-dependent fashion and cell intrinsic Stat6 was required for mediating this suppressive function. Other IL-4 receptor signaling pathways including the ERK/MAPK and PI3K pathways in macrophages were apparently not involved, since IL-4-exposed Stat6<sup>-/-</sup> macrophages had no suppressive activity.



---

The potent inhibitory activity of AAM is comparable to that of myeloid-derived suppressor cells (MDSC) or Foxp3-expressing Tregs [113, 114]. MDSC can inhibit T cell proliferation through depletion of L-arginine by both Arg1 and iNOS up-regulation [115-117]. Additionally, ROS production by MDSC induces post-translational modification of T cell receptors and may cause antigen-specific T cell unresponsiveness [113, 118]. MDSC also indirectly affect T cell activation by induction of Tregs, which require MDSC production of IL-10 and TGF- $\beta$  [119]. Tregs inhibit T cell proliferation through the secretion of IL-10 and TGF- $\beta$ , but cell-cell contact-dependent mechanisms have also been reported, presumably via membrane-bound TGF- $\beta$  [120-122].

One mechanism by which AAM can inhibit T cell proliferation is metabolic starvation. *L. major*-infected mice showed impaired proliferation of CD4<sup>+</sup> T cells caused by Arg1-mediated L-arginine depletion, and Arg1-inhibition restored T cell responses at the site of pathology [123]. However, Arg1 expression is not restricted through Stat6 since a novel TLR-dependent, but Stat6-independent pathway of Arg1 expression has been identified [68, 124]. Therefore, Arg1-mediated suppressive function is not strictly AAM-dependent. Relm- $\alpha$  is another Stat6-controlled secretory product of AAM which has been reported to suppress the activity of Th2 cells by limiting Th2-cytokine expression after *S. mansoni* challenge [125]. In addition to AAM, epithelial cells and eosinophils also produce Relm- $\alpha$  and could be involved in Relm- $\alpha$ -mediated inhibition of Th2 cytokine production [125, 126]. Our experiments demonstrated that Stat6 is also critical for the ability of IL-4-exposed macrophages to induce PD-L2, a ligand for the inhibitory receptor PD-1 on T cells. We showed that retroviral transduction of PD-L2 in Stat6<sup>-/-</sup> macrophages was sufficient to inhibit T cell proliferation. T cell proliferation was restored when PD-L2 was blocked on AAM, indicating the dominant role of PD-L2 as a Stat6-dependent inhibitory ligand on AAM. Interestingly, although Stat6 appears to be required for IL-4-mediated PD-L2 up-regulation on AAM, there is no Stat6 binding site in the PD-L2 promoter [80]. How Stat6 regulates PD-L2 expression remains to be established.

We compared PD-L2<sup>+</sup> and PD-L2<sup>-</sup> macrophages to other established markers for AAM and identified a direct correlation of PD-L2 expression and expression of Relm- $\alpha$ , Arg1 and Ym1. This finding now facilitates the identification and isolation of viable AAM for

further functional studies. Since Relm- $\alpha$ , Arg1 and Ym1 are secreted by AAM, the mannose receptor (CD206) has been proposed as surface marker for AAM [60]. However, in our hands the currently available antibodies against murine CD206 showed a relatively poor staining and were not suitable for flow-cytometric studies. Reese et al. previously reported the generation of an Arg1/YFP-reporter mouse which can be used to isolate Arg1-expressing macrophages [127]. However, Arg1<sup>+</sup> macrophages in this reporter mouse are not restricted to the alternative phenotype and can also include TLR-activated macrophages [124]. Therefore, PD-L2 appears to be a more specific, useful and distinctive marker for AAM.

The expression of PD-L2 on AAM during Th2-biased immune responses like helminth infections and allergic inflammation might serve to prevent uncontrolled activation of the immune system to avoid tissue damage. This hypothesis is supported by the observation that AAM are required to protect mice from lethal infection with *S. mansoni* [72]. During *N. brasiliensis* infection PD-L2 was up-regulated on lung and bronchoalveolar macrophages and expression was Stat6-dependent as Stat6<sup>-/-</sup> mice lack PD-L2 on the surface of macrophages. Interestingly, PD-L2 expression increased over time, with a peak on days 13 and 16 after infection. Studies have shown that macrophages isolated from lungs 13-15 days after *N. brasiliensis* infection exhibited an increased capacity to inhibit proliferation of CD4<sup>+</sup> T cells compared to macrophages isolated on day four post infection [71]. The relatively late expression of PD-L2 during infection with *N. brasiliensis* compared to the rapid increase of Th2-type immune responses on day nine to ten indicates that the initial Th2 response should be fast and strong, whereas an overwhelming response needs to be subsequently controlled by inhibitory mechanisms at later time points.

Although PD-L2 expression on macrophages requires IL-4/IL-13, the cellular source of these cytokines *in vivo* has not been well established and can include Th2 cells and cells of the innate immune system, such as eosinophils, mast cells and basophils. AAM could be detected in severe-combined immunodeficient (SCID) mice at early stages of infection, which indicates that innate IL-4/IL-13 producing cells are sufficient for their generation [128]. However, T cells were required to sustain AAM accumulation at later time points of infection [69]. Ohnmacht et al. have previously shown that activated basophils can induce

---

AAM [129]. As we demonstrated here using complete IL-4/IL-13 knockout mice and mice lacking IL-4/IL-13 only in CD4<sup>+</sup> T cells, IL-4/IL-13 production from T cells is indeed required for PD-L2<sup>+</sup> AAM accumulation at later stages of infection. Since most IL-4 production is attributed to T cells, the source and thereby the amount of secreted IL-4/IL-13 may have an effect on PD-L2 surface expression on AAM [130].

Apart from AAM, PD-L2 expression is mainly restricted to DCs, bone marrow-derived mast cells and B1 B cells in the peritoneum, whereas PD-L1 is expressed constitutively on monocyte-derived cells, epithelial cells, endothelial cells and many tumors [77]. The *in vivo* role of PD-L1 has been studied more extensively than that of PD-L2. PD-L1 expression on tumors inhibits the activity of tumor-specific cytotoxic T cells [131]. Apoptosis of CD8<sup>+</sup> T cells in the liver is reduced in PD-L1<sup>-/-</sup> mice, and T cell responses in these mice are increased [132, 133]. These results demonstrate an important inhibitory role for PD-L1 *in vivo*, whereas PD-L2 seems to play a minor role, probably due to the more restricted expression and requirement of Th2-biased immune responses for PD-L2 induction [77]. Distinct roles for PD-L1 and PD-L2 have been shown in murine asthma models. PD-L1 expression inhibited IFN- $\gamma$  production of invariant natural killer T (iNKT) cells which mitigated airway hyperreactivity, whereas PD-L2 down-regulated iNKT cell function and IL-4 production, thereby modulating the severity of asthma [134]. The effect of PD-L2 has mostly been analyzed in complete PD-L2<sup>-/-</sup> mice. Mice lacking PD-L2 showed decreased IFN- $\gamma$  and IL-2 production associated with increased IL-4 responses after CD4<sup>+</sup> T cell stimulation with activated DCs, indicating that PD-L2 serves as a co-stimulator of Th1 responses [135, 136]. However, the effect of PD-L2 in these studies was restricted to DCs and thereby disregarded the induced expression of PD-L2 on macrophages during a Th2-type immune response. A recent report evaluated the role of PD-L2 under highly Th2-polarizing conditions and demonstrated that PD-L2<sup>-/-</sup> mice generated an enhanced type 2 immune response with enhanced IL-4 production and increased levels of eosinophils and serum IgE after *N. brasiliensis* infection [137]. Interestingly, PD-L1 and PD-L2 can also act as co-stimulatory ligands, as shown in cultures of T cells from PD-1<sup>-/-</sup> mice, and it has been proposed that a second receptor with activating properties exists for these ligands [138]. In addition, retrograde signaling for both ligands has been suggested, which requires further investigation [133, 139].

---

We observed that PD-1 was transiently induced on Th2 cells *in vivo* after infection of mice with *N. brasiliensis*. Consistent with these results, recent studies have shown that PD-1 is expressed on T follicular helper (T<sub>FH</sub>) cells differentiated from Th2 cells in response to helminth infection [140, 141]. T<sub>FH</sub> cells up-regulate PD-1 expression during the course of infection [140]. Further studies identified that also exhausted T cells are characterized by sustained expression of PD-1 [142]. Exhausted T cells fail to proliferate and exert effector functions such as cytotoxicity and cytokine secretion in response to antigen stimulation. Blockade of PD-1 and PD-ligand interactions can reverse T cell exhaustion [142]. In an autoimmune setting, PD-1 is essential for maintaining T cell anergy and preventing autoimmunity [136]. Interestingly, we observed enhanced and prolonged expression of PD-1 on Th2 cells of Stat6<sup>-/-</sup> mice after *N. brasiliensis* infection. Additionally, wild type Th2 cells down-regulated PD-1 after day 13 whereas Stat6<sup>-/-</sup> Th2 cells maintained PD-1 expression for at least one more week. This could be due to delayed worm expulsion in Stat6<sup>-/-</sup> mice, which might cause prolonged activation of T cells. Alternatively, PD-L2 expression in wild type mice could either inhibit expansion of PD-1<sup>+</sup> CD4<sup>+</sup> T cells or cause down-regulation of PD-1. Our experiments with mixed bone marrow chimeras generated with bone marrow from wild type and Stat6<sup>-/-</sup> mice revealed that expression of PD-1 on Th2 cells was higher in the Stat6<sup>-/-</sup> population than in the wild type population, indicating that PD-1 expression is partly directly regulated by Stat6 in a cell-intrinsic manner. Additionally, blocking of PD-L2 *in vivo* during infection with *N. brasiliensis* resulted in significantly higher levels of PD-1<sup>+</sup> Th2 cells, suggesting that PD-L2 on AAM attenuates the Th2 response at the site of infection by engaging PD-1 on IL-4 expressing T cells. We conclude that a cooperation of both PD-L2 on AAM and Stat6-dependent cell intrinsic factors is required for the regulation of PD-1 expression on Th2 cells. The affinity of PD-1 to PD-L2 is 2-6-fold higher than that of PD-1 to PD-L1 [143]. As studies have shown that the PD-1/PD-L1 interaction produces a Th2 response with more IL-4 production, PD-L2 up-regulation at later time points of infection may dampen the effect of PD-L1 through binding with a higher affinity to PD-1 and further down-regulation of the PD-1 receptor [134].

Expulsion of *N. brasiliensis* adult worms from the intestinal lumen seems to be Stat6-dependent [38]. The failure of Stat6<sup>-/-</sup> mice to expel *N. brasiliensis* is not a result of

decreased IL-4 production, as IL-4<sup>-/-</sup> mice retained the capacity to expel this parasite. In contrast, mice that lack IL-4R $\alpha$  have impaired worm expulsion [38]. These observations suggest that IL-13, the only cytokine other than IL-4 that can efficiently activate Stat6 through IL-4R $\alpha$ , might be involved in the expulsion of *N. brasiliensis*. Our experiments with anti-PD-L2 blocking antibody treatment of wild type mice during *N. brasiliensis* infection demonstrated that the IL-4 and/or IL-13-dependent expression of PD-L2 is associated with increased worm expulsion. These results indicate that Stat6-dependent PD-L2 expression on AAM contributes importantly to the protection against *N. brasiliensis* (Figure 42).

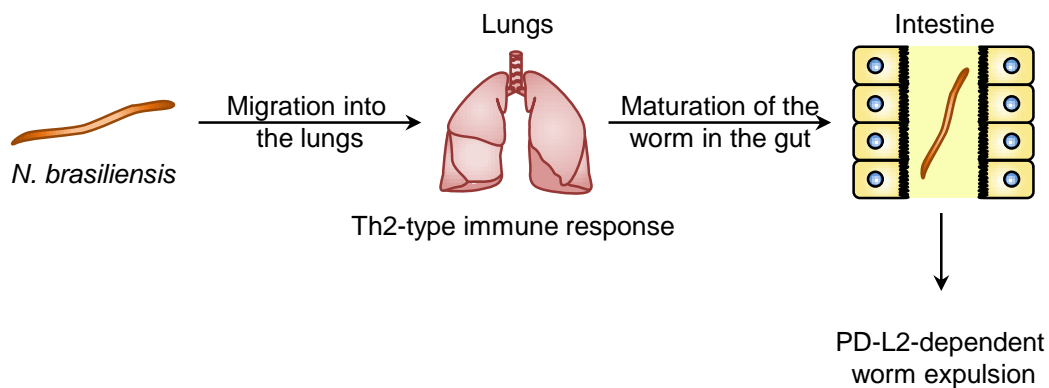


**Figure 42: PD-L2-dependent worm expulsion.**

*N. brasiliensis* larvae are carried by blood circulation to the lungs, where an inflammatory immune response is induced. The larvae are coughed up, enter the intestine and attach to the intestinal wall where they develop into adult worms. During different stages of development, *N. brasiliensis* causes local inflammation first in the lung and subsequently in the small intestine with local and systemic Th2-type responses. Adult worms are expelled from the gut. The Th2 cytokines IL-4 and IL-13 might facilitate expulsion of adult parasites by inducing the expression of PD-L2 on AAM.

Another unresolved issue was the requirement of Stat6 for mobilization and recruitment of macrophages. Earlier studies reported that Stat6<sup>-/-</sup> mice show increased numbers of progenitors of the myeloid lineage [144]. Our experiments with mixed bone marrow chimeras generated with bone marrow from wild type and Stat6<sup>-/-</sup> mice demonstrated that Stat6 was not required in macrophages for development or tissue recruitment to the site of infection. Interestingly, BrdU incorporation was increased in splenic and peritoneal macrophages after *N. brasiliensis* infection, although the parasite does not affect these sites. Furthermore, wild type macrophages seemed to survive better in the lung and

peritoneum, suggesting that Stat6-dependent cell-intrinsic factors could prolong the lifespan of macrophages in selected tissues.

CCR2 and CCR5 are two chemokine receptors that are important players in the trafficking and survival of monocytes and macrophages [104, 145]. However, the involvement of CCR2 in promoting macrophage accumulation seems to be dependent on the macrophage phenotype. It has been reported that the recruitment of inflammatory (thioglycollate-elicited), but not resting peritoneal macrophages requires CCR2 [104]. We observed CCR2- and CCR5-independent macrophage recruitment after *N. brasiliensis* infection to the site of infection.

A prototypic macrophage membrane molecule highly restricted to mature macrophages subpopulations residing in tissues is the F4/80 glycoprotein. Studies have shown that the F4/80 molecule is not essential for survival after challenge with *L. monocytogenes* [97]. Furthermore, recruitment of macrophages into tissues of infected organs can occur even in the absence of F4/80. Since *L. monocytogenes* induces a Th1-type immune response, we used the *N. brasiliensis* infection model to analyze macrophage recruitment in F4/80-deficient mice during a Th2-type inflammation. These experiments showed that the F4/80 molecule also seems to play a minor role during Th2-type immune responses in tissue specific macrophage accumulation. Further analysis are required to investigate whether AAM differentiate during helminth infection from circulating precursors or from resident macrophages following local proliferation and switching to an alternative phenotype.

Finally, we were able to demonstrate that AAM can respond to pro-inflammatory stimuli and CAM to anti-inflammatory stimuli. Following overnight incubation of AAM with LPS, there was a down-regulation of the alternative activation marker PD-L2. This reduction was accompanied by an up-regulation of PD-L1. IL-4 treatment appeared to promote an alternatively activated phenotype in CAM through expression of PD-L2. This suggests that the differentiation state of macrophages remains flexible and that macrophages might be able to change their phenotype during infection. Thereby the length and order of cytokine treatment seems to be important for the regulation of macrophage function [146]. Studies using mice infected with the nematode *B. malayi* as a source of

macrophages with an alternatively activated phenotype showed that these macrophages were still responsive to treatment with LPS/IFN- $\gamma$ , changed their gene expression profile, and acquired bactericidal activity [147]. The capacity of macrophages to maintain phenotypic and functional plasticity might be important for the regulation of infection: first for antigen elimination through bactericidal and phagocytic activity of CAM and later with anti-inflammatory signals from AAM to help to remodel injured tissues and prevent excessive inflammation. Additionally, studies have shown that tumor-bearing mice systemically treated with IL-12 altered the functional responses of macrophages from a predominantly anti-inflammatory to a more pro-inflammatory phenotype, indicating that macrophage polarization may also have therapeutic potential [148].

In this study we have demonstrated that selective up-regulation of PD-L2 on macrophages has the ability to subvert the immune system by inhibiting T cell proliferation. Therefore, expression of PD-L2 on AAM is an important mechanism by which AAM mediate a reduction in immunopathology during Th2-type immune responses [149]. An overview of the identified functions of AAM during Th2-type inflammation is shown in Figure 43. The induced expression of PD-L2 on AAM is Stat6-dependent, whereas the expression of this ligand on DCs is constant and does not require Stat6 during the course of *N. brasiliensis* infection. However, it would be of further interest to investigate whether the suppressive activity of PD-L2 on T cells and the requirement of this ligand for worm expulsion are restricted to the expression on AAM. To address this question it would be helpful to generate mice in which macrophages only lack PD-L2. There is currently limited information on the homing of CAM and AAM. Transferring *in vitro* differentiated or *in vivo* generated AAM or CAM into recipient mice could help to further define the homing behavior of activated macrophages. Additionally, phenotypic plasticity studies of macrophages could be performed by transferring AAM into mice infected with lymphocytic choriomeningitis virus, which induces a strong Th1 immune response. In parallel experiments the flexibility of CAM in a Th2-type environment could be analyzed by transferring CAM into *N. brasiliensis* infected mice. Transferring AAM into mice in which experimental allergic encephalomyelitis has been induced could be a useful tool to investigate whether AAM can suppress auto-reactive T cell responses and whether AAM home to the central nervous system and interact with effector T cells. Finally, a better

understanding of the contribution of AAM to fibrosis, tissue remodeling and immunosuppression might help to identify new therapeutic targets for patients suffering chronic Th2-associated diseases.

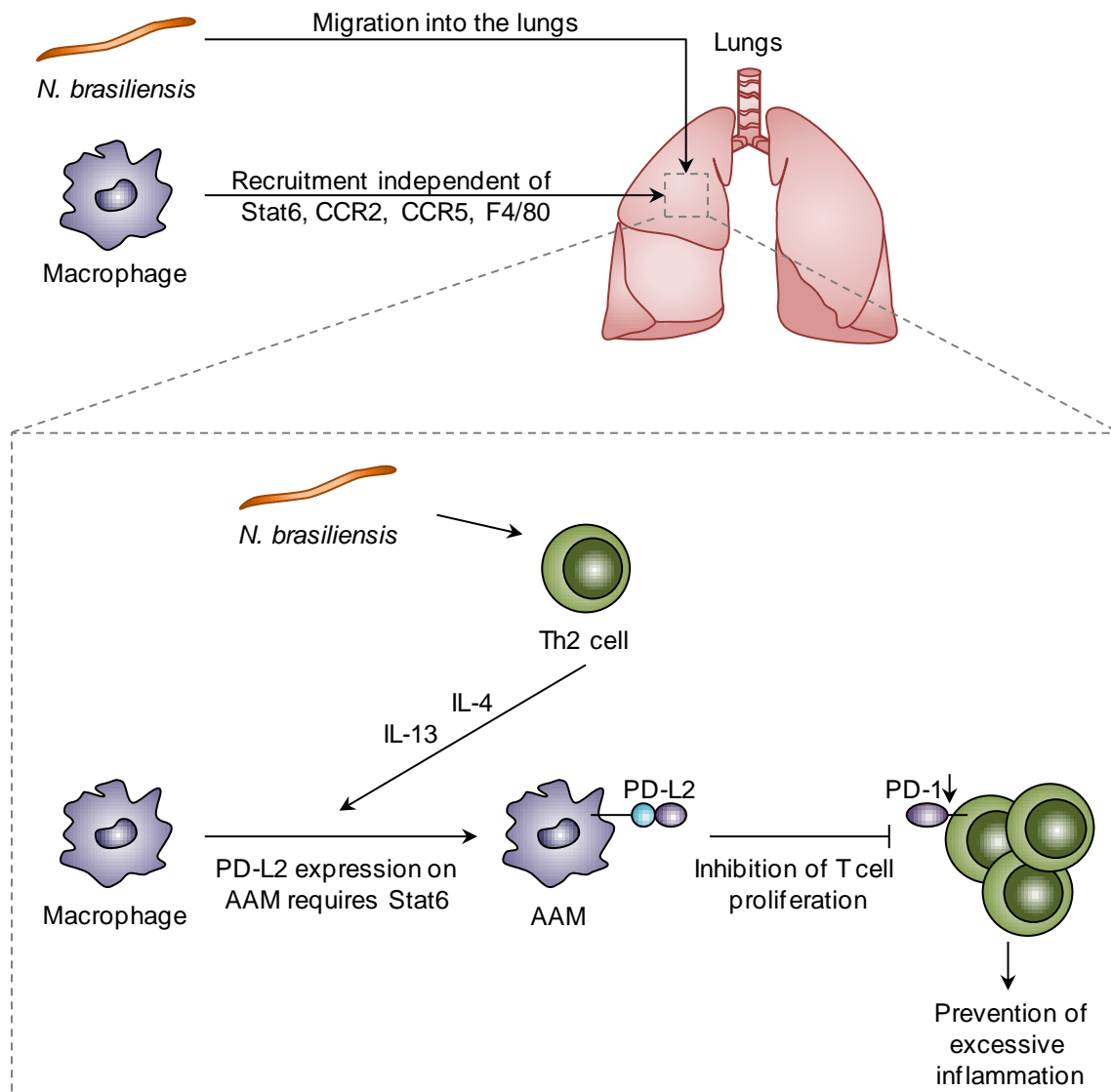


**Figure 43: Model of the protective function of AAM during helminth infection.**

The entry of *N. brasiliensis* into the lungs results in the differentiation of naïve  $CD4^+$  T cells toward Th2 cells. Macrophages are recruited to the site of infection through a Stat6-, CCR2-, CCR5- and F4/80-independent mechanism and acquire an alternative activated phenotype in the presence of IL-4 and IL-13 from Th2 cells. AAM inhibit T cell proliferation by Stat6-dependent expression of the PD-1-ligand PD-L2 and thereby control an overwhelming immune response.



---

## LIST OF FIGURES

Figure 1: IL-4R signaling pathway. ....	5
Figure 2: Macrophage origin and development. ....	6
Figure 3: Innate and adaptive immune activation of macrophages.....	8
Figure 4: Classical and alternative activation of macrophages. ....	10
Figure 5: B7:CD28 family members. ....	12
Figure 6: Schematic of the PD-L2 IRES GFP vector used for the transduction of PD-L2 into macrophages. ....	36
Figure 7: Transfection of Phoenix E cells for virus production and transduction of macrophages. ....	39
Figure 8: Surface expression of F4/80 on bone marrow-derived macrophages.....	40
Figure 9: T cell proliferation in the presence of control wild type bone marrow-derived macrophages. ....	41
Figure 10: Suppression of T cell proliferation by IL-4-exposed macrophages.....	42
Figure 11: Cell-cell contact-dependent T cell suppression by IL-4-exposed macrophages. ....	43
Figure 12: High purity of control or IL-4-treated BMDM.....	44
Figure 13: Stat6-regulated gene expression profile of macrophages. ....	45
Figure 14: Quantitative RT-PCR analysis of selected genes based on the microarray analysis. ....	46
Figure 15: Stat6-dependent expression of PD-L2 on the surface of IL-4-exposed BMDM.....	49
Figure 16: Comparison of IL-4-induced expression of PD-L2 on BMDM to other B7 family members. ....	50
Figure 17: Comparison of IL-4-induced expression of PD-L2 on peritoneal macrophages to other B7 family members. ....	51
Figure 18: Comparison of B7 family members on control and IL-4-exposed bone marrow-derived DCs. ....	52
Figure 19: PD-L2 surface expression: kinetics and correlations with AAM markers. ....	53
Figure 20: Cell intrinsic requirement of Stat6 for PD-L2 expression. ....	54
Figure 21: Plasticity of PD-L1 and PD-L2 surface expression on AAM and CAM.....	55
Figure 22: PD-L2-mediated inhibition of CD4 <sup>+</sup> T cell proliferation.....	56

## LIST OF FIGURES

---

Figure 23: Analysis of PD-L2 expression on WT naïve splenocytes. ....	57
Figure 24: Retroviral vector encoding murine PD-L2. ....	58
Figure 25: Retroviral expression of PD-L2 in Stat6 <sup>-/-</sup> macrophages. ....	59
Figure 26: PD-L2 expression on macrophages <i>in vivo</i> during <i>N. brasiliensis</i> infection....	61
Figure 27: PD-L1 expression on macrophages <i>in vivo</i> after <i>N. brasiliensis</i> infection.....	62
Figure 28: Stat6-dependent PD-L2 expression in lung tissue of <i>N. brasiliensis</i> infected mice.....	63
Figure 29: Analysis of T cell derived IL-4/IL-13 for PD-L2 expression on AAM <i>in</i> <i>vivo</i> .....	64
Figure 30: Overview of BrdU treatment in <i>N. brasiliensis</i> infected mixed bone marrow chimeras. ....	65
Figure 31: BrdU staining of macrophages in mixed bone marrow chimeras after <i>N.</i> <i>brasiliensis</i> infection.....	66
Figure 32: Analysis of Stat6 requirement for accumulation of macrophages after infection. ....	67
Figure 33: Analysis of CCR2 requirement for recruitment of macrophages after infection. ....	68
Figure 34: Analysis of CCR5 requirement for recruitment of macrophages after infection. ....	69
Figure 35: Analysis of F4/80 requirement for recruitment of macrophages after infection. ....	70
Figure 36: Analysis of PD-1 expression on Th2 cells after <i>N. brasiliensis</i> infection.....	71
Figure 37: PD-1 expression on Th2 cells during <i>N. brasiliensis</i> infection. ....	72
Figure 38: Overview of the generation of mixed bone marrow chimeras. ....	73
Figure 39: PD-1 expression on Th2 cells in mixed bone marrow chimeras. ....	74
Figure 40: Efficiency of anti-PD-L2 treatment <i>in vivo</i> . ....	75
Figure 41: Effect of anti-PD-L2 treatment after <i>N. brasiliensis</i> infection. ....	77
Figure 42: PD-L2-dependent worm expulsion.....	83
Figure 43: Model of the protective function of AAM during helminth infection.....	86

---

---

## LIST OF TABLES

Table 1:	Equipment.....	15
Table 2:	Computer software.....	16
Table 3:	Consumable material .....	16
Table 4:	Reagents.....	17
Table 5:	Commercial kits.....	19
Table 6:	Cytokines .....	19
Table 7:	Enzymes.....	19
Table 8:	Media .....	20
Table 9:	Buffer and cell culture media .....	20
Table 10:	Anti-mouse antibodies .....	21
Table 11:	Anti-rabbit antibodies .....	22
Table 12:	Isotypes .....	22
Table 13:	Streptavidin.....	22
Table 14:	Primer sequences .....	22
Table 15:	Mouse strains .....	23
Table 16:	Rat strain.....	24
Table 17:	Cell lines .....	24
Table 18:	Bacterial strain.....	24
Table 19:	Gene expression analysis of control and IL-4-treated BMDM. ....	47

---

## ABBREVIATIONS

AAM	alternatively activated macrophages
Ab	antibody
ACK	ammonium chloride-potassium
APC	antigen presenting cells
APC	allophycocyanin
Arg1	arginase1
BAL	bronchoalveolar lavage
bp	base pair
BCR	B cell receptor
BES	N,N-Bis(2-hydroxyethyl)-2-aminoethanesulfonic acid
BM	bone marrow
BMDC	bone marrow-derived dendritic cells
BMDM	bone marrow-derived macrophages
BrdU	5-bromo-2'-deoxyuridine
BSA	bovine serum albumin
CAM	classically activated macrophages
CCR	chemokine (C-C motif) receptor
CD	cluster of differentiation
cDC	conventional dendritic cell
cDNA	complementary deoxyribonucleic acid
CFSE	carboxyfluorescein succinimidyl ester
CTLA-4	cytotoxic T-lymphocyte antigen-4
Cre	Cre recombinase
d	day
DAPI	4', 6'-diamidino-2-phenylindol
dATP	deoxyadenosine triphosphate
DC	dendritic cell
dCTP	deoxycytidine triphosphate
DEPC	diethylpyrocarbonate
dGTP	deoxyguanosine triphosphate
DMEM	Dulbecco's Modified Eagle's Medium
DNA	deoxyribonucleic acid
dNTP	deoxynucleoside triphosphate
DTT	dithiothreitol
dTTP	deoxythymidine triphosphate
EDTA	ethylenediaminetetraacetic acid
eGFP	enhanced green fluorescent protein
ERK	extracellular-signal-regulated kinases
FACS	fluorescence activated cell sorter

---

Fcgr	Fc receptor, IgG, low affinity IV
FCS	fetal calf serum
F/F	flox/flox
FITC	fluorescein isothiocyanate
FIZZ1	found in inflammatory zone 1
Foxp3	forkead box P3
FSC	forward scatter
GATA-3	GATA-binding protein 3
GEO	Gene Expression Omnibus
GFP	green fluorescent protein
GM-CSF	granulocyte macrophage colony-stimulating factor
Grb-2	Growth factor receptor-bound protein 2
h	hour
hi	high
HSC	hematopoietic stem cell
IFN	interferon
Ig	immunoglobulin
IL	interleukin
iNKT	invariant natural killer T cell
iNOS	inducible nitric oxide synthase
i.p.	intraperitoneal
IRES	internal ribosome entry site
IRS	insulin receptor substrate
Itga	integrin alpha
ITIM	immunoreceptor tyrosine-based inhibitory motif
i.v.	intravenous
JAK	Janus kinase
L3	third-stage larvae
LN	lymph node
LPS	lipopolysaccharide
LU	lung
M $\phi$	macrophages
mAb	monoclonal antibody
MAPK	mitogen-activated protein kinase
M-CSF	macrophage colony-stimulating factor
MDSC	myeloid-derived suppressor cells
MHC	major histocompatibility complex
min	minute
MLN	mesenteric lymph node
MR	mannose receptor
mRNA	messenger ribonucleic acid

---

---

NK cells	natural killer cells
NKT cells	natural killer T cells
NO	nitric oxide
n.s.	not significant
PAMP	pathogen-associated molecular patterns
PBS	phosphate buffered saline
PCR	polymerase chain reaction
PD-1	programmed death-1
pDC	plasmacytoid dendritic cell
PD-L	programmed death-ligand
PE	phycoerythrin
PEC	peritoneal exudate cells
PECy	phycoerythrin-cychrome
PerCP	peridinin chlorophyll protein
PI3K	phosphoinositide 3-kinase
PPAR	peroxisome proliferator-activated receptor
R	receptor
Relm $\alpha$ (retnla)	resistin-like molecule alpha
RNA	ribonucleic acid
ROR- $\gamma$ t	retinoid acid-related orphan nuclear hormone receptor- $\gamma$ t
ROS	reactive oxygen species
rpm	rounds per minute
RPMI	Roswell Park Memorial Institute
RT	real time
Scd	stearoyl-coenzyme A desaturase
SCID	severe-combined immunodeficient
SD	standard deviation
SE	standard error
sec	seconds
SH2	Src homology 2 domain
SHIP	SH2-containing inositol-5-phosphatase
SP	spleen
Sqle	squalene epoxidase
SSC	side scatter
Stat	signal transducer and activator of transcription
T-bet	T-box transcription factor
TCR	T cell receptor
T <sub>FH</sub>	T follicular helper cell
TGF	transforming growth factor
Th	T helper cell
TLR	Toll-like receptor
TNF	tumor necrosis factor
Treg	regulatory T cell

---

WT	wild type
$\gamma_c$	common $\gamma$ -chain
Ym1 (chi3l3)	chitinase 3-like 3

---

## ACKNOWLEDGEMENTS

The Institute for Immunology at the Ludwig-Maximilians-University is a dynamic and motivating research institute and it has been a privilege to undertake my PhD in such a collaborative environment. First I want to express my sincere gratitude to my supervisor Prof. David Vöhringer for giving me the chance to join his laboratory and for providing this interesting project as well as supporting me with his inspiring ideas and discussions.

I am very grateful to my supervisor at the Technical University Munich, Prof. Dirk Haller, for the time and energy to read this thesis and for his support throughout this work. My thanks also go to Prof. Michael Schemann for his agreement to act as chairman.

Special thanks go to the colleagues at the Vöhringer laboratory for their scientific but especially for the mental support as well as for the fun we had and for the continuous supply of chocolate. My thanks go to Caspar Ohnmacht, Alexander Seidl, Marc Panzer, Stefanie Wirth, Isabell Schiedewitz, Adriana Turqueti-Neves and Christian Schwartz.

I would like to thank Dr. Reinhard Hoffmann for providing microarray analysis and Femke Muskens for generating and providing retroviral constructs. Thanks to the 4<sup>th</sup> floor animal room staff, particularly Andrea Bol and Wolfgang Mertl for keeping the mouse house running. Special thanks also go to Marian Turner and Sandra Baumann for helpful comments.

Ich möchte mich ganz herzlich bei meiner Mutter für ihre Liebe und ihre uneingeschränkte Unterstützung bedanken und meinem Bruder für seine besondere Fähigkeit, mich auf den Boden der Tatsachen zurück zu holen und nicht zu vergessen, danke für die jährlichen Skiurlaube.

Mein ganz besonderer Dank gilt meinem Mann Christoph, für seine fortwährende Unterstützung und Geduld während meiner Promotion und für seine ruhige, ausgeglichene, liebevolle Art, die mein Leben so sehr bereichert.



---

## REFERENCES

1. Murphy, K.N., Travers, P., Walport, M., *Janeway's Immunobiology*. Seventh ed. 2007: Garland Science.
2. Mosmann, T.R. and R.L. Coffman, *TH1 and TH2 cells: different patterns of lymphokine secretion lead to different functional properties*. *Annu Rev Immunol*, 1989. **7**: p. 145-73.
3. Szabo, S.J., et al., *A novel transcription factor, T-bet, directs Th1 lineage commitment*. *Cell*, 2000. **100**(6): p. 655-69.
4. Murphy, K.M. and S.L. Reiner, *The lineage decisions of helper T cells*. *Nat Rev Immunol*, 2002. **2**(12): p. 933-44.
5. Abbas, A.K., K.M. Murphy, and A. Sher, *Functional diversity of helper T lymphocytes*. *Nature*, 1996. **383**(6603): p. 787-93.
6. Zheng, W. and R.A. Flavell, *The transcription factor GATA-3 is necessary and sufficient for Th2 cytokine gene expression in CD4 T cells*. *Cell*, 1997. **89**(4): p. 587-96.
7. Zhang, D.H., et al., *Transcription factor GATA-3 is differentially expressed in murine Th1 and Th2 cells and controls Th2-specific expression of the interleukin-5 gene*. *J Biol Chem*, 1997. **272**(34): p. 21597-603.
8. Paul, W.E. and J. Zhu, *How are T(H)2-type immune responses initiated and amplified?* *Nat Rev Immunol*. **10**(4): p. 225-35.
9. Coffman, R.L. and T.R. Mosmann, *CD4+ T-cell subsets: regulation of differentiation and function*. *Res Immunol*, 1991. **142**(1): p. 7-9.
10. Langrish, C.L., et al., *IL-23 drives a pathogenic T cell population that induces autoimmune inflammation*. *J Exp Med*, 2005. **201**(2): p. 233-40.
11. Veldhoen, M., et al., *TGFbeta in the context of an inflammatory cytokine milieu supports de novo differentiation of IL-17-producing T cells*. *Immunity*, 2006. **24**(2): p. 179-89.
12. Ivanov, II, et al., *The orphan nuclear receptor RORgamma directs the differentiation program of proinflammatory IL-17+ T helper cells*. *Cell*, 2006. **126**(6): p. 1121-33.
13. Acosta-Rodriguez, E.V., et al., *Surface phenotype and antigenic specificity of human interleukin 17-producing T helper memory cells*. *Nat Immunol*, 2007. **8**(6): p. 639-46.
14. Sakaguchi, S., et al., *Immunologic self-tolerance maintained by activated T cells expressing IL-2 receptor alpha-chains (CD25). Breakdown of a single mechanism of self-tolerance causes various autoimmune diseases*. *J Immunol*, 1995. **155**(3): p. 1151-64.
15. Fontenot, J.D., M.A. Gavin, and A.Y. Rudensky, *Foxp3 programs the development and function of CD4+CD25+ regulatory T cells*. *Nat Immunol*, 2003. **4**(4): p. 330-6.
16. von Herrath, M.G. and L.C. Harrison, *Antigen-induced regulatory T cells in autoimmunity*. *Nat Rev Immunol*, 2003. **3**(3): p. 223-32.
17. Nelms, K., et al., *The IL-4 receptor: signaling mechanisms and biologic functions*. *Annu Rev Immunol*, 1999. **17**: p. 701-38.

18. Lee, F., et al., *Isolation and characterization of a mouse interleukin cDNA clone that expresses B-cell stimulatory factor 1 activities and T-cell- and mast-cell-stimulating activities*. Proc Natl Acad Sci U S A, 1986. **83**(7): p. 2061-5.
19. Yoshimoto, T. and W.E. Paul, *CD4pos, NK1.1pos T cells promptly produce interleukin 4 in response to in vivo challenge with anti-CD3*. J Exp Med, 1994. **179**(4): p. 1285-95.
20. Dubucquoi, S., et al., *Interleukin 5 synthesis by eosinophils: association with granules and immunoglobulin-dependent secretion*. J Exp Med, 1994. **179**(2): p. 703-8.
21. Hsieh, C.S., et al., *Differential regulation of T helper phenotype development by interleukins 4 and 10 in an alpha beta T-cell-receptor transgenic system*. Proc Natl Acad Sci U S A, 1992. **89**(13): p. 6065-9.
22. Coffman, R.L., et al., *B cell stimulatory factor-1 enhances the IgE response of lipopolysaccharide-activated B cells*. J Immunol, 1986. **136**(12): p. 4538-41.
23. Vitetta, E.S., et al., *Serological, biochemical, and functional identity of B cell-stimulatory factor 1 and B cell differentiation factor for IgG1*. J Exp Med, 1985. **162**(5): p. 1726-31.
24. Kawakami, T. and S.J. Galli, *Regulation of mast-cell and basophil function and survival by IgE*. Nat Rev Immunol, 2002. **2**(10): p. 773-86.
25. Dabbagh, K., et al., *IL-4 induces mucin gene expression and goblet cell metaplasia in vitro and in vivo*. J Immunol, 1999. **162**(10): p. 6233-7.
26. Noelle, R., et al., *Increased expression of Ia antigens on resting B cells: an additional role for B-cell growth factor*. Proc Natl Acad Sci U S A, 1984. **81**(19): p. 6149-53.
27. Conrad, D.H., et al., *Effect of B cell stimulatory factor-1 (interleukin 4) on Fc epsilon and Fc gamma receptor expression on murine B lymphocytes and B cell lines*. J Immunol, 1987. **139**(7): p. 2290-6.
28. Ohara, J. and W.E. Paul, *Up-regulation of interleukin 4/B-cell stimulatory factor 1 receptor expression*. Proc Natl Acad Sci U S A, 1988. **85**(21): p. 8221-5.
29. Gordon, S., *Alternative activation of macrophages*. Nat Rev Immunol, 2003. **3**(1): p. 23-35.
30. Russell, S.M., et al., *Interleukin-2 receptor gamma chain: a functional component of the interleukin-4 receptor*. Science, 1993. **262**(5141): p. 1880-3.
31. Hilton, D.J., et al., *Cloning and characterization of a binding subunit of the interleukin 13 receptor that is also a component of the interleukin 4 receptor*. Proc Natl Acad Sci U S A, 1996. **93**(1): p. 497-501.
32. Hou, J., et al., *An interleukin-4-induced transcription factor: IL-4 Stat*. Science, 1994. **265**(5179): p. 1701-6.
33. Keegan, A.D., et al., *An IL-4 receptor region containing an insulin receptor motif is important for IL-4-mediated IRS-1 phosphorylation and cell growth*. Cell, 1994. **76**(5): p. 811-20.
34. Kaplan, M.H., et al., *Stat6 is required for mediating responses to IL-4 and for development of Th2 cells*. Immunity, 1996. **4**(3): p. 313-9.
35. Knott, M.L., et al., *The roles of eotaxin and the STAT6 signalling pathway in eosinophil recruitment and host resistance to the nematodes Nippostrongylus brasiliensis and Heligmosomoides bakeri*. Mol Immunol, 2009. **46**(13): p. 2714-22.
36. Fulkerson, P.C., et al., *Pulmonary chemokine expression is coordinately regulated by STAT1, STAT6, and IFN-gamma*. J Immunol, 2004. **173**(12): p. 7565-74.

37. Khan, W.I., et al., *Stat6 dependent goblet cell hyperplasia during intestinal nematode infection*. Parasite Immunol, 2001. **23**(1): p. 39-42.
38. Urban, J.F., Jr., et al., *IL-13, IL-4Ralpha, and Stat6 are required for the expulsion of the gastrointestinal nematode parasite Nippostrongylus brasiliensis*. Immunity, 1998. **8**(2): p. 255-64.
39. Franke, T.F., et al., *Direct regulation of the Akt proto-oncogene product by phosphatidylinositol-3,4-bisphosphate*. Science, 1997. **275**(5300): p. 665-8.
40. Tauber, A.I., *Metchnikoff and the phagocytosis theory*. Nat Rev Mol Cell Biol, 2003. **4**(11): p. 897-901.
41. Pollard, J.W., *Trophic macrophages in development and disease*. Nat Rev Immunol, 2009. **9**(4): p. 259-70.
42. Gordon, S. and P.R. Taylor, *Monocyte and macrophage heterogeneity*. Nat Rev Immunol, 2005. **5**(12): p. 953-64.
43. van oud Alblas, A.B. and R. van Furth, *Origin, Kinetics, and characteristics of pulmonary macrophages in the normal steady state*. J Exp Med, 1979. **149**(6): p. 1504-18.
44. Bouwens, L., et al., *Quantitation, tissue distribution and proliferation kinetics of Kupffer cells in normal rat liver*. Hepatology, 1986. **6**(4): p. 718-22.
45. Mosser, D.M. and J.P. Edwards, *Exploring the full spectrum of macrophage activation*. Nat Rev Immunol, 2008. **8**(12): p. 958-69.
46. Kono, H. and K.L. Rock, *How dying cells alert the immune system to danger*. Nat Rev Immunol, 2008. **8**(4): p. 279-89.
47. Taylor, P.R., et al., *Macrophage receptors and immune recognition*. Annu Rev Immunol, 2005. **23**: p. 901-44.
48. Akira, S., K. Takeda, and T. Kaisho, *Toll-like receptors: critical proteins linking innate and acquired immunity*. Nat Immunol, 2001. **2**(8): p. 675-80.
49. Nimmerjahn, F. and J.V. Ravetch, *Fc gamma receptors: old friends and new family members*. Immunity, 2006. **24**(1): p. 19-28.
50. Barrington, R., et al., *The role of complement in inflammation and adaptive immunity*. Immunol Rev, 2001. **180**: p. 5-15.
51. Anderson, C.F. and D.M. Mosser, *Cutting edge: biasing immune responses by directing antigen to macrophage Fc gamma receptors*. J Immunol, 2002. **168**(8): p. 3697-701.
52. Dalton, D.K., et al., *Multiple defects of immune cell function in mice with disrupted interferon-gamma genes*. Science, 1993. **259**(5102): p. 1739-42.
53. Young, H.A., *Unraveling the pros and cons of interferon-gamma gene regulation*. Immunity, 2006. **24**(5): p. 506-7.
54. Van Ginderachter, J.A., et al., *Classical and alternative activation of mononuclear phagocytes: picking the best of both worlds for tumor promotion*. Immunobiology, 2006. **211**(6-8): p. 487-501.
55. Pfeffer, K., et al., *Mice deficient for the 55 kd tumor necrosis factor receptor are resistant to endotoxic shock, yet succumb to L. monocytogenes infection*. Cell, 1993. **73**(3): p. 457-67.
56. Green, S.J., et al., *Leishmania major amastigotes initiate the L-arginine-dependent killing mechanism in IFN-gamma-stimulated macrophages by induction of tumor necrosis factor-alpha*. J Immunol, 1990. **145**(12): p. 4290-7.

- 
57. Zhang, S., et al., *Delineation of diverse macrophage activation programs in response to intracellular parasites and cytokines*. PLoS Negl Trop Dis. **4**(3): p. e648.
  58. O'Shea, J.J. and P.J. Murray, *Cytokine signaling modules in inflammatory responses*. Immunity, 2008. **28**(4): p. 477-87.
  59. MacMicking, J., Q.W. Xie, and C. Nathan, *Nitric oxide and macrophage function*. Annu Rev Immunol, 1997. **15**: p. 323-50.
  60. Stein, M., et al., *Interleukin 4 potently enhances murine macrophage mannose receptor activity: a marker of alternative immunologic macrophage activation*. J Exp Med, 1992. **176**(1): p. 287-92.
  61. Odegaard, J.I., et al., *Macrophage-specific PPARgamma controls alternative activation and improves insulin resistance*. Nature, 2007. **447**(7148): p. 1116-20.
  62. MacKinnon, A.C., et al., *Regulation of alternative macrophage activation by galectin-3*. J Immunol, 2008. **180**(4): p. 2650-8.
  63. Rauh, M.J., et al., *SHIP represses the generation of alternatively activated macrophages*. Immunity, 2005. **23**(4): p. 361-74.
  64. Martinez, F.O., L. Helming, and S. Gordon, *Alternative activation of macrophages: an immunologic functional perspective*. Annu Rev Immunol, 2009. **27**: p. 451-83.
  65. Stutz, A.M., et al., *The Th2 cell cytokines IL-4 and IL-13 regulate found in inflammatory zone 1/resistin-like molecule alpha gene expression by a STAT6 and CCAAT/enhancer-binding protein-dependent mechanism*. J Immunol, 2003. **170**(4): p. 1789-96.
  66. Welch, J.S., et al., *TH2 cytokines and allergic challenge induce Ym1 expression in macrophages by a STAT6-dependent mechanism*. J Biol Chem, 2002. **277**(45): p. 42821-9.
  67. Rutschman, R., et al., *Cutting edge: Stat6-dependent substrate depletion regulates nitric oxide production*. J Immunol, 2001. **166**(4): p. 2173-7.
  68. Hesse, M., et al., *Differential regulation of nitric oxide synthase-2 and arginase-1 by type 1/type 2 cytokines in vivo: granulomatous pathology is shaped by the pattern of L-arginine metabolism*. J Immunol, 2001. **167**(11): p. 6533-44.
  69. Loke, P., et al., *Alternative activation is an innate response to injury that requires CD4+ T cells to be sustained during chronic infection*. J Immunol, 2007. **179**(6): p. 3926-36.
  70. Chang, N.C., et al., *A macrophage protein, Ym1, transiently expressed during inflammation is a novel mammalian lectin*. J Biol Chem, 2001. **276**(20): p. 17497-506.
  71. Siracusa, M.C., et al., *Dynamics of lung macrophage activation in response to helminth infection*. J Leukoc Biol, 2008. **84**(6): p. 1422-33.
  72. Herbert, D.R., et al., *Alternative macrophage activation is essential for survival during schistosomiasis and downmodulates T helper 1 responses and immunopathology*. Immunity, 2004. **20**(5): p. 623-35.
  73. Sharpe, A.H. and G.J. Freeman, *The B7-CD28 superfamily*. Nat Rev Immunol, 2002. **2**(2): p. 116-26.
  74. Ishida, Y., et al., *Induced expression of PD-1, a novel member of the immunoglobulin gene superfamily, upon programmed cell death*. Embo J, 1992. **11**(11): p. 3887-95.
  75. Dong, H., et al., *B7-H1, a third member of the B7 family, co-stimulates T-cell proliferation and interleukin-10 secretion*. Nat Med, 1999. **5**(12): p. 1365-9.
-

- 
76. Latchman, Y., et al., *PD-L2 is a second ligand for PD-1 and inhibits T cell activation*. *Nat Immunol*, 2001. **2**(3): p. 261-8.
  77. Keir, M.E., et al., *PD-1 and its ligands in tolerance and immunity*. *Annu Rev Immunol*, 2008. **26**: p. 677-704.
  78. Parry, R.V., et al., *CTLA-4 and PD-1 receptors inhibit T-cell activation by distinct mechanisms*. *Mol Cell Biol*, 2005. **25**(21): p. 9543-53.
  79. Okazaki, T., et al., *PD-1 immunoreceptor inhibits B cell receptor-mediated signaling by recruiting src homology 2-domain-containing tyrosine phosphatase 2 to phosphotyrosine*. *Proc Natl Acad Sci U S A*, 2001. **98**(24): p. 13866-71.
  80. Loke, P. and J.P. Allison, *PD-L1 and PD-L2 are differentially regulated by Th1 and Th2 cells*. *Proc Natl Acad Sci U S A*, 2003. **100**(9): p. 5336-41.
  81. Nishimura, H., et al., *Development of lupus-like autoimmune diseases by disruption of the PD-1 gene encoding an ITIM motif-carrying immunoreceptor*. *Immunity*, 1999. **11**(2): p. 141-51.
  82. Nishimura, H., et al., *Autoimmune dilated cardiomyopathy in PD-1 receptor-deficient mice*. *Science*, 2001. **291**(5502): p. 319-22.
  83. Yamazaki, T., et al., *Expression of programmed death 1 ligands by murine T cells and APC*. *J Immunol*, 2002. **169**(10): p. 5538-45.
  84. Liang, S.C., et al., *Regulation of PD-1, PD-L1, and PD-L2 expression during normal and autoimmune responses*. *Eur J Immunol*, 2003. **33**(10): p. 2706-16.
  85. Tseng, S.Y., et al., *B7-DC, a new dendritic cell molecule with potent costimulatory properties for T cells*. *J Exp Med*, 2001. **193**(7): p. 839-46.
  86. Freeman, G.J., et al., *Engagement of the PD-1 immunoinhibitory receptor by a novel B7 family member leads to negative regulation of lymphocyte activation*. *J Exp Med*, 2000. **192**(7): p. 1027-34.
  87. Butte, M.J., et al., *Programmed death-1 ligand 1 interacts specifically with the B7-1 costimulatory molecule to inhibit T cell responses*. *Immunity*, 2007. **27**(1): p. 111-22.
  88. de Silva, N.R., et al., *Soil-transmitted helminth infections: updating the global picture*. *Trends Parasitol*, 2003. **19**(12): p. 547-51.
  89. Ogilvie, B.M. and D.J. Hockley, *Effects of immunity of *Nippostrongylus brasiliensis* adult worms: reversible and irreversible changes in infectivity, reproduction, and morphology*. *J Parasitol*, 1968. **54**(6): p. 1073-84.
  90. Maizels, R.M. and M. Yazdanbakhsh, *Immune regulation by helminth parasites: cellular and molecular mechanisms*. *Nat Rev Immunol*, 2003. **3**(9): p. 733-44.
  91. Mohrs, M., et al., *Analysis of type 2 immunity in vivo with a bicistronic IL-4 reporter*. *Immunity*, 2001. **15**(2): p. 303-11.
  92. Lee, P.P., et al., *A critical role for Dnmt1 and DNA methylation in T cell development, function, and survival*. *Immunity*, 2001. **15**(5): p. 763-74.
  93. Voehringer, D., et al., *Efficient generation of long-distance conditional alleles using recombineering and a dual selection strategy in replicate plates*. *BMC Biotechnol*, 2009. **9**: p. 69.
  94. McKenzie, G.J., et al., *Simultaneous disruption of interleukin (IL)-4 and IL-13 defines individual roles in T helper cell type 2-mediated responses*. *J Exp Med*, 1999. **189**(10): p. 1565-72.
  95. Perez de Lema, G., et al., *Chemokine receptor Ccr2 deficiency reduces renal disease and prolongs survival in MRL/lpr lupus-prone mice*. *J Am Soc Nephrol*, 2005. **16**(12): p. 3592-601.
-

- 
96. Luckow, B., et al., *Reduced intragraft mRNA expression of matrix metalloproteinases Mmp3, Mmp12, Mmp13 and Adam8, and diminished transplant arteriosclerosis in Ccr5-deficient mice.* Eur J Immunol, 2004. **34**(9): p. 2568-78.
  97. Schaller, E., et al., *Inactivation of the F4/80 glycoprotein in the mouse germ line.* Mol Cell Biol, 2002. **22**(22): p. 8035-43.
  98. Kuipers, H., et al., *Contribution of the PD-1 ligands/PD-1 signaling pathway to dendritic cell-mediated CD4+ T cell activation.* Eur J Immunol, 2006. **36**(9): p. 2472-82.
  99. Cepko, C. and W. Pear, *Overview of the retrovirus transduction system.* Curr Protoc Mol Biol, 2001. **Chapter 9**: p. Unit9 9.
  100. Hirano, M., et al., *IgEb immune complexes activate macrophages through FcgammaRIV binding.* Nat Immunol, 2007. **8**(7): p. 762-71.
  101. Takeda, K., et al., *Impaired IL-13-mediated functions of macrophages in STAT6-deficient mice.* J Immunol, 1996. **157**(8): p. 3220-2.
  102. Loke, P., et al., *Alternatively activated macrophages induced by nematode infection inhibit proliferation via cell-to-cell contact.* Eur J Immunol, 2000. **30**(9): p. 2669-78.
  103. Serbina, N.V. and E.G. Pamer, *Monocyte emigration from bone marrow during bacterial infection requires signals mediated by chemokine receptor CCR2.* Nat Immunol, 2006. **7**(3): p. 311-7.
  104. Kurihara, T., et al., *Defects in macrophage recruitment and host defense in mice lacking the CCR2 chemokine receptor.* J Exp Med, 1997. **186**(10): p. 1757-62.
  105. Wu, L., et al., *CCR5 levels and expression pattern correlate with infectability by macrophage-tropic HIV-1, in vitro.* J Exp Med, 1997. **185**(9): p. 1681-91.
  106. Dehmel, S., et al., *Chemokine receptor Ccr5 deficiency induces alternative macrophage activation and improves long-term renal allograft outcome.* Eur J Immunol. **40**(1): p. 267-78.
  107. Zhao, A., et al., *Th2 cytokine-induced alterations in intestinal smooth muscle function depend on alternatively activated macrophages.* Gastroenterology, 2008. **135**(1): p. 217-225 e1.
  108. Allen, J.E., R.A. Lawrence, and R.M. Maizels, *APC from mice harbouring the filarial nematode, Brugia malayi, prevent cellular proliferation but not cytokine production.* Int Immunol, 1996. **8**(1): p. 143-51.
  109. MacDonald, A.S., et al., *Requirement for in vivo production of IL-4, but not IL-10, in the induction of proliferative suppression by filarial parasites.* J Immunol, 1998. **160**(3): p. 1304-12.
  110. Loke, P., et al., *IL-4 dependent alternatively-activated macrophages have a distinctive in vivo gene expression phenotype.* BMC Immunol, 2002. **3**: p. 7.
  111. Taylor, M.D., et al., *F4/80+ alternatively activated macrophages control CD4+ T cell hyporesponsiveness at sites peripheral to filarial infection.* J Immunol, 2006. **176**(11): p. 6918-27.
  112. Rodriguez-Sosa, M., et al., *Chronic helminth infection induces alternatively activated macrophages expressing high levels of CCR5 with low interleukin-12 production and Th2-biasing ability.* Infect Immun, 2002. **70**(7): p. 3656-64.
  113. Ostrand-Rosenberg, S. and P. Sinha, *Myeloid-derived suppressor cells: linking inflammation and cancer.* J Immunol, 2009. **182**(8): p. 4499-506.
  114. Shevach, E.M., *Mechanisms of foxp3+ T regulatory cell-mediated suppression.* Immunity, 2009. **30**(5): p. 636-45.
-

- 
115. Pesce, J.T., et al., *Arginase-1-expressing macrophages suppress Th2 cytokine-driven inflammation and fibrosis*. PLoS Pathog, 2009. **5**(4): p. e1000371.
  116. Bronte, V., et al., *IL-4-induced arginase 1 suppresses alloreactive T cells in tumor-bearing mice*. J Immunol, 2003. **170**(1): p. 270-8.
  117. Bronte, V., et al., *L-arginine metabolism in myeloid cells controls T-lymphocyte functions*. Trends Immunol, 2003. **24**(6): p. 302-6.
  118. Kusmartsev, S. and D.I. Gabrilovich, *Inhibition of myeloid cell differentiation in cancer: the role of reactive oxygen species*. J Leukoc Biol, 2003. **74**(2): p. 186-96.
  119. Huang, B., et al., *Gr-1+CD115+ immature myeloid suppressor cells mediate the development of tumor-induced T regulatory cells and T-cell anergy in tumor-bearing host*. Cancer Res, 2006. **66**(2): p. 1123-31.
  120. Groux, H., et al., *A CD4+ T-cell subset inhibits antigen-specific T-cell responses and prevents colitis*. Nature, 1997. **389**(6652): p. 737-42.
  121. Asseman, C., et al., *An essential role for interleukin 10 in the function of regulatory T cells that inhibit intestinal inflammation*. J Exp Med, 1999. **190**(7): p. 995-1004.
  122. Nakamura, K., A. Kitani, and W. Strober, *Cell contact-dependent immunosuppression by CD4(+)CD25(+) regulatory T cells is mediated by cell surface-bound transforming growth factor beta*. J Exp Med, 2001. **194**(5): p. 629-44.
  123. Modolell, M., et al., *Local suppression of T cell responses by arginase-induced L-arginine depletion in nonhealing leishmaniasis*. PLoS Negl Trop Dis, 2009. **3**(7): p. e480.
  124. El Kasmi, K.C., et al., *Toll-like receptor-induced arginase 1 in macrophages thwarts effective immunity against intracellular pathogens*. Nat Immunol, 2008. **9**(12): p. 1399-406.
  125. Nair, M.G., et al., *Alternatively activated macrophage-derived RELM- $\alpha$  is a negative regulator of type 2 inflammation in the lung*. J Exp Med, 2009. **206**(4): p. 937-52.
  126. Munitz, A., et al., *Resistin-like molecule alpha enhances myeloid cell activation and promotes colitis*. J Allergy Clin Immunol, 2008. **122**(6): p. 1200-1207 e1.
  127. Reese, T.A., et al., *Chitin induces accumulation in tissue of innate immune cells associated with allergy*. Nature, 2007. **447**(7140): p. 92-6.
  128. Reece, J.J., M.C. Siracusa, and A.L. Scott, *Innate immune responses to lung-stage helminth infection induce alternatively activated alveolar macrophages*. Infect Immun, 2006. **74**(9): p. 4970-81.
  129. Ohnmacht, C. and D. Voehringer, *Basophil effector function and homeostasis during helminth infection*. Blood, 2009. **113**(12): p. 2816-25.
  130. Sherman, M.A., *The role of STAT6 in mast cell IL-4 production*. Immunol Rev, 2001. **179**: p. 48-56.
  131. Dong, H., et al., *Tumor-associated B7-H1 promotes T-cell apoptosis: a potential mechanism of immune evasion*. Nat Med, 2002. **8**(8): p. 793-800.
  132. Dong, H., et al., *B7-H1 determines accumulation and deletion of intrahepatic CD8(+) T lymphocytes*. Immunity, 2004. **20**(3): p. 327-36.
  133. Latchman, Y.E., et al., *PD-L1-deficient mice show that PD-L1 on T cells, antigen-presenting cells, and host tissues negatively regulates T cells*. Proc Natl Acad Sci U S A, 2004. **101**(29): p. 10691-6.
-

- 
134. Akbari, O., et al., *PD-L1 and PD-L2 modulate airway inflammation and iNKT-cell-dependent airway hyperreactivity in opposing directions*. *Mucosal Immunol.* **3**(1): p. 81-91.
  135. Shin, T., et al., *In vivo costimulatory role of B7-DC in tuning T helper cell 1 and cytotoxic T lymphocyte responses*. *J Exp Med*, 2005. **201**(10): p. 1531-41.
  136. Keir, M.E., et al., *Tissue expression of PD-L1 mediates peripheral T cell tolerance*. *J Exp Med*, 2006. **203**(4): p. 883-95.
  137. Ishiwata, K., et al., *Costimulator B7-DC attenuates strong Th2 responses induced by Nippostrongylus brasiliensis*. *J Immunol.* **184**(4): p. 2086-94.
  138. Wang, S., et al., *Molecular modeling and functional mapping of B7-H1 and B7-DC uncouple costimulatory function from PD-1 interaction*. *J Exp Med*, 2003. **197**(9): p. 1083-91.
  139. Nguyen, L.T., et al., *Cross-linking the B7 family molecule B7-DC directly activates immune functions of dendritic cells*. *J Exp Med*, 2002. **196**(10): p. 1393-8.
  140. Zaretsky, A.G., et al., *T follicular helper cells differentiate from Th2 cells in response to helminth antigens*. *J Exp Med*, 2009. **206**(5): p. 991-9.
  141. King, I.L. and M. Mohrs, *IL-4-producing CD4+ T cells in reactive lymph nodes during helminth infection are T follicular helper cells*. *J Exp Med*, 2009. **206**(5): p. 1001-7.
  142. Barber, D.L., et al., *Restoring function in exhausted CD8 T cells during chronic viral infection*. *Nature*, 2006. **439**(7077): p. 682-7.
  143. Youngnak, P., et al., *Differential binding properties of B7-H1 and B7-DC to programmed death-1*. *Biochem Biophys Res Commun*, 2003. **307**(3): p. 672-7.
  144. Broxmeyer, H.E., et al., *Th1 cells regulate hematopoietic progenitor cell homeostasis by production of oncostatin M*. *Immunity*, 2002. **16**(6): p. 815-25.
  145. Tyner, J.W., et al., *CCL5-CCR5 interaction provides antiapoptotic signals for macrophage survival during viral infection*. *Nat Med*, 2005. **11**(11): p. 1180-7.
  146. Stout, R.D., et al., *Macrophages sequentially change their functional phenotype in response to changes in microenvironmental influences*. *J Immunol*, 2005. **175**(1): p. 342-9.
  147. Mylonas, K.J., et al., *Alternatively activated macrophages elicited by helminth infection can be reprogrammed to enable microbial killing*. *J Immunol*, 2009. **182**(5): p. 3084-94.
  148. Watkins, S.K., et al., *IL-12 rapidly alters the functional profile of tumor-associated and tumor-infiltrating macrophages in vitro and in vivo*. *J Immunol*, 2007. **178**(3): p. 1357-62.
  149. Huber, S., et al., *Alternatively activated macrophages inhibit T-cell proliferation by Stat6-dependent expression of PD-L2*. *Blood*, 2010. **116**(17): p. 3311-20.



---

# CURRICULUM VITAE

## Personal

---

Silke Huber (née Schmechel)

Date of Birth: 08 January 1981

Nationality: German

Marital status: married

## Employment

---

- Since Jan. 2011 Study Director in the Immunoanalytics group of BSL Bioservice, Planegg, Germany
- Oct. 2007 – Dec. 2010 PhD at the Institute for Immunology at the Ludwig-Maximilians University, Munich, Germany (Prof. Dr. D. Vöhringer)  
Title: *Phenotypic and functional characterization of alternatively activated macrophages*
- Nov. 2006 – Sep. 2007 Research associate in the Mucosal Immunology Division at the Department of Gastroenterology, Munich University Hospital, Germany (Dr. med. A. Konrad-Zerna)

## Education

---

- Oct. 2006 Degree: *Master of Science* (Grade: 1.4)  
Main subject: Biomedicine
- April 2006 – Oct. 2006 Master's Thesis at the Department of Biofunctionality at the Technical University Munich, Germany (Prof. Dr. D. Haller)  
Title: *The relevance of pattern recognition receptors for the activation of intestinal epithelial cells in TLR2 and TLR4 deficient mice*
- Oct. 2004 – Oct. 2006 Master in Nutritional Science at the Technical University Munich, Germany
- Aug. 2004 Degree: *Bachelor of Science* (Grade: 1.6)
- April 2004 – July 2004 Bachelor's Thesis at the Department of Food Technology at the Technical University Munich, Germany (Prof. Dr. K.-H. Engel)  
Title: *In-vitro studies of ferulic acid metabolism of phytosterols*
- Oct. 2001 – Sep. 2004 Bachelor in Nutritional Science at the Technical University Munich, Germany
- Aug. 1993 – June 2000 Georg-Büchner-Gymnasium Seelze, Germany (Grade: 1.9)

**Internships and temporary employment abroad**

---

Sep. – Dec. 2005	Internship at the Department of Immunology of the National Autonomous University of Mexico, Mexico (Dr. E.G. Zepeda)
Aug. – Oct. 2004	Internship at the Department of Gastroenterology, Hannover Medical School, Germany (Prof. Dr. med. S. C. Bischoff)
Aug. – Oct. 2003	Internship at the Department of Physiology, University of Barcelona, Spain (Prof. J.M. Planas)
Sep. 2000 – July 2001	Au pair and Spanish language school at the Escola Oficial d'Idiomes in Barcelona, Spain

**Congresses**

---

May 2010	5 <sup>th</sup> ENII EFIS/EJI Summer School in Advanced Immunology, Sardinia, Italy ( <i>oral and poster presentation</i> )
Sep. 2009	European Congress of Immunology, Berlin, Germany ( <i>Poster presentation</i> )
March 2008	4 <sup>th</sup> German Spring School on Immunology, Ettal, Germany
July 2006	German consortium of inflammatory bowel disease, Mainz, Germany

**Workshops**

---

May 2010	Workshop on Presenting Professionally, Ludwig-Maximilians University, Munich, Germany
Nov. 2009	Workshop on Publishing in Peer-Reviewed Journals, Ludwig-Maximilians University, Munich, Germany
Jan. 2006	Scientific course on Fluorescence Activated Cell Sorting (FACS Calibur, FACSCComp, CellQuest Pro) Company Becton Dickinson, Heidelberg, Germany

**Financial Support**

---

GlaxoSmithKline, travel grant  
European Network of Immunology, registration waiver fellowship  
Munich University association, travel grant

---

## **ERKLÄRUNG**

Hiermit erkläre ich, dass ich die vorliegende Doktorarbeit selbständig angefertigt habe. Es wurden nur die in der Arbeit ausdrücklich benannten Quellen und Hilfsmittel benutzt. Wörtlich oder sinngemäß übernommenes Gedankengut habe ich als solches kenntlich gemacht.

---

Ort, Datum

---

Unterschrift